# Planning a Mobile Photo Enforcement Program by Mapping Program Goals to Deployment Decisions

by

Yang Li

A thesis submitted in partial fulfillment of the requirements for the degree of

Doctor of Philosophy

in

TRANSPORTATION ENGINEERING

Department of Civil and Environmental Engineering
University of Alberta

# ABSTRACT

This thesis develops a methodical, evidence-based mobile photo enforcement (MPE) resource deployment program. The goal is to provide a framework for enforcement agencies to adopt, which is transparent in its goals and efficient in attainment of these goals. Specifically, we provide a method that assists agencies map their traffic safety goals directly to the allocation of enforcement resources. Currently operating MPE programs tend to be "black boxes," leading to questions regarding their efficacy and aims.

The MPE deployment problem was identified to consist of three phases: 1) quantifying MPE deployment goals, 2) increasing MPE coverage of deployment goals, and 3) efficient scheduling of MPE resources. In the first phase, we identify a set of deployment objectives that are often set out by many governments managing MPE programs. Quantitative measures corresponding to the objectives are proposed in order to facilitate deployment decisions that lead to goal attainment. In phase two, a neighborhood-level resource allocation model is developed to assign monthly operator shifts to city neighborhoods. The model employs multi-objective optimization so that multiple, possibly conflicting, deployment objectives can be considered simultaneously. To further interpret the model solutions (known as the Pareto front), we use clustering techniques and response surface methods to represent the Pareto front and analyze front tradeoffs, respectively. The third and final deployment phase, assigns operator shifts to neighborhoods to visit groups of roadway locations within each, to continually attain the goals set in the previous stage. In addition, a binary integer programming model is applied to schedule shifts (two per day) for an entire month. The scheduling model is developed to minimize violations of the time halo effects of enforcement,

by minimizing visits to an operator task over consecutive shifts (i.e., over which the time halo of enforcement is still in effect).

The proposed three-phase approach is applied to an MPE program in the City of Edmonton, in the province of Alberta, Canada. First, we explored the deployment results of six priorities identified in the Alberta provincial enforcement guidelines, using five years (2010-14) of historical data from Edmonton's MPE program. Second, three priorities that received the most enforcement attention were used in the resource allocation model. The model provided various Pareto optimal solutions for one month (September 2014), using metrics that quantified each of the three priorities, calculated from three years (2012-14) of historical data. To reduce decision fatigue for agencies, solutions were further partitioned into several clusters, where each cluster's representative solution is considered a candidate plan for resource allocations to neighborhoods. The tradeoffs between cluster solutions were also examined using a polynomial model, from which the quantitative relationship between three objectives implied in any candidate plans is revealed. Finally, our scheduling model creates a plan for operator shifts to their location visit tasks for an entire month of two shifts per day, using the neighborhood allocations from the second stage. Resulting schedules were found to increase the resource utilization efficiency by 14% compared to a randomly generated plan.

This thesis contributes to the literature and practice by 1) developing a systematic and optimized resource allocation and scheduling method for MPE programs for the first time in the literature, 2) increasing the transparency of the decision-making process of enforcement agencies in designing an MPE program. The proposed method uses optimization techniques in both MPE resource allocation and resource scheduling, to assign limited resources in an efficient manner. The method

directs enforcement coverage by optimizing metrics quantified for high-level program goals, resulting in a more transparent and evidence-based MPE program operation.

**Keywords** mobile photo enforcement, resource allocation, scheduling, geographic information system (GIS), multi-objective optimization, tradeoff analysis, Dantzig-Wolfe, column generation.

# PREFACE

### Published

1. **Li, Y.**, Kim, A. M., El-Basyouny, K., & Li, R, "Using GIS to interpret automated speed enforcement guidelines and guide deployment decisions in mobile photo enforcement programs", *Transportation Research Part A: Policy and Practice*, 86, 141–158.

2. **Li, Y.**, Xie, J., Kim, A. M., & El-Basyouny, K., "Investigating tradeoffs between optimal mobile photo enforcement program plans", *Journal of Multi‐Criteria Decision Analysis*. Accepted December 2018.

3. **Li, Y.**, Kim, A. M., & El-Basyouny, K., "Linking Program Goals to Deployment Decisions: Creating A Transparent and Efficient Mobile Photo Enforcement Program", *in 98th Transportation Research Board Annual Meeting Online Compendium*. Accepted November 2018.

4. **Li, Y.**, Kim, A., & El-Basyouny, K., "Scheduling resources in a mobile photo enforcement program", *in Transportation Information and Safety (ICTIS)*, 2017 4th International Conference, pp. 645–652. *IEEE*.

### Under Review

5. **Li, Y.**, Kim, A., & El-Basyouny, K., "Interactive allocation of mobile photo enforcement resources with multiple program objectives." Under review.

### In Preparation

6. **Li, Y.** & Kim, A. M. "Allocating and scheduling resources for a mobile photo enforcement program." In preparation for submission in February 2019.

# DEDICATION

*To my mother Boping Meng and*

*my husband Haoyang (Kyle) Wang*

*with love*

# ACKNOWLEDGMENTS

I feel lucky to conduct my doctoral research under the co-supervision of Dr. Amy Kim and Dr. Karim El-Basyouny. I would like to sincerely thank them for their tireless guidance, which enabled me to successfully complete the arduous doctoral program on time and master the high-level qualities required for the traffic engineering profession.

In addition, my thanks to the Traffic Safety Section, in the City of Edmonton, for funding the research project for my doctoral study and providing historical data used in this thesis. As well, thanks to the staff of the Traffic Safety Section for helping me better understand the research project under study.

I would also like to thank my officemates and colleagues at University of Alberta for their support and companionship, especially Ran Li, Yunzhuang Zheng, and Can Zhang for many good technical discussions; Kathy Hui, Matt Woo, Kasturi Mahajan, Suliman Gargoum, Ai Teng, and Negar Tavafzadeh for our great team work in the ITEUA student chapter; and also Aalyssa Atley and Rachelle Foss for their proof-reading support.

As well, thanks Dr. Amy Kim, Dr. Karim El-Basyouny, Dr. Tae Kwon, Dr. John Doucette, and Dr. Hooman Askari Nasab for participating in my candidacy exam, and Dr. Amy Kim, Dr. Karim El-Basyouny, Dr. Tae Kwon, Dr. Ata Khan, Dr. Hooman Askari Nasab, and Dr. Nicholas Beier for participating in my final defense.

Finally, my thanks go to my husband who unconditionally supports the attainment of my unrestrained and vigorous ideas, and to my mother whose constant love and encouragement sustain me throughout my life.

# TABLE OF CONTENTS

# LIST OF TABLES

# LIST OF FIGURES

# LIST OF SYMBOLS

### Acronyms

| | | |
|---|---|---|
| ASE | = | automated speed enforcement |
| BIP | = | binary integer programming |
| COE | = | City of Edmonton |
| ECP | = | epsilon constraint problem |
| EPDO | = | equivalent property damage only |
| EPK | = | equivalent property damage only collision frequency per kilometer |
| FTPP | = | freeway traffic police patrol |
| GDE3 | = | generalized differential evolutionary 3 algorithm |
| GIS | = | Geographic Information Systems |
| LSAP | = | location and schedule assignment |
| MCL | = | maximal covering location |
| MOEA | = | multi-objective evolutionary algorithm |
| MOLP | = | multi-objective linear programming |
| MP | = | master problem |
| MPE | = | mobile photo enforcement |
| MRA | = | mobile photo enforcement resource allocation |
| MRS | = | mobile photo enforcement resource scheduling |
| PF | = | Pareto front |
| RLMP | = | restricted linear programming master problem |
| SCL | = | set covering location |
| SP | = | sub-problem |
| SVI | = | speed violation indicator |
| SZD | = | school zone density |
| WSP | = | weighted sum problem |

**Notations**

| | | |
|---|---|---|
| $m$ | = | enforcement site index |
| $R_m$ | = | expected radius of enforcement distance halo effect at site $m$ in meters |
| $R_0$ | = | baseline radius of distance halo effect in meters |
| $y_m$ | = | total enforcement level at site $m$ in hours |
| $Y$ | = | average citywide level of enforcement in hours |
| $x_n$ | = | number of operator shifts assigned to neighborhood $n$ in a given month, $n \in [1, \dots, N]$ |
| $n$ | = | neighborhood index, $n = 1, \dots, N$ |
| $EPK_n$ | = | EPDO collision frequency per kilometer (km) for neighborhood $n$ |
| $SVI_n$ | = | speed violation indicator for neighborhood $n$ |
| $SZD_n$ | = | number of school zones per square kilometer (sq.km) for neighborhood $n$ |
| $P$ | = | number of total shifts in one month |
| $L_n$ | = | minimum allowable shifts that may be allocated to neighborhood $n$ in one month |
| $U_n$ | = | maximum allowable shifts that may be allocated to neighborhood $n$ in one month |
| $\alpha_g$ | = | weight given to deployment metric $EPK$ in the $g$th iteration |
| $\beta_g$ | = | weight given to deployment metric $SVI$ in the $g$th iteration |
| $\gamma_g$ | = | weight given to deployment metric $SZD$ in the $g$th iteration |
| $g$ | = | iteration index, $g = 1, \dots, G$ |
| $\varepsilon_g^1$ | = | lower bound value given to deployment objective $SVI$ in the $g$th iteration |
| $\varepsilon_g^2$ | = | lower bound value given to deployment objective $SZD$ in the $g$th iteration |
| $a(i)$ | = | average distance between any data point $i$ in cluster $a$ and all other points in the same cluster |
| $b(i)$ | = | average distance of the point $i$ to all the points of a neighboring cluster $b$ |
| $e$ | = | curve elasticity |
| $d$ | = | number of sites to be visited per operator per shift |
| $N^{(1)}$ | = | set of neighborhoods identified in Stage 1 |
| $M_n$ | = | number of predetermined enforcement sites included in neighborhood $n$ |
| $j$ | = | task index |
| $J_n$ | = | number of tasks included in neighborhood $n$ |
| $c_{mj}$ | = | 1 if the $m^{th}$ site is used in the $j^{th}$ candidate task, and 0 otherwise |

| | | |
|---|---|---|
| $C^n$ | = | a $M_n \times J_n$ binary matrix containing all the possible tasks for neighborhood $n$ |
| $W_m$ | = | weight of enforcement site $m$ |
| $EPK_m$ | = | EPDO collision frequency per kilometer (km) for site $m$ |
| $SVI_m$ | = | speed violation indicator for site $m$ |
| $SZD_m$ | = | number of school zones for site $m$ |
| $w_{EPK}$ | = | weight given to deployment metric $EPK$ |
| $w_{SVI}$ | = | weight given to deployment metric $SVI$ |
| $w_{SZD}$ | = | weight given to deployment metric SZD |
| $W_j^n$ | = | weight of task $j$ in neighborhood $n$ |
| $x_j^n$ | = | number of monthly shifts allocated to candidate task $j$ in neighborhood $n$ |
| $x_{ij}$ | = | 1 if visit occurs at task $j$ in shift $i$, 0 otherwise |
| $i$ | = | shift index, $i = 1, \dots, I$ |
| $I$ | = | total number of shifts of the given month |
| $J$ | = | total number of tasks identified across all neighborhoods, $J = \sum_{n \in N^{(1)}} J_n$ |
| $c_{ij}$ | = | cost of allocating an operator visit at task $j$ in shift $i$ |
| $dl_i$ | = | minimum number of visits required for shift $i$ |
| $du_i$ | = | maximum number of visits allowed for shift $i$ |
| $t$ | = | number of consecutive shifts over which time halo effects are observed |
| $mod$ | = | remainder of $1 + (i - 1)$ divided by $I$ |
| $K_j$ | = | number of all possible schedules of distributing $x_j$ visits within $I$ shifts |
| $S_j$ | = | Set of feasible shift schedules for task $j$ |
| $\lambda_j^k$ | = | 1 if shift schedule $x_j^k$ is selected for task $j$, 0 otherwise |

# 1 INTRODUCTION

## 1.1 BACKGROUND

### *1.1.1 The Controversy over MPE Deployment*

Despite the demonstrated effectiveness of mobile photo enforcement (MPE) for improving road safety, enforcing speed limits through MPE programs is highly controversial. Enforcement agencies and academics in safety research typically support the use of MPE programs, which dispatch operators driving vehicles equipped with photo radar equipment to roadway locations in order to detect and photograph vehicles violating speed limits, for reducing speeds and improving road safety. In fact, according to a review of studies around the world conducted from the late 1990s to early 2000s by Rodier et al. (2007), an MPE program is proven to reduce speeding vehicles and collisions by up to 82% and 51%, respectively. And, because speeding is one main cause of traffic collisions—30% of global traffic fatalities are attributed to speeding problems (OECD/ECMT, 2006)—an MPE program is an effective means of reducing accidents. Even simply increasing the perceived risk of detection, can create general deterrence to speed violations.

However, due to a lack of understanding among the community, fostered by limitations with deployment strategies, those in opposition (mostly members of the public) tend to associate the program with issuing tickets to raise revenue. A series of US opinion polls show that one in three people oppose the use of photo radar for managing speed (Rodier et al., 2007). And, yet, in the face of this concern, few enforcement agencies have provided deployment strategies that transparently link placement decisions back to program goals (typically aligned with road safety). To solve this issue, some studies have begun to focus on how to establish such a deployment strategy, as described in the next section.

### *1.1.2 Deployment Strategies for MPE*

Contrary to potential misconception, the road safety goals of the MPE program are to reduce collisions, reduce speed violations, and improve the safety of vulnerable road users. To meet these goals, many government guidelines that manage automated speed enforcement techniques (MPE

is within the scope of this technology) have directed agencies to deploy their programs following a number of priorities. The most common goals in the automated speed enforcement guidelines (NHTSA, 2008; Alberta Justice and Solicitor General, 2014; Victoria Police Traffic Camera Office, 2006; Queensland Police, 2016; Humberside Police, 2008) are as follows:

- High collision sites to reduce accidents;
- High speed violation sites to reduced speeding vehicles;
- School zones, construction zones, high pedestrian volume sites, and sites with community speeding complaints to improve pedestrian's safety.

When developing MPE deployment strategies, agencies should allocate enforcement resources (operators and vehicles) to the above priority locations (Delaney, Diamantopoulou, & Cameron, 2003). Moreover, enforcement resources should cover more such locations, resulting in greater program safety (Delaney et al., 2003; R. Li, El-Basyouny, Kim, & Gargoum, 2016; Newstead & Cameron, 2003).

In addition to location, MPE resources also need to be allocated based on time. This is because the equipment (cameras) of the MPE program is not fixed at a certain location, instead, the operator drives a vehicle that carries the camera to different locations at different times. The time halo effect is where drivers' speeding behaviors are reduced after the end of enforcement operations, due to the "memory" of having observed prior enforcement at that particular site. The time halo effect can last several hours to days (Hauer, Ahlin, & Bowser, 1982; Armour, 1986; Cairney, 1988; Vaa, 1997; Gouda & El-Basyouny, 2016). But, it is known that enforcement tends to lose its effect once drivers adapt to the schedule of enforcement operations (OECD, 1990). By generating a highly varied operation schedule, the enforcement effect may last longer (R. Q. Brackett & Beecher, 1980; Robert Quinn Brackett & Edwards, 1977; Bjørnskau & Elvik, 1992; Newstead & Cameron, 2003). All of the above suggestions for MPE deployment strategies are qualitative, and thus quantitative methods are required to assist enforcement agencies implement these systems.

### 1.1.3 Current Resource Allocation and Scheduling Approach

Regardless of the considerations for deployment, there is inadequate guidance for agencies, as little research has been done on quantitative methods for assigning MPE resources to designated locations and times. A random scheduling model, which was conceived by Edwards and Brackett (1978), further developed and implemented by Leggett (1988), and improved by Kim et al. (2016), has been thus far the main method for deploying MPE programs discussed in the literature. The random resource scheduling model generates a pairing between the operator's work time and the enforcement location through indiscriminate matching. The model emphasizes increasing the variability of enforcement activities over time—namely, unpredictability to motorists. However, the use of the random scheduling method makes it difficult for MPE agencies to address other targets, such as increasing enforcement spatial coverage and considering resource availability limits.

Although research into MPE deployment is very limited, resource allocation and scheduling issues have been extensively studied in other research areas, but they are usually solved separately. For example, optimization techniques have been widely applied to help decision makers determine how to allocate limited resources in location and time in order to best achieve some predefined objective(s). Maximum covering location model (Church & Velle, 1974) and set covering location model (Toregas, Swain, ReVelle, & Bergman, 1971) are both widely used to determine the optimal location and number of police stations, fire stations and emergency centers, to meet pre-set program objectives (Toregas et al., 1971; Church & Velle, 1974; Larson, 1974; Church, Sorensen, & Corrigan, 2001; Curtin, Qiu, Hayslett-McCall, & Bray, 2005; Daskin, 1982). Additionally, the integer programming model, based on set covering theory, is the fundamental formulation of most resource scheduling models in the fields of aviation, public transit, and vehicle routing (Desaulniers, Desrosiers, Dumas, Solomon, & Soumis, 1997; Desaulniers, Desrosiers, & Solomon, 2002; Desrochers & Soumis, 1989; Desrosiers, Soumis, & Desrochers, 1984; Gamache, Soumis, Marquis, & Desrosiers, 1999). Similarly, the optimization model establishes an optimal scheduling plan between personnel tasks and time by satisfying specified target and resource constraints. In view of the successful use of optimization techniques for resource allocation and scheduling issues, these approaches can also be used for MPE, specifically, to improve the allocation efficiency of MPE program resources.

## 1.2 PROBLEM STATEMENT AND MOTIVATION

The decision-making process of most enforcement agencies when deploying MPE programs is a "black box" that lacks a transparent and defensible structure. As noted, this has led to controversy surrounding the use of MPE, regardless of its positive impact on managing speeds and collisions. Therefore, a method is necessary that assists MPE agencies to assign enforcement resources over locations and times based on road safety goals. Additionally, considering the limited nature of enforcement resources, the method should utilize assets efficiently in the achievement of these goals. But, the literature has been systematically studied, revealing there is no such method.

Establishing a goal-oriented and efficient MPE resource allocation method requires solving the following problems:

- Although a set of MPE deployment priorities associated with road safety goals have been proposed, they are qualitative. Few studies have discussed how to identify these MPE deployment priorities, and to what extent they achieve the goals.

- To accomplish a greater MPE program effect, a deployment strategy is to cover more target locations. However, how to assign resources to increase MPEs coverage of target roadway locations has not been discussed in the literature. Additionally, enforcement locations are associated with multiple and different deployment priorities, so the question remains, how to consider them at the same time?

- When scheduling MPE resources, the existing random scheduling method can be used to increase the program's unpredictability over time, but it may waste program resources, which are usually limited. Therefore, the problem arises of to how to change enforcement presence between roadway locations in order to sustain a dynamic enforcement operation, while ensuring efficient resource utilization?

The motivation of this thesis is to solve the above problems, and thus establish a deployment method for the MPE program that can map multiple goals into decisions and use resources efficiently. With this method, MPE agencies' decision-making processes will follow a quantitative process from defining goals through resource allocation to resource scheduling.

Although the MPE program is the focus of this thesis, the larger vision of this work is that it is a first step in designing a broader range of traffic enforcement programs that utilize a variety of technologies. The technologies used for the MPE program designed in this thesis are one of several different types available to carry out such a program. In addition, other technologies such as electronic driver speed feedback signs are used to deter speeding and indirectly, the consequences of speeding. This work provides a foundation for designing programs that incorporate multiple technologies and deterrence mechanisms, to ultimately improve urban traffic safety.

## 1.3 THESIS OBJECTIVES

Given the motivation of this thesis, we will explore the three main research questions raised in the preceding section: 1) quantification of MPE deployment goals, 2) MPE resource coverage of deployment goals, and 3) efficient scheduling of MPE resources. For solving each question, the specific research objectives are as follows.

- *Quantification of MPE deployment goals:* Establish deployment criteria to enable MPE agencies to prioritize enforcement resource allocation to roadway locations where the goals (i.e., reducing collisions, reducing speed violations, and increasing pedestrian safety) can be met. Quantitative measures for each deployment criterion will be developed to assess and compare the level of enforcement needs related to each safety goal. These criteria and measures will bring transparency into the process of allocating resources to locations and are expected to help reach city-wide safety targets.

- *MPE resource coverage of deployment goals:* Develop a method to allocate MPE resources to enforcement priority locations identified by the deployment criteria and metrics mentioned above. Because the MPE program may have different deployment priorities at different points in time (such as prioritizing high collision sites to reduce collisions in winter, and prioritizing school zones during the return to school in September), the proposed method considers multiple deployment goals simultaneously. The method uses optimization techniques to achieve efficient use of resources.

- *Efficient scheduling of MPE resources:* Design a method to schedule resources to chosen enforcement locations. Based on the principle of increasing the unpredictability of MPE

resource's time allocation so as to yield longer enforcement effects, the resource time allocation method presented in this thesis aims to produce an optimal but varied enforcement pattern.

Each of the above objectives is addressed in a section of this thesis. Figure 1-1 shows the connections (and workflow) between these objectives.

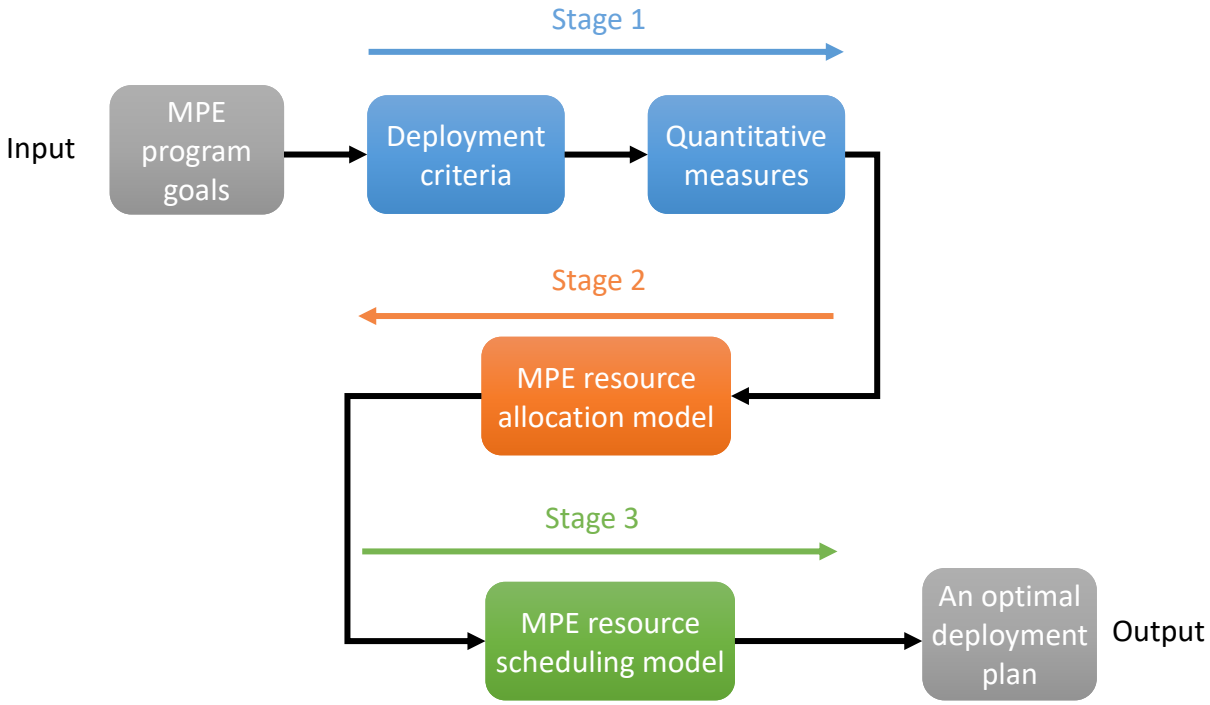


**Figure 1-1 Thesis work flow.**

The first stage of the research (blue boxes) converts user input qualitative MPE program goals to quantitative deployment criteria and measures. These are then input to the second stage (orange box), which produces a set of resource allocation solutions. After the MPE agency chooses a solution, it is input into the resource scheduling model (Stage 3, green box). The scheduling model further allocates enforcement resources to individual enforcement locations over time, resulting in an optimal resource deployment plan.

Overall, this thesis aims to deliver an evidence-based decision structure for conducting an MPE program. This thesis contributes to the literature and practice by 1) developing both a systematic and optimized resource allocation and scheduling method for MPE programs for the first time in

the literature, 2) increasing the transparency of the decision-making process of enforcement agencies when designing an MPE program. The proposed method uses optimization techniques in both MPE resource allocation and resource scheduling, to assign limited resources in an efficient manner. The method directs enforcement coverage by optimizing metrics quantified for high-level program goals, resulting in a more transparent and evidence-based MPE program operation.

## 1.4 THESIS STRUCTURE

The remainder of this thesis is organized into the following six chapters.

Chapter 2 presents a literature review of the work done on MPE resource allocation. Section 2.1 outlines the six prevalent criteria published in various countries for guiding the deployment of automated speed enforcement programs. Existing methods for allocating and scheduling MPE resources are studied in Sections 2.2 and 2.3, respectively. Section 2.4 concludes the chapter.

Chapter 3 describes the sources of data used for the development of MPE both resource allocation and scheduling models proposed in this thesis. To validate the model outcomes, two case studies were examined. Section 3.1 describes how to use and process data to quantitatively interpret the deployment principles of MPE programs. Section 3.2 introduces the data collected for model development and application.

Chapters 4, 5, and 6 provide a detailed introduction of the MPE deployment methods and procedure steps designed in this thesis, corresponding to the implementation of the three specific objectives illustrated in Section 1.3.

Chapter 4 elaborates on how we identify MPE deployment priorities that are aligned with guiding principles through the following sections: Section 4.1—an introduction to this chapter; Section 4.2—an exploration of operations of the Edmonton's MPE program, in relation to six major criteria identified in the provincial enforcement guidelines; Section 4.3—a further discussion of enforcement coverage while considering enforcement's distance halo effect; Section 4.4—summary of this chapter.

- *A version of this chapter has been published as **Li, Y.**, Kim, A. M., El-Basyouny, K., & Li, R, "Using GIS to interpret automated speed enforcement guidelines and guide deployment decisions in mobile photo enforcement programs", Transportation Research Part A: Policy and Practice, 86, 141–158.*

Chapter 5 introduces the MPE resource allocation (MRA) model through the following sections: Section 5.1—an introduction to this chapter, Section 5.2—mathematical formulation of the MRA model proposed in this chapter, Section 5.3—two methods to generate the optimal resource allocation solutions (i.e., a Pareto front) for the MRA model, Section 5.4—MRA Pareto front generation results, Section 5.5—Pareto front result analysis, Section 5.6—summary of this chapter.

- *A version of this chapter related to MRA model has been published as **Li, Y.**, Kim, A. M., & El-Basyouny, K., "Linking Program Goals to Deployment Decisions: Creating A Transparent and Efficient Mobile Photo Enforcement Program", in 98th Transportation Research Board Annual Meeting. Accepted November 2018.*

- *Another version of this chapter related to MRA model is being reviewed for a potential journal publication as **Li, Y.**, Kim, A. M., & El-Basyouny, K., "Interactive Allocation of Mobile Photo Enforcement Resources with Multiple Program Objectives". Under review.*

- *A version of this chapter related to MPA Pareto front analysis has been published as **Li, Y.**, Xie, J, Kim, A. M., & El-Basyouny, K., "Investigating Tradeoffs between Optimal Mobile Photo Enforcement Program Plans", Journal of Multi-Criteria Decision Analysis. Accepted December 2018.*

Chapter 6 presents the MPE resource scheduling (MRS) model. This chapter contains the following sections: Section 6.1—an introduction of this chapter, Section 6.2—mathematical formulation of the MRS model developed in this chapter, Section 6.3—an introduction of the Dantzig-Wolfe decomposition and column generation approaches to solve the MRS model, Section 6.4—a model application to the MPE program in Edmonton, Section 6.5— a sensitivity analysis of model parameters, Section 6.6—summary of this chapter.

- *A version of this chapter related to a preliminary model design has been published as **Li, Y.**, Kim, A. M., & El-Basyouny, K., "Scheduling resources in a mobile photo enforcement program", in Transportation Information and Safety (ICTIS), 2017 4th International Conference on (pp. 645–652). IEEE.*

- *Another version of this chapter focusing on the scheduling problem is being prepared for a potential journal publication as* ***Li, Y.****, & Kim, A. M., "Allocating and scheduling resources for a mobile photo enforcement program". In preparation.*

Finally, Chapter 7 concludes this thesis and includes a brief discussion of future research. Sections 7.1-7.4 describes in turn the overview, findings, contributions, and limitations of the research presented in this thesis.

# 2 LITERATURE REVIEW

The MPE deployment goals were first collected from a review of the implementation guidelines of the automated speed enforcement (ASE) program running in multiple countries.

## 2.1 ASE GUIDING PRINCIPLES

Local, provincial, or national governments in the U.S., Canada, Australia, and the U.K. published a number of Automated speed enforcement (ASE) guidelines during the early 2000s. All of these guidelines have similar principles that primarily focus on outlining where to deploy enforcement cameras. They recognize that making good decisions regarding ASE deployment during program design and operation is essential to a program's effectiveness (NHTSA, 2008; Victoria Police Traffic Camera Office, 2006). Specifically, six considerations for enforcement attention are most commonly addressed in deployment guidelines; these include 1) high collision sites, 2) high speed violation sites, 3) school zones, 4) construction zones, 5) high pedestrian volume sites, and 6) sites with community speeding complaints. Local enforcement agencies should identify and prioritize these sites accordingly, in order to efficiently manage their resources and safety outcomes.

### *2.1.1 High Collision Site*

As the most prevalent transportation concern, traffic collisions are responsible for over 1.2 million fatalities and 20 million injuries every year worldwide (Mohan, 2006). Roughly 90 people are killed on U.S. roads and five on Canadian roads nearly every day; however, these figures are decreasing gradually with government intervention (NHTSA, 2015; Transport Canada, 2015). ASE programs are one intervention shown to significantly reduce the frequency and severity of collisions. Previous studies indicate that ASE reduce collisions by 8.9% to 51%, and collision-related injuries and fatalities by 12% to 50% (Coleman et al., 1996; Elvik, 1997; Berkuti & Osburn, 1998; Chen, Wilson, Meckle, & Cooper, 2000; Christie, Lyons, Dunstan, & Jones, 2003; Hess, 2004; Goldenbeld & van Schagen, 2005; OECD/ECMT, 2006). And, in Canada, ASE programs have been successfully operating in the cities of Edmonton, Calgary, and Winnipeg. Empirical data from Edmonton shows that ASE is effective in reducing collisions by 14% to 20% (R. Li, El-Basyouny, & Kim, 2015). Given that the primary objective of ASE programs is to reduce traffic

accidents, and in turn improve traffic safety, prioritizing high collision and collision risk sites in the guidelines is critical.

Although all ASE guidelines indicate the need to deploy enforcement cameras to high collision sites, the elements that identify these sites vary among jurisdictions. Guidelines in both the Province of Alberta (Canada) and the State of Victoria (Australia) identify high collision sites as an MPE deployment focus (Alberta Justice and Solicitor General, 2014; Victoria Police Traffic Camera Office, 2006), but present little detail, otherwise. In contrast, the U.S. Department of Transportation, the State of Queensland in Australia, and the County of Humberside in the U.K. all propose criteria for evaluating high collision sites in their guidelines. Four key elements – collision frequency, collision severity, exposure measure of collision risks, and data analysis period – are most commonly included in the evaluation procedures (NHTSA, 2008; Humberside Police, 2008). One criteria for identifying collision sites is the equivalent-property-damage-only (EPDO) frequency per kilometer (km) over three years (Humberside Police, 2008). The EPDO method converts all collisions into property damage only collisions by assigning weighting factors to different collision severities, including fatalities, injuries, and property damage only(AASHTO, 2010). Therefore, it can effectively combine both the collision frequency and collision severity into one factor that assigns higher weights to crashes with higher severity. In addition, the County of Humberside uses road length as an exposure measure against EPDO collision frequency (Humberside Police, 2008), to measure and compare risk to the exposed population experiencing collisions over a certain distance traveled (Jørgensen, Koornstra, Broughton, Glansdorp, & Evans, 1999). Road length data can be collected relatively easily since a large number of cities have well-maintained databases of this information.

### *2.1.2 High Speed Violation Sites*

Given the ASE program's ultimate goal is to reduce traffic accidents, speeding contributes to more than 20% of total fatalities on Canadian roads (Transport Canada, 2010, 2011), making it evident that speed is the leading cause of collisions, by increasing both the likelihood and severity of crashes (OECD/ECMT, 2006). As such, reducing vehicle speed is the mechanism through which this goal is achieved, and ASE programs are seen to deter speeding by 15% to 88% (Lamm &

Kloeckner, 1984; Coleman et al., 1996; Davis, 2001; Retting & Farmer, 2003; Cities of Beaverton and Portland, 1997).

As the allocation of ASE to high speed violation sites plays a key role in addressing traffic safety concerns, nearly all guidelines stipulate that higher priority be placed on these locations. Most guidelines' treatment of high-speed violation sites is similar to that of high collision sites; although the importance of deploying cameras to these sites is identified, as demonstrated by both the Province of Alberta and the State of Queensland, each discussing the criticality of enforcing these sites, further information is not given on how to identify and assign enforcement resources (Alberta Justice and Solicitor General, 2014; Queensland Police, 2016). The State of Victoria uses reports of speeding problems from governments, authorities, and police officers to identify high speed violation sites (Victoria Police Traffic Camera Office, 2006). However, these reports are subjective and difficult to verify or quantify, and the guidelines do not demonstrate how to go from a report to a clearly identified problem location.

In contrast, the U.S. Department of Transportation and the County of Humberside propose using data on travel speeds or the percentage of vehicles violating the speed limit to screen high speed violation sites. The U.S. guidelines highlight several data sources to be used for identifying high speed violation sites, including average speed, 85$^{th}$ percentile of speed, speed range and dispersion, percentage of speeding vehicles and number of citations (NHTSA, 2008). The County of Humberside guidelines use the 85$^{th}$ percentile of free flow speed to identify high speed violation sites (Humberside Police, 2008).

### *2.1.3 School Zones*

Children are the most vulnerable road users and require the greatest protection. About one third of child deaths worldwide are caused by traffic collisions (Peden, 2008), and children of school age (from 5 to 19 years of age) are the main victims of road collisions (Joel Warsh, Rothman, Slater, Steverango, & Howard, 2009). Furthermore, they are more likely to be struck by a vehicle when walking to school, especially within 300 meters of the school (Joel Warsh et al., 2009).

Hence, ASE initiatives for school zones have been included in many jurisdictions' ASE program guidelines. For instance, the Province of Alberta, the U.S. Department of Transportation, and the

State of Victoria all address school zones as a priority for deployment. In addition, conducting ASE in school zones acts for the public as a demonstration of law enforcement attention, which promotes overall public buy-in for a program (NHTSA, 2008). Again, however, no guidelines provide details on identifying school zones for enforcement. Because the number of collisions involving school children decreases as the distance from the school increases (Joel Warsh et al., 2009), there is a need to identify specific regions around schools where children are at significant vehicle collision risk.

### 2.1.4 Construction Zones

In addition to the high risk of school zones, workers in construction zones are exposed to the risk of both injury and fatality from passing vehicles. According to the Federal Highway Administration (FHWA), 1.6% of total road collisions in the U.S. in 2010 occurred in construction zones. More than 2,000 U.S. workers were hit in construction zones every year from 2003 to 2008 (FHWA, 2015). In these collisions, speeding is the primary risk to the safety of construction workers on the road, accounting for 31% of work zone fatalities in 2008 in the U.S. (FHWA, 2015). Therefore, speed enforcement cameras are needed to protect workers in these zones. In addition, enforcement at construction zones is an effective method of promoting ASE programs to the public (NHTSA, 2008). Despite the fact that ASE attention at construction zones is addressed in the guidelines of the U.S. Department of Transportation, the Province of Alberta, the State of Victoria, and the State of Queensland these guidelines also only mention this enforcement priority, and lack detailed instructions on how to deploy enforcement resources. The State of Victoria provides one identification instruction, calling for an assessment of construction locations, construction time periods and the traffic at construction zones to inform deployment decisions (Victoria Police Traffic Camera Office, 2006). However, the guidelines are still difficult to implement based on the rather general information provided.

### 2.1.5 High Pedestrian Volume Sites

In addition to school children and construction workers, other pedestrians also need protection from speeding vehicles. Urban areas often have high pedestrian volumes, and subsequently, a high number of pedestrian collisions. For instance, in Edmonton, districts with shopping, restaurants, and nightlife historically have experienced high numbers of pedestrian collisions (The Office of

Traffic Safety, 2013). According to the National Highway Traffic Safety Administration (NHTSA), in 2003 about 12 pedestrians died and 180 pedestrians were injured each day on roads in the U.S. (NHTSA, 2013). Moreover, in a collision, the vehicle's speed determines the pedestrian's likelihood of survival. A pedestrian has a 20% chance of surviving when hit by a vehicle traveling at 50km/h; however, the likelihood of survival increases to 90% if the vehicle speed decreases to 30km/h (Walz, Niederer, & Kaeser, 1986; Waiz, Hoefliger, & Fehlmann, 1983; OECD/ECMT, 2006). The Province of Alberta guidelines require local enforcement agencies to identify high pedestrian volume sites and prioritize enforcement efforts for those sites (Alberta Justice and Solicitor General, 2014). However, the guidelines do not provide quantitative measurements for identifying high pedestrian volume sites. In addition, pedestrian volume is expensive and almost impossible to collect citywide.

### *2.1.6 Sites with Community Speeding Complaints*

Complaints about speeding in residential areas are one of the most common citizen grievances to police (Scott & Maddox, 2001; Weisel, 2004). Although fewer crashes occur on local roads than on arterial and collector roads, assigning ASE priority to a residential area can mitigate community concerns, and is yet another way by which an ASE program's profile can be raised to gain citizen support for enforcement programs. The guidelines from the Province of Alberta, the State of Victoria, the State of Queensland, and the U.S. dictate that enforcement efforts should address community complaints. But, similarly, these guidelines only mention dedicating enforcement attention to sites with community complaints about speeding, without further describing how to evaluate these sites.

## 2.2 RESOURCE ALLOCATION APPROACHES

Randomized resource allocation is a foremost method discussed in the literature for MPE deployment. The method was conceived by Edwards and Brackett (1978) and further developed by Leggett (1988), with the single focus of high collision sites. Specifically, Leggett (1988) randomly matched a set of identified high collision sites with a set of two-hour segments in a day. Then the matched sets are assigned within the coverage area of each police division accordingly. This random scheduling approach was later extensively tested in MPE programs operated in

Australia (L. M. W. Leggett, 1997) and New Zealand (Graham, Bean, & Matthews, 1992), where an average of one-third of road casualties were reduced during each test deployment.

To further consider multiple types of deployment goals, Kim et al. (2016) introduce a priority index into the randomized resource allocation method. The priority index computes the severity level of each site by converting the gravity of high collision sites, high speed violation sites, and sites with other concerns into one factor using weights. Ranking all enforcement sites by highest to lowest index values, a monthly candidate enforcement site list is created, and sites are then randomly allocated to enforcement resources over that month. It is concluded that the added site selection method may increase enforcement coverage by 24% (Kim et al., 2016). However, the priority index values depend on the weights assigned to deployment goals, which are difficult to obtain and are therefore based on program managers' judgment and experience.

Research on how to allocate MPE resources appear to have been given to improving the perception of randomness of MPE deployment, rather than how to more efficiently and effectively utilize resources. In contrast, many studies have been conducted since the early 1970s on how to optimally allocate emergency facilities, such as fire stations, police stations, or emergency medical service (EMS) stations (Toregas et al., 1971; Church & Velle, 1974; Larson, 1974; Church et al., 2001; Curtin et al., 2005; Daskin, 1982). The purpose of emergency facilities is to successfully respond to demand over time, such that their resource allocation problem is a demand-covering problem with constraints on service time or distance (Berman, Drezner, & Krass, 2010; ReVelle & Eiselt, 2005; Huntley, 1970). One typical approach to solving this problem is the set covering location (SCL) model. It aims to identify the minimum number of emergency facilities needed and their optimal locations, by ensuring that the facilities cover all the demand for emergency services in a city within a maximal service distance (Toregas et al., 1971). However, the SCL model requires a total coverage for demand, which is difficult to achieve when resources are limited. The maximal covering location (MCL) model is then proposed to determine the optimal locations of a fixed number of emergency facilities, attempting to cover as much demand as possible with limited resources, by focusing on areas with high demands (Church & Velle, 1974).

Considering most emergency facilities are stationary (Curtin et al., 2005; Larson, 1974; Ma, 2003), Yin (2006) investigates how to optimally allocate a fixed number of mobile police patrol vehicles

to freeway segments. A min-max optimization model is proposed, which aims to minimize the maximal total patrol travel time spent handling worst-case freeway incidents. As the model is developed based on the worst-case scenario, the optimal resource allocation plan obtained is independent of time and therefore independent of demand (that changes over time). Adler et al. (2014) develops a maximal covering model, which attempts to allocate a fixed number of freeway traffic police patrol (FTPP) vehicles based on demands that change over time. The model is a multi-criteria optimization that accounts for several deployment goals simultaneously. Adopting multi-criteria optimization in allocating resources produces a set of optimal solutions (known as Pareto front, or PF) rather than a single solution. This allows decision makers' flexibility in imposing their priorities and mandates on the resource allocation. Despite the goals of FTPP programs differing from those of MPE programs (the former, focusing on timely response to calls for service and general road policy duties, while the latter on identifying speed violators and reducing speeds at various roadway locations), the general benefits are similar.

When presented with a PF in the multi-objective solution space, however, enforcement agencies can face difficulties. First, in many real-life multi-objective optimization problems, the PF can be very large or can even contain an infinite number of solutions; the greater the number of considered objectives, the larger the expected size is of the PF. It is, therefore, difficult to make a choice from a large PF. Second, although each solution on the PF informs the value given to each objective, the exchange of the objective values between solutions is not directly revealed. This creates inconvenience for MPE agencies when they compare a large number of solutions and choose the desired tradeoff.

There are two main approaches to reducing the number of solutions to represent a PF: 1) define objective preferences and establish utility functions (Branke, Deb, Dierolf, Osswald, & others, 2004; Mattson, Mullur, & Messac, 2004; Taboada, Baheranwala, Coit, & Wattanapongsakorn, 2007), and 2) cluster analysis (Morse, 1980; Rosenman & Gero, 1985; Taboada et al., 2007; Taboada & Coit, 2007; Zitzler & Thiele, 1999). The first-category approach requires multiple iterative calculation and most also require a-priori determinations and estimates of preferences between objectives. Conversely, clustering techniques (the second approach to generating a PF representation) do not require significant computational efforts and prior preference information.

Approaches to analyze tradeoffs among conflicting objectives are mainly focused on plotting results of two axes (with two objectives) in a discrete PF or a hypersurface (three or more objectives). The tradeoff between any two objective functions when moving from one solution to another along a PF is the slope of the line connecting the two solutions in the two-objective space (Miettinen, 1999). Hence, by connecting the solutions on the PF with smooth curves or surfaces, the objective tradeoff implied can be analyzed in an efficient manner in a PF with a large number of data points. For instance, Bai et al. (2011) used polynomial regression to generate pairwise tradeoff curves for five performance objectives considered in a highway asset management program. Goel et al. (2007) applied the response surface method to simultaneously analyze the tradeoffs of three goals related to a rocket injector design program. The authors constructed a polynomial model to build a (optimized) tradeoff surface for the three goals considered. However, tradeoffs were analyzed on a 2D contour map of the surface for simplicity. Note that the higher the objective dimension is, the more complex and difficult it is to interpret tradeoffs on a hypersurface. Therefore, when there are more than two objectives to consider, the easiest method is to perform a pairwise comparison of objective tradeoffs in 2D while keeping other dimensions constant (Bai et al., 2011).

## 2.3 RESOURCE SCHEDULING APPROACHES

As discussed in the preceding section, resource allocation methods aiming to increase the unpredictable appearance of enforcement activities have been thus far the primary method studied for deploying and scheduling MPE programs in the literature. By randomly matching operator shifts and enforcement locations, a better road safety outcome is expected over a fixed scheduling scheme: 30% greater reduction in collisions (L. M. W. Leggett, 1997), and 33% greater reduction of speeding vehicles (Kim et al., 2016). However, randomly matching shifts and locations makes it difficult for MPE agencies to consider program goals (other than perception of randomness) and resource utilization efficiency.

Adler et al. developed a two-stage location and schedule assignment (LSAP) model to sequentially achieve the goals of 1) expanding enforcement coverage and 2) varying enforcement schedules, with constrained resources (2014). The LSAP model is designed for freeway traffic police patrol (FTPP) programs, which conduct general traffic law enforcement and handle incidents/calls for

services on interurban roads. The review of how the LSAP model achieves the former goal in Stage 1 has been specifically discussed in Section 2.2.

In Stage 2 of the LSAP model, Adler et al. (2014) proposed utilizing the potential of distance and time halo effects of enforcement in order to produce a dynamic work schedule. Distance halo effect is the distance over which the enforcement affects driver behavior upstream and downstream of the enforcement location (Christie et al., 2003; Hess, 2004). Time halo effect is the length of time during which the enforcement effect continues, even if enforcement vehicles have left the area (Vaa, 1997). These two effects are considered in two steps. The concept of distance halo is used in the first step to find a representative subset of the Pareto optimal resource allocation solutions identified in Stage 1 of the LSAP model. A MAXMIN integer programming sub-model is used to determine the subset, which covers the highest number of locations and achieves the most balanced shift distributions between locations. The second step uses the shift distributions determined in the previous step as an input, and sequences the shifts within the planning horizon by considering the time halo effect. A binary integer programming sub-model is used to minimize instances where shifts are continuously allocated to the same location while the time halo effect remains. This second-stage model yields a highly-varied schedule, which is expected to increase enforcement unpredictability. In addition, this model provides a significant improvement over a fixed deployment plan actually implemented; it avoided three-quarters of unnecessary sequential visits during a two-shift time halo.

Following Adler et al. (2014), Li et al. (2017) established a binary integer programing model for scheduling MPE resources. The enforcement locations of Edmonton's MPE program are predetermined, and account for distance halo effects between locations. Therefore, Li et al.'s scheduling model focuses on accounting for the time halo of enforcement. The results of utilizing a two-shift time halo show that 90% of enforcement visits were non-sequential (not violating time halo effects).

However, the time halo duration assumed in the scheduling models of Adler et al. (2014) and Li et al. (2017) is up to three shifts. For example, in Adler et al. (2014), the maximum time halo is three shifts for a problem instance of 250 shifts and 19 location covering sets. Similarly, Li et al.'s model can only manage a two-shift time halo in an instance of 449 shifts and 145 site combinations.

When solving the problem instances described above, the memory of most commercial integer programming solvers will be exhausted once the specified maximum acceptable time halo is exceeded. This is because the model formulations represent schedule elements as decision variables, leading to an exponential increase in the number of possible solutions with the size of the schedule. Most commercial solvers typically use the standard branch and bound algorithm to solve integer programming (IP) problems. This algorithm is an enumeration method. It branches each decision variable of the model into two possibilities (0 and 1), and then solves a linear programming (LP) relaxation of the original IP problem under each branch in order to obtain the IP's bound (objective value of the LP relaxation problem) applied to the next branch. Thus, the number of possible solutions enumerated in the models of Adler et al. and Li et al. equal two to the power of the number of schedule elements, which must exceed the available memory on a workstation when the number of elements is large.

Most resource scheduling problems, when formulated as integer programs, define decision variables using the column or row of a schedule. When the branch and bound is applied, branching on this type of variable is more efficient than branching on a single scheduled element, and tighter bounds can be obtained (Ernst, Jiang, Krishnamoorthy, & Sier, 2004). This formulation strategy can be found in many scheduling problems in transportation, such as air crew pairing (Desaulniers et al., 1997) and rostering (Gamache et al., 1999), urban transit crew scheduling (Desrochers & Soumis, 1989), and vehicle routing scheduling (Desrosiers et al., 1984). Specifically, a column or row is often defined as a path connecting arcs and nodes in vehicle routing problems, or an itinerary connecting flights in airline crew scheduling problems.

Airline crew scheduling and rostering is the largest application of staff scheduling problems across all industries (Ernst et al., 2004). The hardest part of solving these problems is that they are very large-scale, complex integer programming problems (Desaulniers et al., 2002). A combined approach has primarily been used to solve these problems: this approach starts by decomposing a scheduling table using the Dantzig-Wolfe algorithm, and then solves the decomposition using a column generation algorithm (Desaulniers et al., 2002; Ernst et al., 2004).

The Dantzig-Wolfe algorithm, named after Dantzig and Wolfe (1960), reformulates a schedule by treating one column of the schedule as a variable, instead of an element in the schedule. The

problem after reformulation is a set covering/partitioning integer programming problem, which is a common representation of most resource scheduling problems (Ernst et al., 2004). In transportation resource scheduling problems, a column of the schedule is defined as a feasible schedule for resources to perform a certain task. When branching occurs on these columns (i.e., set covering problem variables), the bounds derived by a branch-and-bound method are tight on the problem objective.

The number of feasible resource schedules (columns) can be exponential to the problem size. Therefore, the number of variables of the set covering problem that is reformulated by the Dantzig-Wolfe algorithm is enormous. To handle this issue, the column generation approach (Ford Jr & Fulkerson, 1958) is usually used in combination with the Dantzig-Wolfe algorithm. Similar to the simplex method, column generation only identifies new columns that can be entered into the problem's variable basis, rather than enumerating all columns.

## 2.4 SUMMARY

We find that ASE guidelines typically focus on six key priorities for their programs. They direct enforcement resources to roadways exhibiting high numbers of collisions and speed violations, in school zones, construction zones, and high-pedestrian areas, and those with community speeding complaints. However, most guidelines provide only qualitative guidance for identifying critical locations. This leads to difficulties when collecting data to measure and compare sites for enforcement attention. Also, when local enforcement agencies make decisions on deploying cameras, precise instructions on how enforcement resources should be allocated to different sites is unclear. To help agencies identify specific deployment priorities and improve deployment decisions, we translate these qualitative descriptions to precise quantitative measures in Chapter 4.

There has been limited research to improve resource allocation and scheduling in MPE programs. This thesis aims to address this gap, and therefore, assist agencies to directly impose program priorities to MPE resource deployment decisions. Despite that the MPE resource allocation and scheduling problem differs somewhat from the freeway traffic police patrol (FTPP) problem, the concepts used to solve FTPP problems (two-stage decomposition and optimization) can be applied to the MPE problem. We decompose MPE resource allocation and scheduling problem into two

optimization sub-problems (see Chapters 5 and 6, respectively). A maximum covering location model combined with multi-objective optimization is used to find the best MPE resource allocation when there are multiple and competing priorities. Then, we use the time halo of enforcement to determine MPE enforcement schedules. The use of time halo has demonstrated to not only produce diverse enforcement schedules, but also make efficient use of resources.

We will also address the following issues when solving the above two optimization sub-problems. Due to many Pareto-optimal allocation solutions obtained from multi-objective optimization, we conduct post-Pareto analyses to further help agencies better understand and apply the solutions. We used a clustering process to identify representative solutions, given that clustering can be easily implemented without user-specified preferences. The response surface method is used to fit an optimal tradeoff surface that (typically) involves more than two enforcement objectives. Finally, resource scheduling problems are typically large and difficult to solve with conventional integer programming. Given the success of Dantzig-Wolfe and column generation methods in solving large resource scheduling problems, we also use these two methods to solve our scheduling problem.

# 3 DATA DESCRIPTION

Citywide geocoded data was gathered from the Traffic Safety Section at the City of Edmonton (COE), who manages the MPE program in Edmonton, Alberta, Canada. We obtained data on traffic collisions, travel speed surveys, schools, construction projects, neighborhoods, and road networks. We also obtained operational data from the Edmonton MPE program, including deployment sites and when sites were enforced (i.e. operator visit data). The data is used for two case studies described in the following two sections.

## 3.1 EVALUATING ASE GUIDELINES

Five years of citywide geocoded data, from January 2010 to December 2014, were used to identify six types of high-priority sites on Edmonton roads. In Edmonton, the total number of speed-related midblock collisions over the five-year study period is 29,573, consisting of 40 fatal collisions, 2,881 injury collisions, and 26,652 property-damage-only collisions. Because a much higher number of collisions occur on arterial roads and collector roads than on local roads, and collisions are the primary motivation for enforcement, this thesis focuses on identifying arterial and collector roads exhibiting need for enforcement attention according to the priorities discussed. Local roads are considered only in regard to community complaints on residential roads.

The arterial and collector road network in Edmonton is segmented into 2,691 sites, with each site representing a segment for enforcement. Specifically, an arterial site refers to an arterial road segment between two adjacent signalized intersections. Whereas, a collector site is determined to be a collector road segment that intersects any arterial or collector roads.

Speed surveys conducted in Edmonton within five years (2010-14) only occur at 720 of the 2,691 segmented sites, so we identify high speed violation sites from these 720 sites. The data used to identify other deployment priorities at the 2,691 sites also included a total of 3,996 construction projects executed during the five-year study period, and 296 schools (including elementary, middle, and high schools).

When considering local sites with community complaints, the potential local sites are aggregated on the neighborhood level. As a result, 388 neighborhoods were identified after aggregation. Grouping the data from local sites by neighborhood allows this thesis to investigate the implications of enforcement on each community.

To compare the deployment priorities found based on the above data with the actual program deployment, the operational data of the Edmonton MPE program from 2010 to 2014 was also collected. During the five-year study period, Edmonton's MPE program operators visited a total of 1,317 sites, including 1,087 arterial and collector sites and 230 local sites. At the time of this study, the MPE program employed 20 operators, who were deployed in 10-hour shifts that occur twice daily, from 6 am to 4 pm, and 4 pm to 2 am. A shift consists of one operator in one vehicle. The average deployment time spent at each arterial and collector site was 166 hours in five years, whereas this time dropped to 11 hours at each local site.

## 3.2 Designing a Deployment Plan

To study the results of our proposed two-stage MPE resource allocation and scheduling model, we applied the model to a case. The case assumes a deployment plan for the Edmonton MPE program operated in September 2014. September was chosen because it is known that the Edmonton MPE program aims to dedicate greater enforcement efforts to school zones at this time of year.

Three years of geocoded data (2012-2014) consisting of 18,198 speed-related midblock collisions, 893 speed survey reports, and 296 schools' information from the COE were used to calculate the model metrics representing the three most important enforcement needs (reducing collisions and speed violations, and increasing the safety of school children). A three-year span was chosen since a constantly updated data is needed to support the rotating monthly plan. Three years are usually the minimum time period for the study of collision data; it is able to provide sufficient sample size that ensures statistical correctness (Abdulhafedh, 2017).

The first stage model allocates resources to city neighborhoods. The collision reports, speed surveys, and school information collected from 2012 to 2014 were assigned to their corresponding neighborhoods in GIS, to calculate the three neighborhood-level metrics. To handle the issue of some geocoded data being positioned along the boundaries of neighborhoods (composed mainly

of arterial roads), all geocoded neighborhood data was shifted 50 meters south and 50 meters east. A 50-meter shift is considered a small movement, such that the collision, speed, and school data originally within a neighborhood is highly unlikely to not remain in the same neighborhood as before; however, boundary data is "moved" northwest into a neighborhood. With this shift, only 0.1% of all collision data are without a neighborhood. Given that such a small amount of the collision data is "homeless" (i.e., not belonging to any neighborhood), it is ignored in the analysis.

The total number of enforcement shifts made in September 2014 was used to fix the total number of shifts available for the model over one month. In September 2014, a total of 458 shifts were deployed to 231 enforcement sites located in 135 neighborhoods across the city. An operator will visit anywhere from one to four sites during one shift, with an average of 6.7 hours spent on the enforcement task itself per 10-hour shift.

Also, the actual monthly shifts made during 2013-2014 in each Edmonton neighborhood were used to determine the restrictions on the number of shifts to be allocated during one month. According to the Edmonton MPE deployment data from 2013-2014, neighborhoods were classified as receiving 1) high attention, 2) medium attention, and 3) no attention. The first group consisted of about 30 neighborhoods that were visited each month over the two years of 2013 and 2014, and assigned a minimum of 240 shifts each month (which is about half the total shifts available per month). This group of neighborhoods had a minimum of eight shifts, and maximum of 49, allocated per month. The medium attention group consisted of 186 neighborhoods that were visited more occasionally, with a minimum of zero and maximum of seven shifts per month. The remaining 172 neighborhoods were not visited at all over the two years. To correspond more closely to the actual resources available to Edmonton's MPE program, we set the constraints for our application using the above information. However, this may change depending on the particular requirements, needs, and governing regulations of the MPE program.

The second stage model scheduled daily site visits within neighborhoods based on the neighborhood-level resource allocations determined by the Stage 1 model. A neighborhood-level deployment result is analyzed, which allocates one-month shifts to 44 neighborhoods containing 130 enforcement sites. Three years (2012-2014) of data on collision statistics, speed surveys, and school location information, which were used to construct the neighborhood-level metrics in Stage

1, are also used to compute site-level metrics consistent with the (three) deployment criteria. Two years (2013-2014) of operational data were gathered and utilized from the COE's MPE program to identify the bounds on the number of visits in each daily shift of the study month.

A study was conducted in 2015 in Edmonton to measure the time halo effects of MPE on arterial and collector roads (Gouda & El-Basyouny, 2016). Nine locations were monitored within a five-week period, during which the time halo effects of enforcement were observed to reach an average of five days after every 20 hours of enforcement. The level of enforcement intensity affected the duration of the time halo; however, a relationship between the enforcement intensity and time halo was not determined. Therefore, we will consider the enforcement time halo duration to be fixed at five days, regardless of the intensity of the applied enforcement. Future work may include developing a modified cost function that accounts for the effect of enforcement intensity on time halo durations.

# 4 QUANTIFICATION OF MPE DEPLOYMENT GOALS

Automated speed enforcement (ASE) guidelines are designed to guide enforcement agencies in operating ASE programs that are effective in improving traffic safety. A better understanding of the governing ASE guidelines and how to implement them can help enforcement agencies to improve decision-making and resource allocation, thereby increasing program effectiveness and efficiency.

## 4.1 INTRODUCTION

In many jurisdictions, the design and operation of automated speed enforcement (ASE) programs are governed by official guidelines. Automated speed camera systems are used to assist police in enforcing speed limits. Specifically, the speed camera is mounted on the roadside or in an enforcement patrol vehicle to detect vehicle speeds, and photograph vehicles violating speed limits. Mobile photo enforcement (MPE) is a subset of ASE technology, with a speed camera mounted on the car. Therefore, the operation of MPE should adhere to ASE program guidelines.

The guidelines outline basic principles for how ASE programs should operate, providing a tool to assist local enforcement agencies in developing a successful ASE program with positive safety outcomes. In particular, ASE guidelines emphasize controlling the deployment of enforcement cameras, to ensure deployment at the right locations, thus increasing the program's effectiveness in improving safety.

However, when implementing guidelines, most descriptions of deployment goals are too qualitative to interpret, impacting the successful identification of specific deployment considerations. Guidelines provide general descriptions of where ASE should be deployed to achieve objectives of reducing speed and collisions, but they do not specifically define how site identification and ASE deployment should be conducted. Local enforcement agencies must rely only on their own interpretations during the design and implementation phase. Consequently, the potential benefits of using the guidelines are not entirely realized.

Research tackling the limitations of existing ASE guidelines is limited. Therefore, this chapter proposes quantitative measures based on the main guiding principles of ASE to facilitate interpretation of the guidelines and deployment decisions that well reflect these principles. A case study is presented to explore the relationship between ASE principles and the interpretation and application of guidelines by a local enforcement agency. The results are visualized using Geographic Information System (GIS) plots, through which this thesis provides insight into the geographic distribution of enforcement throughout the city, in terms of where enforcement should take place and where it is actually conducted. Two MPE program indicators – spatial coverage and intensity – are used to investigate the interpretation and application of the provincial ASE guidelines. Given that MPE activities have distance halo effects, which are safety effects that extend upstream and downstream of the camera site (Vaa, 1997), this thesis also considers these. Coverage of the MPE program is also considered using a measure of the distance halo effect. The results of this chapter can help enforcement agencies gain greater clarity on how to improve program performance with the help of ASE guidelines, in order to achieve increased efficiency and effectiveness.

## 4.2 Quantitative Interpretation of ASE Guidelines and GIS Visualization

In this section, quantitative measures are proposed and used to identify each of the six deployment priorities described in Section 2.1, for the road network of Edmonton. Then, each criterion is visualized on a GIS map of the city. The COE has a mobile photo enforcement (MPE) program that involves dispatching mounted photo radar cameras in unmarked/marked patrol vehicles to sites to photograph the license plates of those that violate speed limits by a predetermined threshold. The operation of MPE in Edmonton must adhere to the ASE guidelines released by the Province of Alberta, which dictate the deployment goals for the six deployment priorities. To illustrate the interpretation and application of the Alberta ASE guidelines by the COE enforcement agency, the deployment information of the MPE program, including spatial coverage and intensity, is visually presented for each deployment priority.

### 4.2.1 High Collision Sites

Although the Alberta guidelines for ASE address enforcement goals for high collision sites, they provide limited instructions on how to identify these sites. Based on the review of ASE guidelines in identifying high collision sites in other jurisdictions, this thesis attempts to do so by assessing four characteristics: collision frequency, severity, exposure measure of collision risks, and the data analysis period. In particular, this thesis employs the EPDO frequency of collisions to account for both frequency and severity, using COE data on collisions resulting in fatality, injury, and property damage over 2000 Canadian Dollars. Moreover, the length of the road segment is used to evaluate the exposure to the risk of collisions, given that this information is available in the COE database. The final measure for evaluating high collision sites is EPDO per kilometer (km) traveled on a road segment over five years.

All the studied collisions (29,573 collisions in total as described in Section 3.1) are converted into corresponding EPDO frequencies, based on a report released by the Capital Region of Alberta in 2010 (de Leur, Thue, & Ladd, 2010). The report specifies that the direct cost of one fatal collision is equivalent to that of 16.6 PDO collisions and the direct cost of one injury collision is equivalent to that of 3.6 PDO collisions (de Leur et al., 2010). Collision severity classification and cost estimates for these different severity levels vary across jurisdictions. Enforcement agencies may amend the computation of EPDO frequencies based on their own classification and cost estimation. However, it is noted that some jurisdictions have very high cost estimations for fatal collisions. For instance, the American Association of State Highway and Transportation Officials (AASHTO) proposed the social cost of one fatal collision to be more than four million US dollars (AASHTO, 2010). Consequently, this high value gives fatal collisions a significant relative weighting when computing EPDO frequencies – in fact, more than 30 times the weight assigned to fatal collisions in Edmonton. This tends to become an issue in that fatal collisions dominate the identification of high collision sites, whereas sites experiencing frequent injury collisions that are also dangerous locations get far less attention. An alternative is to adopt a collision cost measure that combines fatal and injury collisions. According to AASHTO, a social collision cost that includes fatal, incapacitating injury, and moderate injury collisions is estimated to be 158,200 US dollars, which is significantly smaller than the four million USD assigned to fatal collisions alone (AASHTO, 2010).

Figure 4-1 identifies the ranking of high collision sites within the top 10% of EPDO collisions per kilometer ($EPK$) over the five-year study period, and shows them marked in red. The average $EPK$ of all road segments is 13.8, but surges to 53.1 in this figure due to the narrowing of the scope to high collision sites only. The density map of high collision sites highlights areas in greatest need of enforcement. As shown in Figure 4-1, high collision sites are clustered in the central neighborhoods of Edmonton, on two major freeways (Yellowhead Trail and Whitemud Drive), as well as some northern, western, and southeastern neighborhoods.

When the geographic allocation of MPE is plotted for the five-year study period, it is observed that 1,087 MPE sites are widely dispersed throughout Edmonton's major urban road network. The MPE sites are represented as circles in Figure 4-1, and the intensity of MPE at each site is represented by the size of the circles. The larger the circle, the longer the enforcement time spent at that site during the five-year period. As seen from Figure 4-1, 85 MPE sites (marked in green) cover high collision sites, and the other 1,002 MPE sites (marked in black) do not precisely overlap with high collision sites.

**MPE Program Coverage on High Collision Sites**

| | High Collision | Others | Total |
|---|---|---|---|
| Number of Sites | 269 | 2,422 | 2,691 |
| Number of Sites Covered by MPE | 47 | 529 | 576 |
| 5-year Average Deployment Hours Per Site | 305.1 | 314.3 | 313.5 |

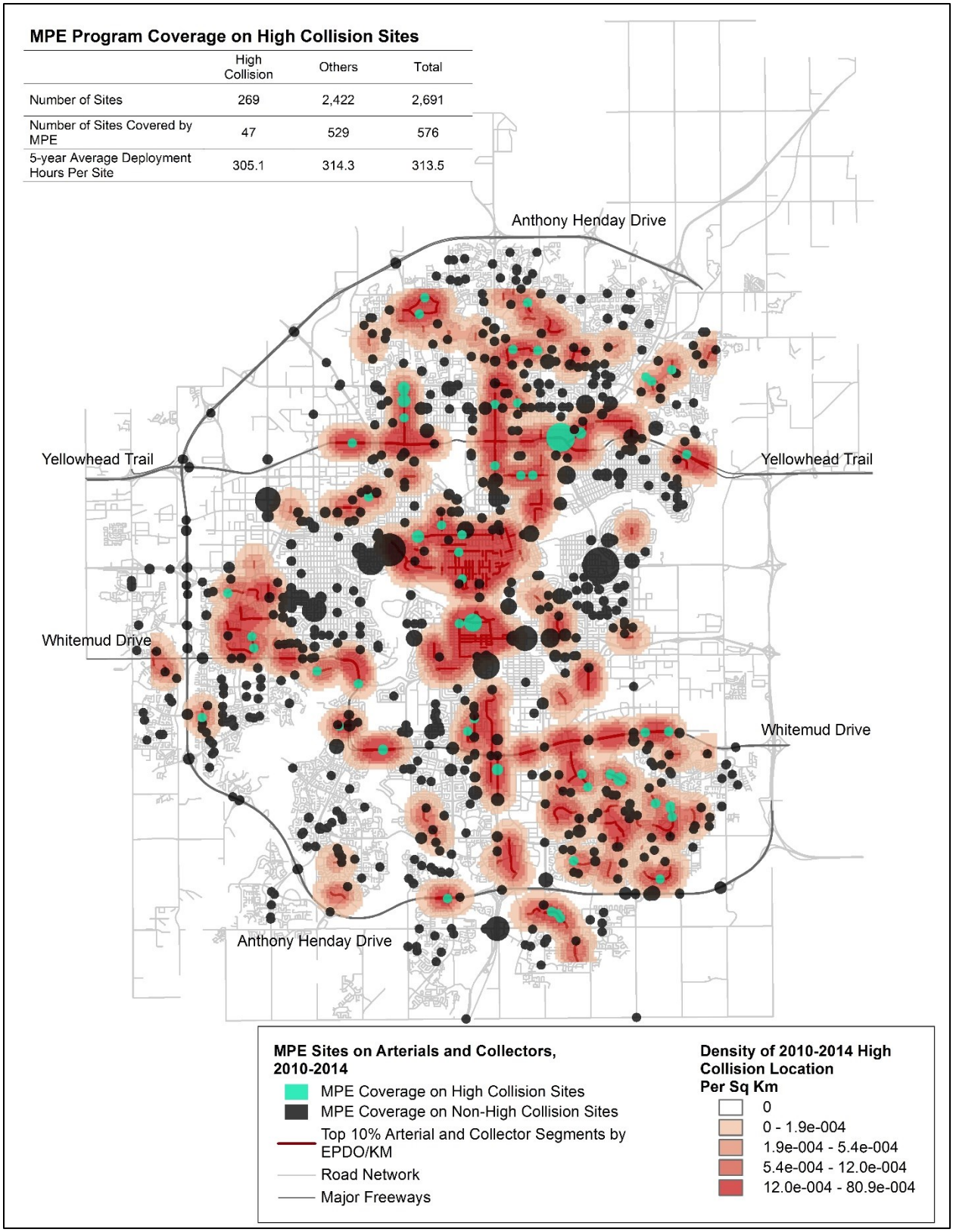


**Figure 4-1 2010-2014 MPE program coverage on high collision sites.**

According to Figure 4-1, 47 of 269 high collision sites were covered by the MPE program, which indicates about 17.5% citywide spatial coverage. The five-year MPE program invested about 305 hours at each high collision site, which indicates that each site was enforced for more than five hours every month. This indicates that the COE enforcement agency took into account high collision sites when making deployment decisions. However, it was observed that the MPE program spent an average of 314.3 hours at sites not identified as high collision sites over the five-year period – about nine hours more than the average time spent at high collision sites. This demonstrates that there were other considerations (such as the other five priorities discussed) for MPE deployment in Edmonton that resulted in greater enforcement intensity at these sites.

### *4.2.2 High Speed Violation Sites*

According to the Alberta guidelines, enforcement should be conducted at locations with high speed violation rates. This thesis identifies high speed violation sites by the percentage of vehicles that exceed the speed limit. More specifically, the top 10% of sites with the highest average percentage of vehicles violating speed limits during the five-year study period is employed as the threshold for screening high speed violation sites.

As shown in Figure 4-2, 72 high speed violation sites have been identified and marked in red. As with high collision sites, a density map is also used to illustrate how the high speed violation sites are clustered throughout the city. Figure 4-2 shows that the sites in question are located mainly on the city's ring road (Anthony Henday Drive), as well as the central, northeastern, and southern portions of the city. According to the five-year speed surveys, approximately 45.6% of surveyed vehicles on the total 720 sites exceeded the speed limit. This high value could be due to a selection bias – speed detectors tend to be placed on roadways that are known to have a high number of speed violations. The average percentage of speeding vehicles surges to 81.9% on the 72 identified high speed violation sites, which is almost double that of all 720 sites.

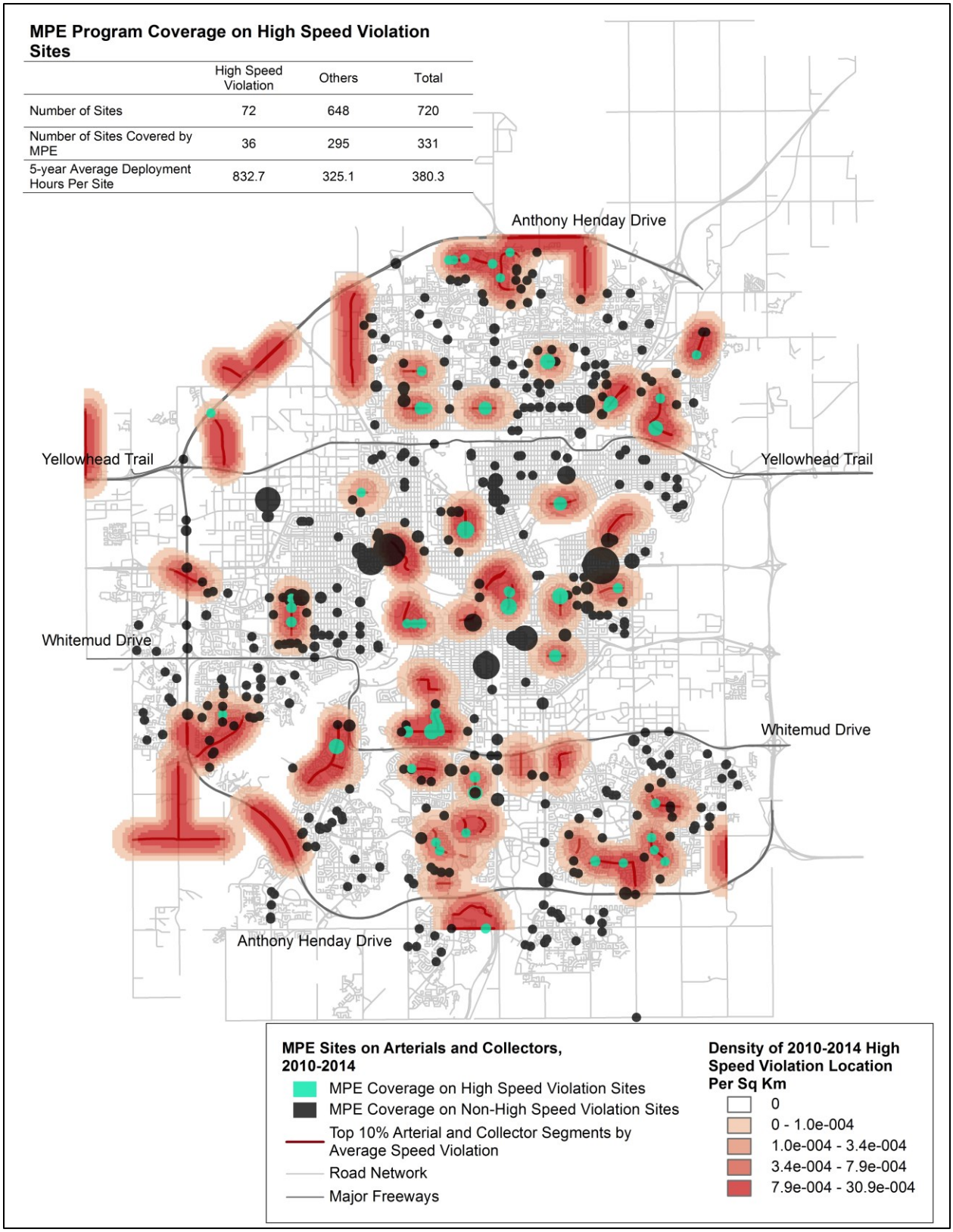


**Figure 4-2 2010-2014 MPE program coverage on high speed violation sites.**

After overlapping the MPE deployment information with the high speed violation sites, only 720 of 1,087 MPE sites are selected for investigation because the other MPE sites do not have speed survey data. Figure 4-2 shows that about half of the high speed violation sites are covered by 97 of the 720 selected MPE sites during the five-year study period. The average deployment time at each high speed violation site is 832.7 hours, which is more than 2.5 times that of other sites. Furthermore, the average number of deployment hours spent on such sites is 2.7 times higher than that spent on high collision sites.

Despite the limited scope of the data, it can be seen that the resources of the five-year MPE program, in terms of the spatial and time coverage, were more invested in locations with speeding problems than those with collision problems. The green circles of Figure 4-2 show how the amount of time spent on high speed violation sites is evenly spread geographically. However, the green circles of Figure 4-1 indicate that MPE deployment is concentrated along specific corridors and areas with high collision rates – along Yellowhead Trail and central areas.

### 4.2.3 School Zones

The locations of primary schools, middle schools, and high schools, and the size of each school zone in Edmonton are the basis for assessing their enforcement priority. Given that data on the individual size of each school zone was not available for this case study, we demarcate a circular area around each school as an enforcement measure. The risk of collisions involving school children is significantly higher within 150 m of the school building, but then decreases substantially beyond distances of 300 m (Joel Warsh et al., 2009). We choose a 250 m school zone radius for enforcement, which accounts for the school property size as well as the traffic areas beyond school boundaries with different road designs and speed limits (Alberta Ministry of Transportation, 2007). Figure 4-3 presents the spatial distribution of 296 schools in Edmonton, which includes primary schools, middle schools, and high schools. As seen from Figure 4-3, school zones received much enforcement attention during the five-years assessed, with 84% of school zones covered by MPE. Of the 1,087 MPE sites, 508 overlap with school zones. The average number of deployment hours spent on school zones is about 300 h per zone over the five-year study period, which is of similar average intensity to that of high collision sites. This result indicates that deployment at school zones has been a focus of the COE MPE program.

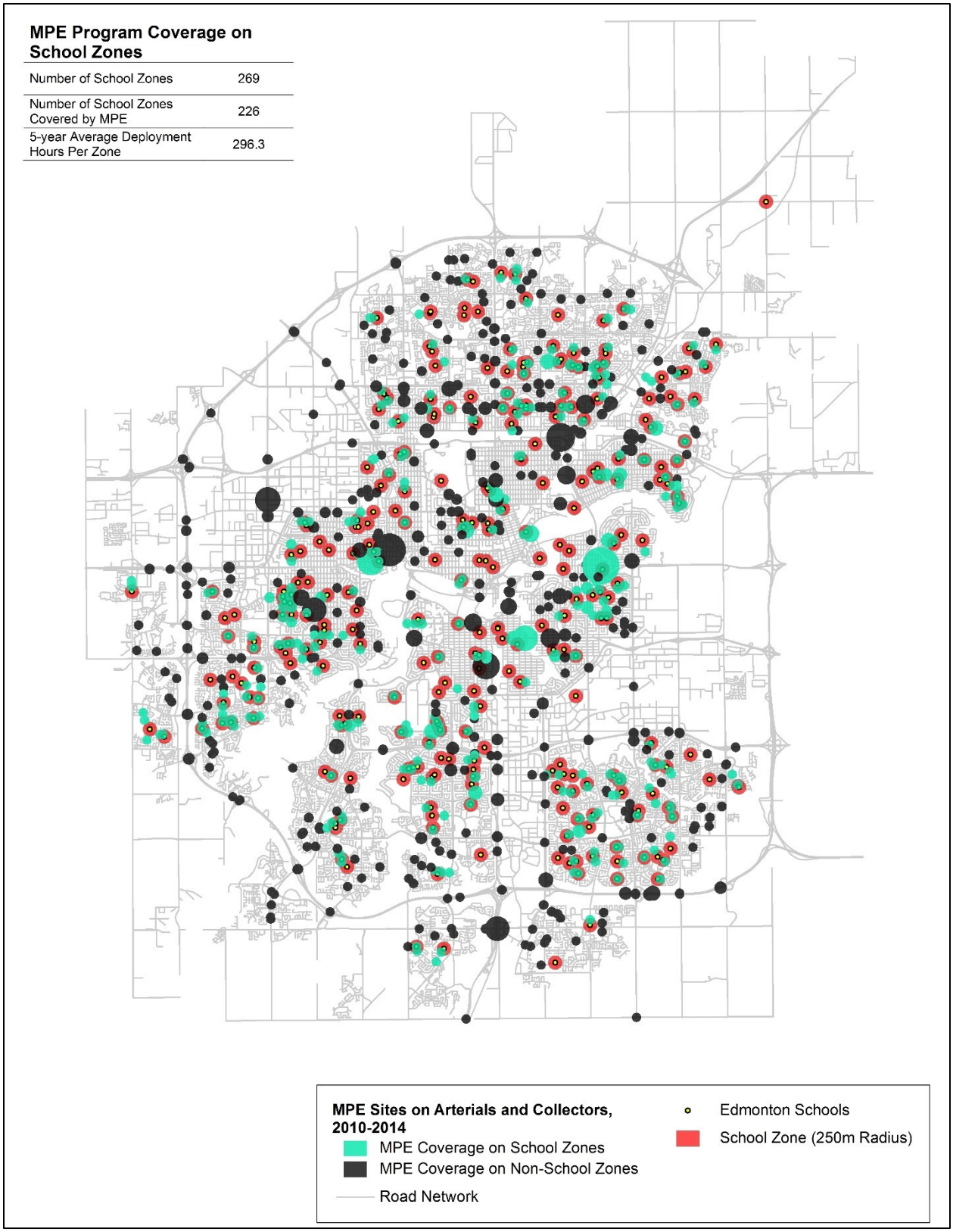


**Figure 4-3 2010-2014 MPE program coverage on school zones.**

### 4.2.4 Construction Zones

The lengths of these construction projects ranged from a few hours to several years. Therefore, deployment priorities should be based on the length of construction projects, as longer projects are expected to experience more collisions. As a result, this thesis has categorized construction projects into long-term projects (duration of one year or longer) and short-term projects (less than a year), and overlapped MPE information with that of construction zones to see what zones were enforced during the five-year study period.

Figure 4-4 illustrates 2,267 short-term projects, highlighted in yellow, and 1,729 long-term projects, marked in brown. Of these, 121 short-term projects and 70 long-term projects were covered by the five-year MPE program. The percentage of construction projects covered is only about 5%. Accordingly, 138 MPE sites and 69 MPE sites precisely cover short-term projects and long-term projects, respectively. When calculating the MPE coverage, apart from spatial coverage, only the MPE conducted within the time period construction projects were ongoing were considered as coverage.

**MPE Program Coverage at Construction Zones**

| | Construction | | Total |
|---|---|---|---|
| | Short Term | Long Term | |
| Number of Construction Zones | 2,267 | 1,729 | 3,996 |
| Number of Construction Zones Covered by MPE | 121 | 70 | 191 |
| 5-year Average Deployment Hours Per Zone | 446.8 | 365.7 | 368.7 |

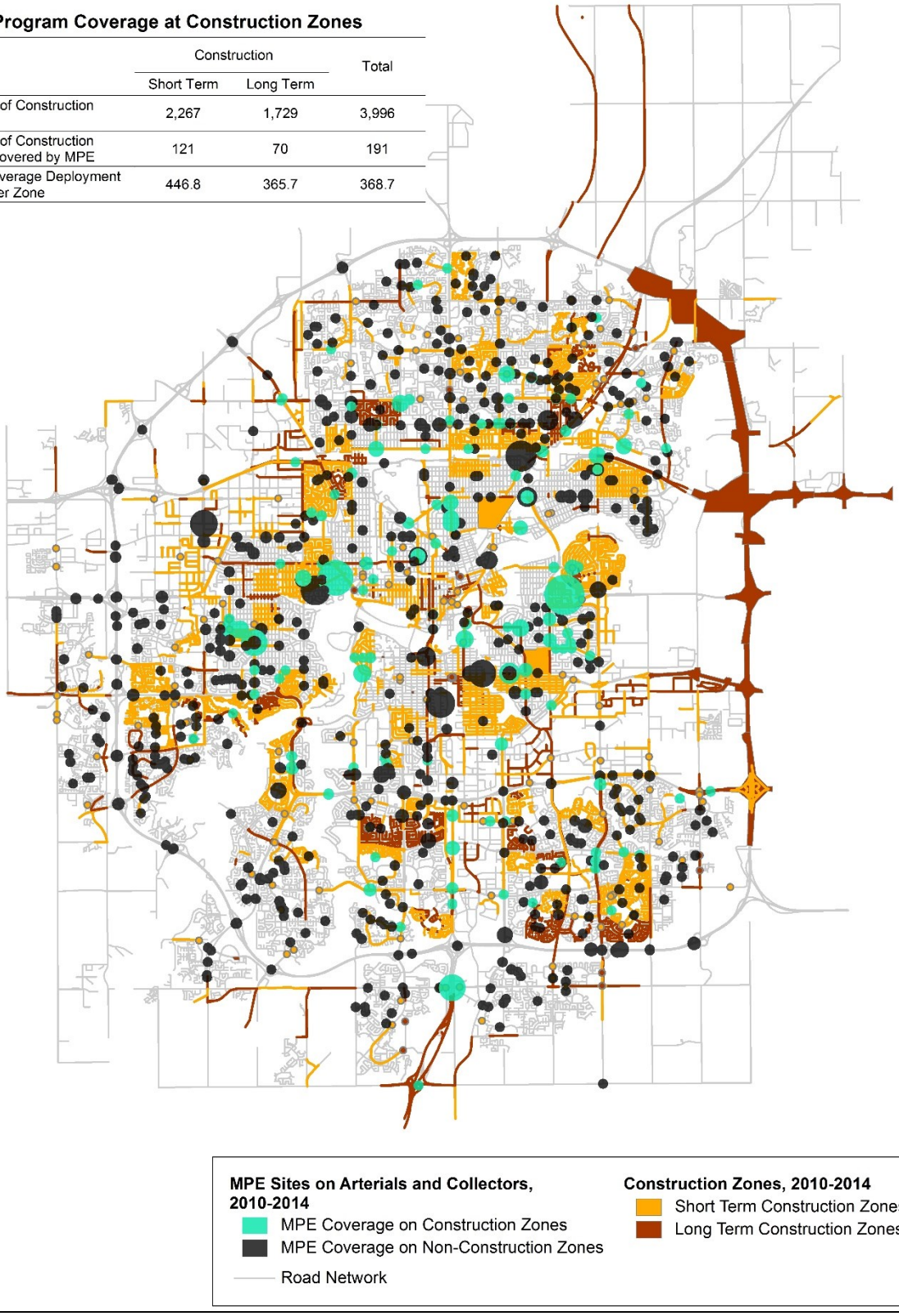


**Figure 4-4 2010-2014 MPE program coverage on construction zones.**

Although spatial MPE coverage on construction zones is relatively low, the coverage time intensity is high in that the average deployment hours per zone is 368.7 hours for the five-year period. The duration of the enforcement at short-term construction zones is somewhat higher than for long-term construction zones, 446.8 and 365.7 hours, respectively. It is noted that the MPE program did not distinguish between projects of different lengths for the amount of enforcement allocated. However, Figure 4-4 shows that short-term construction projects were mainly distributed within inner city areas, whereas long-term projects were primarily located along the city boundary or on highways. Long-term construction projects may have had lower enforcement intensity because traffic was diverted from these facilities during the project. However, owing to the fact that further information on construction zones was not available for this analysis, further investigation is needed to reach a concise conclusion.

### 4.2.5 High Pedestrian Volume Sites

Shopping districts, transit stations, colleges, universities, and other such places often have a large number of pedestrians. However, enforcement sites in and around these areas cannot be identified if pedestrian volumes are not available, which is typically the case as pedestrian volumes in these areas are not typically collected as part of on-going regular traffic data collection programs. Speed-related collision data involving pedestrians can be used as an alternative to evaluate MPE deployment priority, as the motivation of enforcement at high pedestrian volume sites is to protect the safety of pedestrians.

Similar to high collision site identification, the most commonly used methods to identify high pedestrian collision sites compute collision indices for sites, then rank all sites in descending order. Four types of collision indices are most commonly used: pedestrian collision frequency, collision density, collision rate per volume, or a combination of these three indicators (Pulugurtha, Krishnakumar, & Nambisan, 2007; Vasudevan, Pulugurtha, & Nambisan, 2007). Given data availability in Edmonton, this thesis computed a pedestrian collision index accounting for collision frequency, density, and severity. The pedestrian collision index is the product of the number of pedestrian collisions per kilometer (km) on a road segment over five years, and the pedestrian EPDO per kilometer (km) on that segment over five years, divided by 100 (Pulugurtha et al., 2007; Vasudevan et al., 2007). The direct costs used to compute EPDO frequencies are the same as those

used to identify high collision sites – one fatal collision is equivalent to that of 16.6 PDO (property damage only) collisions, and one injury collision is equivalent to that of 3.6 PDO collisions (de Leur et al., 2010).

As a result, roadway segments in Edmonton experiencing pedestrian-involved speed-related collisions are assessed. A high pedestrian collision site is identified as having a pedestrian crash index above or equal to the median value for all sites assessed, and the results are shown in Figure 4-5.

**MPE Program Coverage on High Pedestrian Collision Sites**

| | High Pedestrian Collision | Others | Total |
|---|---|---|---|
| Number of Sites | 151 | 2,540 | 2,691 |
| Number of Sites Covered by MPE | 20 | 556 | 576 |
| 5-year Average Deployment Hours Per Site | 330.4 | 312.9 | 313.5 |

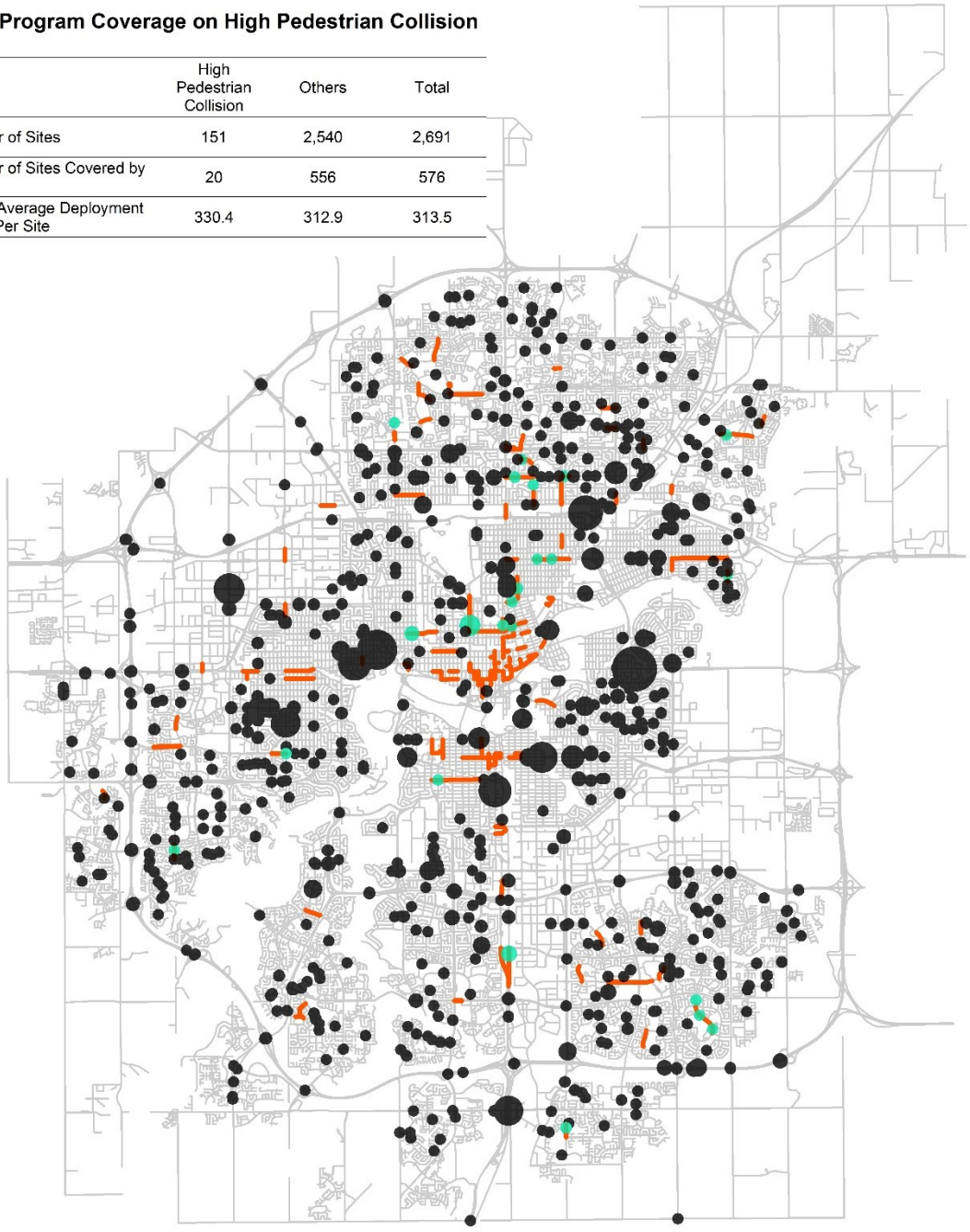

**MPE Sites on Arterials and Collectors, 2010-2014**

- MPE Coverage on High Pedestrian Collision Sites
- MPE Coverage on Non-High Pedestrian Collision Sites
- Road segment with pedestrian collision index greater than or equal to the median in 2010-2014
- Road Network

**Figure 4-5 2010-2014 MPE program coverage on high pedestrian collision sites.**

A total of 151 MPE sites were found to be located at high pedestrian collision sites. A significant proportion of the high pedestrian collision sites are clustered in central areas of Edmonton (including downtown, Whyte Avenue shopping and entertainment district, and University of Alberta), with others scattered at various locations around the city. Of the 1,087 MPE sites, 39 cover 20 high pedestrian collision sites. This resulted in about 13% MPE coverage of high pedestrian collision sites, about 25% lower than the spatial coverage of high collision sites. This lower coverage of pedestrian sites is likely due to the greater difficulty of operating MPE in central areas of Edmonton, in turn because of the limited number of places at which enforcement vehicles can locate. However, the average deployment intensity at high pedestrian collision sites is 330.4 hours per site during the five-year analysis period, which is 25 hours higher than that of high collision sites. Because there is a high likelihood of severe injury when pedestrians are struck by a speeding vehicle (OECD/ECMT, 2006), these high pedestrian collision sites merit ongoing attention by the COE enforcement agency.

### 4.2.6 Sites with Community Speeding Complaints

The frequency of collisions, severity level of collisions, and percentage of speeding vehicles on local roads in residential areas are much lower than for arterial and collector roads. Specifically, the five-year average EPDO frequency of local sites is 5.5 $EPK$, which is only about 40% of the average EPDO frequency for arterial and collector sites. In addition, the percentage of vehicles violating the speed limit is 21.1% at local sites, which is less than half of the average figure for arterial and collector sites. For optimal resource allocation, more enforcement efforts should be exerted to other critical sites experiencing a higher risk of collisions. However, given that enforcement at local sites can mitigate community concerns and improve the enforcement program's profile, this type of site could still be a consideration when evaluating deployment decisions, with a low number of visits and enforcement times being appropriate.

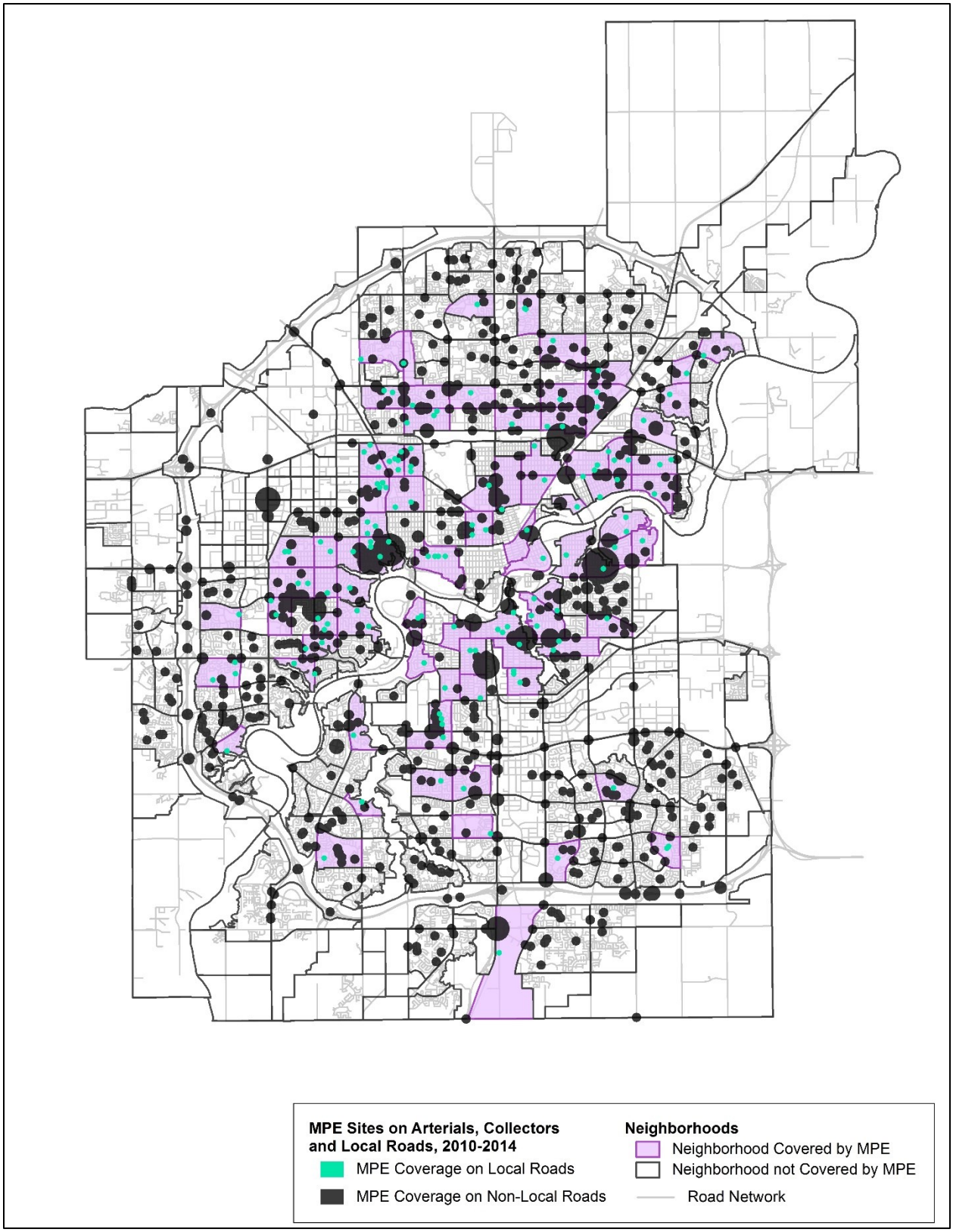


**Figure 4-6 2010-2014 MPE program coverage on local roads in neighborhoods.**

Since speeding complaint records were not available for this case study, this thesis only reviewed the MPE program resources devoted to these neighborhood sites. As shown in Figure 4-6, Edmonton is divided into 388 clearly defined neighborhoods. Apart from 1,087 MPE sites enforced on arterial and collector sites, MPE was deployed to another 230 local sites (marked in green), which were in neighborhoods adjacent to central areas of the city. This number indicates that enforcement in residential areas was a priority of the COE enforcement agency. The 230 local MPE sites cover 83 neighborhoods (colored in purple). The average deployment time spent on each neighborhood is 31.3 hours over the five-year period, which is more than 10 times less the intensity spent on other deployment priorities. This thesis presents only an idea of how to review this type of site. Further work on measuring the risk of neighborhoods using data on community complaints can be carried out, so that deployment decisions for these sites can be made based on a more thorough evaluation.

### *4.2.7 MPE Program Coverage Overview*

Based on the analysis of MPE program coverage for the six deployment priorities, Figure 4-7 illustrates an overview of MPE program deployment from 2010 to 2014. A total of 1,317 MPE sites are divided into three groups: 732 sites covering one priority only, 190 sites covering two or more priorities simultaneously, and 395 sites with none of the high-priority deployment considerations identified by the Alberta ASE guidelines.

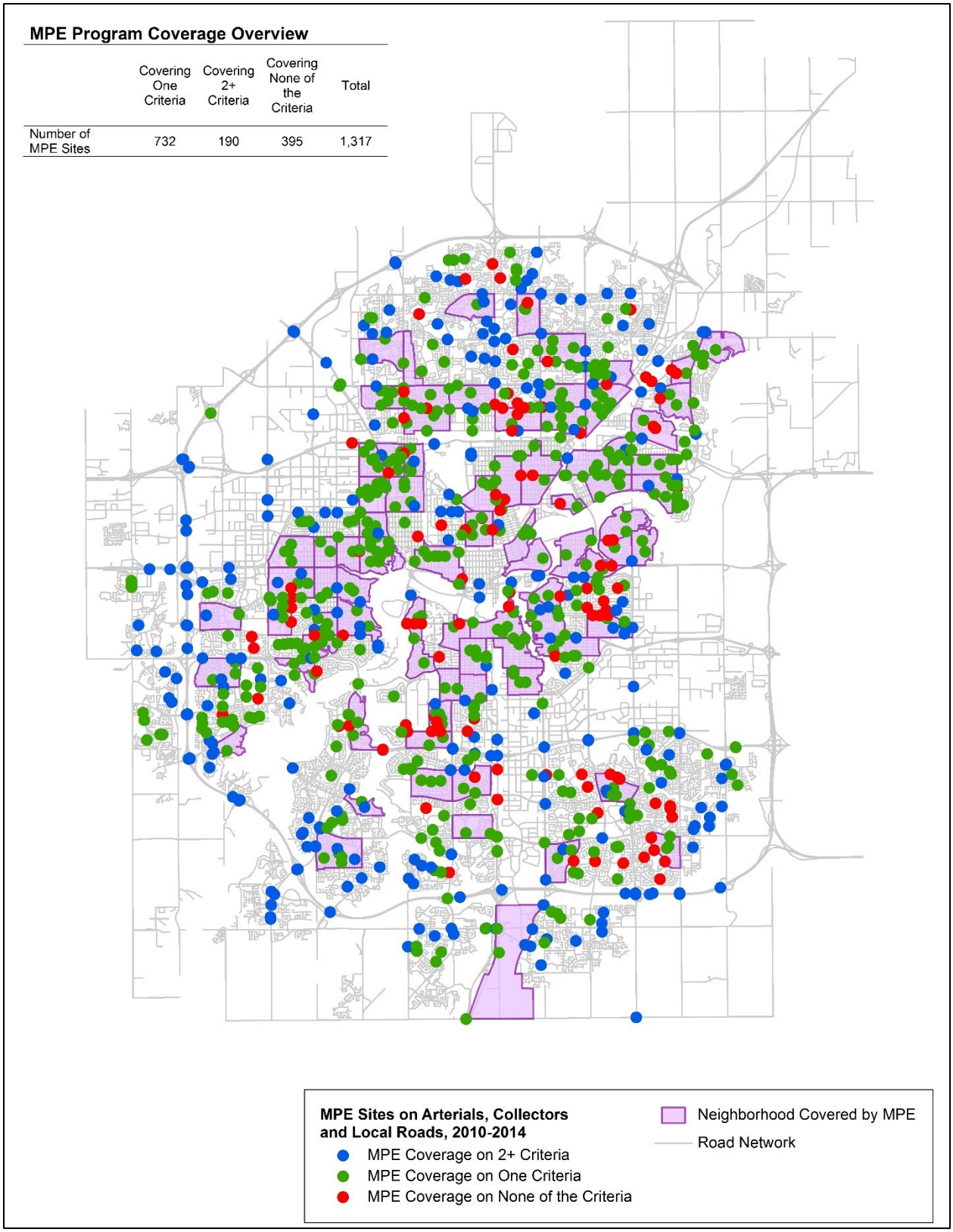


**Figure 4-7 2010-2014 MPE program coverage overview.**

The greatest benefit gained from visualizing MPE program coverage is that enforcement agencies can observe which sites are identified as priority sites during the study period and allocate resources to these locations. Figure 4-7 shows that a total of 922 MPE sites were allocated to locations within the scope of the six addressed enforcement priorities in this thesis. Of these 922 sites, one-fifth were covered by two or more priorities (marked as blue points); and four-fifths of the locations were covered by only one priority (marked as green points). Based on this information, enforcement agencies can further improve their management of (often very limited) resources. Agencies can invest more resources at locations identified to have two or more deployment priorities, to increase program efficiency. Alternately, enforcement agencies can also identify and dedicate more resources to locations with particular priorities, if there should be mandates to target specific priorities at certain times of the year. Chapter 5 introduced the determination of optimal resource allocation strategies when there are multiple deployment priorities and aims.

As seen from Figure 4-7, there were 395 sites marked in red that did not cover any of the proposed six priorities. There are three major reasons why this would occur. First, we only accounted for six of the most commonly identified deployment priorities and did not consider other priorities that are also included in the Province of Alberta's ASE guidelines or by the COE, such as multi-lane roadways, playground zones, etc. These sites might have been enforced with the purpose of achieving other goals or considerations. Second, we attempted to provide a quantitative interpretation for each of the six criteria. However, it is worth mentioning that while there are other ways to define each criterion, we only presented one definition. Third, certain locations that were identified as priority sites in this study might not have been operationally enforceable. Because of all the above reasons, some sites did not meet any of the criteria identified in this study.

## 4.3 COVERAGE ACCOUNTING FOR DISTANCE HALO EFFECT

Achieving maximum citywide coverage may be very difficult for local enforcement agencies, owing to the fact that there are a number of deployment goals but limited resources. However, sites that have been enforced by ASE may experience distance halo effects, which are safety effects that extend upstream and downstream of the camera site (Vaa, 1997). In the review of MPE spatial coverage, this section investigates the geospatial relationship between high-priority deployment considerations and historical deployment priorities, taking distance halo effects into consideration.

The distance range of this effect varies across studies. Nilsson (1992) states that the distance halo effect for MPE in urban areas can reach up to 500 meters upstream and 500 meters downstream. In contrast, Champness et al. (2005) conclude that the distance halo effect of a mobile overt speed camera program extends 1000 meters downstream, but is insignificant for upstream traffic. Elvik (2011) concludes that the level of enforcement intensity significantly affects the scope of the enforcement safety effects. Therefore, this thesis has established a function to estimate the range of the distance halo effect based on deployment intensity.

The function of the estimated radius of the MPE distance halo effect is shown in Equation (4-1):

$$R_m = R_0 * [0.5 + 0.124 * ln(y_m/Y)] \quad (4\text{-}1)$$

where:

$m$ = enforcement site index
$R_m$ = expected radius of enforcement distance halo effect at site $m$ in meters
$R_0$ = baseline radius of distance halo effect in meters
$y_m$ = total enforcement level at site $m$ in hours
$Y$ = average citywide level of enforcement in hours

Equation (4-1) is based on the logarithmic formulation constructed by Elvik (2011). The relative level of enforcement is calculated by dividing the total enforcement hours of each deployment site by the average total deployment hours of all the sites. In this thesis, the average deployment hours of the 1,317 MPE sites operating during the five-year study period is 139.1 hours. Considering that the maximum distance halo effect of the MPE program in urban areas is 500 meters (Nilsson, 1992), the radius constraints are such that the minimum distance halo should not be less than zero meters and the maximum should not be greater than 500 meters. Furthermore, a 250 m baseline radius is adopted; when the deployment hours at a site are less than the average citywide deployment intensity, the distance halo is estimated less than the baseline. Therefore, the fewer deployment resources allocated, the smaller the distance halo effect predicted, and vice versa.

As in the review of spatial coverage, the GIS layer of MPE sites accounting for distance halo effects is overlapped with the locations of high-priority deployment considerations. Because reducing collisions and speed is the ultimate objective of enforcement, this section investigates

only high collision and high-speed violation sites to illustrate the distance halo effect. The MPE coverage accounting for the distance halo effects is visually compared with these two priorities, respectively, and the findings are discussed below.

### 4.3.1 High Collision Sites

The distance halo effects of the five-year MPE program are mapped for high collision sites in Figure 4-8. The sizes of the blue circles on the maps are calculated based on Equation (4-1), which considers the degree of enforcement of each site, and reflects the estimated distance halo effect of surrounding areas. In summary, 19% of 1,087 enforcement sites generated distance halo effects within a radius of 250 to 500 meters; whereas, the other 81% of enforcement sites generated effects covering less than a 250-meter radius.

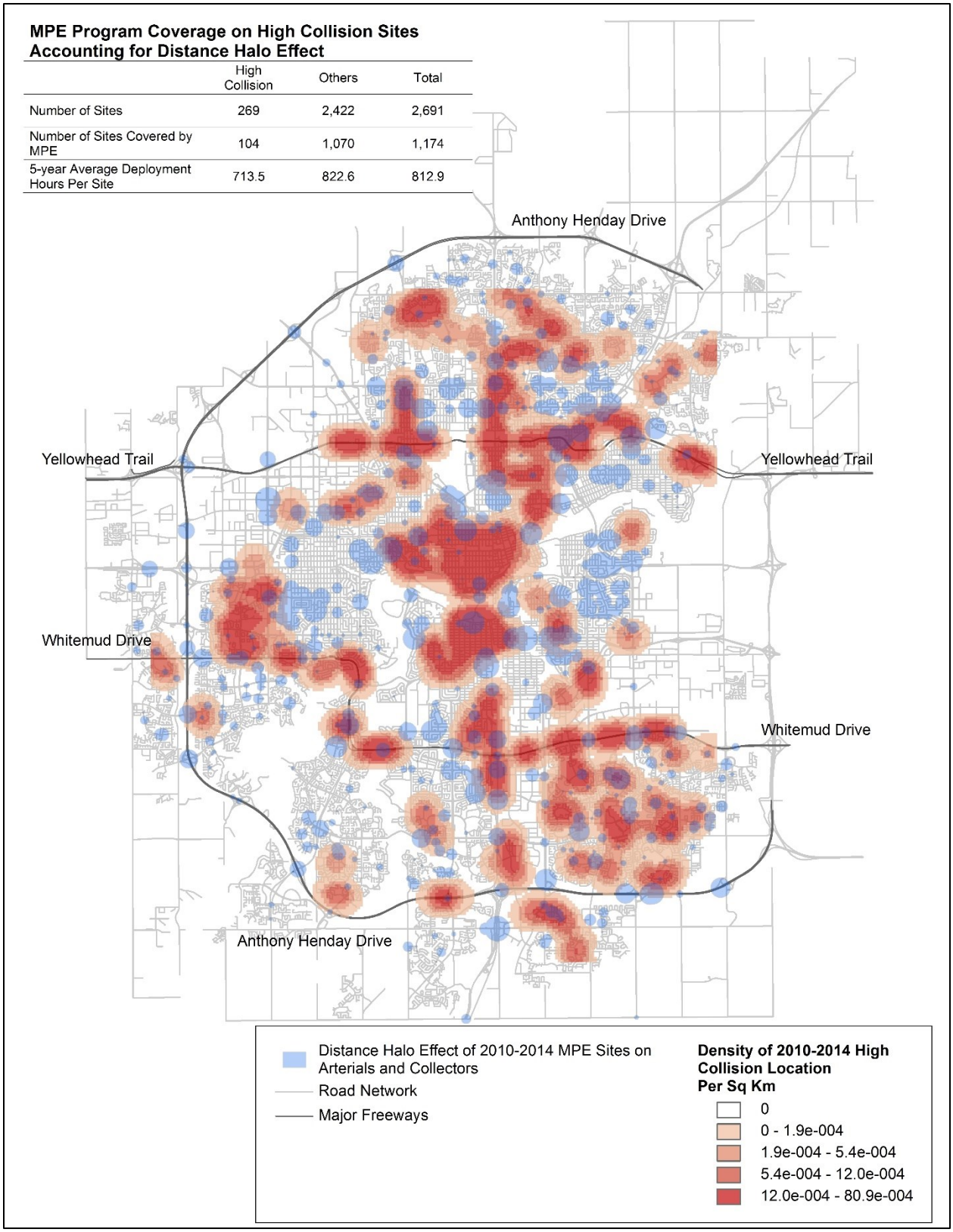


**Figure 4-8 2010-2014 MPE program coverage on high collision sites accounting for distance halo effect.**

Without considering the distance halo effect, the spatial coverage of the MPE program for high collision sites does not account for high collision sites adjacent to MPE deployment locations. For instance, 18 high collision sites are identified along the Yellowhead Trail and Whitemud Drive freeways. The number of MPE deployment sites on these two freeways is also very high, with a total of 38 MPE sites. However, only one third of these high collision sites is precisely covered by MPE. It is observed that 66% of these enforcement sites are located on an overpass or underpass of interchanges, which may be due to ease of camera placement. In contrast, most high collision sites are located between freeway interchanges, with only three located at interchanges. Although these 38 MPE sites may have deterrence effects on high collision sites nearby, these effects cannot be determined without the distance halo effect.

When evaluating MPE program coverage with the distance halo effect, the coverage of high collision sites increases from 47 to 104, doubling the citywide coverage to 38.7% (Figure 4-8). In addition, the number of enforcement sites influencing high collision sites expands from 85 to 171 when the spatial deterrent effect of each MPE operation is considered. Furthermore, the average deployment time at each high collision site doubles, adding to 713.5 hours per site for the five-year study period.

### *4.3.2 High Speed Violation Sites*

As with high collision sites, the five-year MPE program performance for high speed violation sites is improved when the distance halo effect is accounted for. As shown in Figure 4-9, the coverage increases by 13.9%, reaching 63.9%. In addition, the number of MPE sites influencing high speed violation sites expands to 146, with the average deployment hours rising to 1,373 per site.

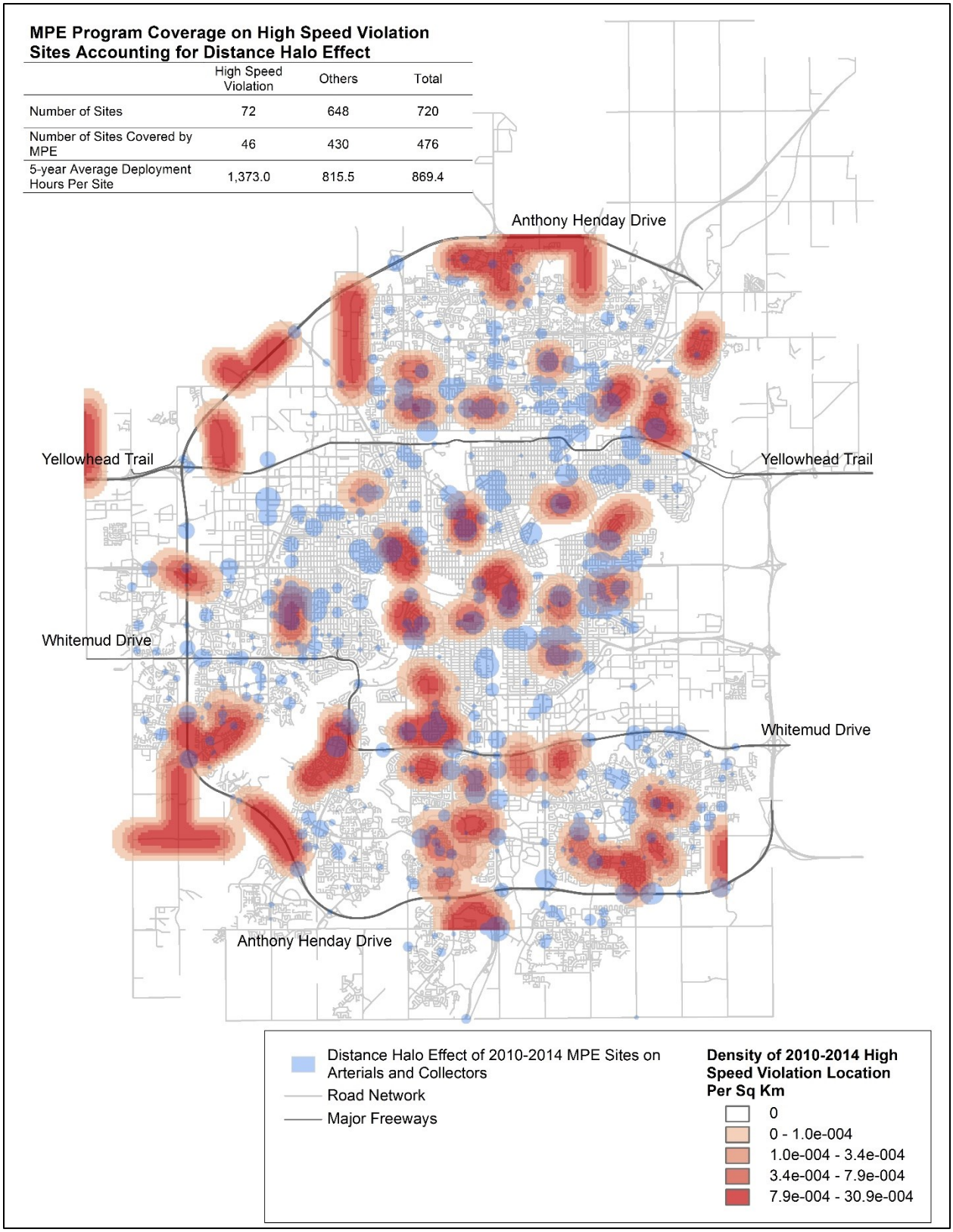


**Figure 4-9 2010-2014 MPE program coverage on high speed violation sites accounting for distance halo effect.**

As a result, the performance of the MPE program in terms of spatial coverage and the level of enforcement intensity are improved when accounting for the distance halo effect. This effect is a more reasonable indicator of MPE deployment performance when assessing spatial coverage and intensity. This method can help enforcement agencies form a better understanding of the extended spatial impact of MPE deployment to high priority sites. However, it may be difficult to incorporate the effects of distance halos as a basis for MPE deployment decisions at this time, given that there has been very limited research on the quantification of distance halo effects with respect to enforcement intensity. This thesis presents a method to estimate the distance halo effect of an MPE program; further research should be conducted in the future to test this estimation method. At this time, it is recommended that enforcement agencies allocate MPE to exact high priority sites rather than within estimated distance halo effect areas.

## 4.4 SUMMARY

This chapter proposed quantitative measures to help agencies conducting ASE programs to identify and evaluate deployment priorities. These priorities are based on six considerations typically identified in ASE guidelines: high collision sites, high speed violation sites, school zones, construction zones, high pedestrian volume sites, and sites with community speeding complaints. A case study from Edmonton, Alberta, Canada, was presented, and five years of data (2010–2014) was used to identify and plot these six priorities using GIS. Maps were also overlaid with deployment data from the COE's MPE program, showing enforcement presence at high priority locations.

Sites at high risk of experiencing collisions and speeding – warranting greater enforcement attention – were identified using quantitative criteria. High collision sites were identified as those with an average of 53.1 $EPK$, while high speed violation sites were identified as those where 81.9% of vehicles violated the speed limit.

Spatial coverage and enforcement intensity were assessed to investigate the interpretation and application of the six Alberta ASE deployment priorities by the COE's MPE program. It was observed that each priority was addressed by the COE program, but at different levels of attention. High speed violation sites and school zones were shown to have received the greatest attention

among the six priorities, with comparatively high spatial coverage and intensity. High speed violation sites received the most enforcement time, with more than 800 deployment hours on average for each site during the five-year study period. In contrast, school zones received more enforcement coverage, at 84%. Additionally, it was found that 30% of MPE resources were not allocated to sites meeting the criteria of any of the six deployment priorities. If the MPE program were to reallocate these resources to sites meeting any of the six priorities, the program may be able to achieve greater safety outcomes.

Furthermore, this chapter introduced a function to assess MPE distance halo effects. After mapping MPE distance halo effects with the locations of high collision sites and high speed violation sites, both spatial coverage and intensity increased. The spatial coverage and average deployment hours on high collision sites doubled and increased by 30% and 60% on high speed violation sites, respectively. These increases indicate that enforcement cameras were located very close to some high priority sites.

# 5 MPE RESOURCE ALLOCATION MODEL

Agencies that manage and operate mobile photo enforcement (MPE) programs must consider program goals when making decisions about how to deploy operators. Usually, there are priorities to target locations with high collisions, speed violations, and pedestrian volumes, and within school zones and construction zones. However, there is no documented MPE design structure that systematically connects these priorities to the deployment decisions made. This chapter proposes a method to aid MPE agencies in applying program goals directly in the efficient allocation of limited program resources. A neighborhood-level MPE resource allocation (MRA) model is developed (Sections 5.2 and 5.3), which uses multi-objective optimization to determine how enforcement is allocated to city neighborhoods. The model is applied to an MPE program in Edmonton, Alberta, Canada, and the solutions are explored using several approaches (Sections 5.4 and 5.5).

Our work 1) allows for enforcement agencies to explicitly map performance outcomes to program goals, thus engendering a more transparent and efficient MPE program, which in turn may help to improve road safety; 2) provides managers with a pool of candidate deployment options that address different program considerations and preferences, and 3) provides managers with insights into the tradeoffs between different deployment solutions available to them.

## 5.1 INTRODUCTION

To make decisions on how to deploy operators within a mobile photo enforcement (MPE) program—a multiple-objective problem—program managers must take several, often conflicting, goals into account. These program-level goals—typical of most MPE programs around the world—include reducing collisions, reducing speed violations, and increasing safety particularly for the most vulnerable pedestrians. When these high-level program goals are considered in deployment decisions, operators are typically directed to roadway locations experiencing high collision rates, high speed limit violations rates, and dense pedestrian traffic particularly comprising school-age children. MPE program presence at these sites can be of varying or equal importance to MPE agencies, depending on any number of factors. Since enforcement resources

are usually limited due to the high costs of manpower and equipment, allocating finite resources to meet multiple goals is a common dilemma for MPE agencies. There is little support available on this topic in the published literature.

This chapter presents an MPE resource allocation (MRA) model that uses multi-objective optimization to consider multiple criteria simultaneously. The three deployment objectives used here prioritize the reduction of collisions at high collision sites, reduction of speed violations at high speed violation sites, and increased safety in school zones. These are part of a larger set of six that are commonly identified in MPE program guidelines (see Chapter 2). These three objectives are used in this research for two reasons. First, addressing the former two (reducing collisions and speed violations) addresses the ultimate safety goals of MPE programs around the world. Second, placing priority on school zones is necessary for protecting children (J. Warsh, Rothman, Slater, Steverango, & Howard, 2009), who are the most vulnerable road users (Peden et al., 2004).

Multi-objective linear programming is used to assign a limited number of enforcement shifts to neighborhoods in a city, directing enforcement coverage according to the three priorities. Three neighborhood-level metrics—equivalent property-damage-only collision frequency per kilometer ($EPK$), speed violation indicator ($SVI$), and school zone density ($SZD$)—are used to quantify each neighborhood's enforcement demand. Determining the enforcement resource allocation on a neighborhood basis is intended to provide planning-level insight on how resources might be allocated to satisfy the three priorities. A neighborhood is the considered unit of study because it is commonly understood, and descriptive data is often available at this level of urban aggregation.

Scalar optimization and evolutionary algorithms, two common types of multi-objective optimization algorithms, are demonstrated to solve the MRA model. Resource allocation solutions from the MRA model make up a Pareto front (PF). In a PF, no solution is absolutely superior over any other; instead, in comparing two solutions, we observe tradeoffs between the (two or more) objectives. To further understand the PF of the MRA solutions, we conduct two PF analysis steps: PF representation and tradeoff analysis. First, the $K$-medoids clustering algorithm is adopted to partition the PF of the MRA model into similar-sized clusters, in order to help agencies managing MPE programs choose from a reduced set of solutions on the PF. $K$-medoids is chosen because of

its ease of implementation. In addition, it is well known for its efficiency in processing large amounts of data, so it was used to handle a large number of PF solutions quickly. Second, we use the response surface method to determine tradeoff patterns on the PF. A quadratic polynomial model is estimated on a PF to construct a continuous surface. From this, we can examine the tradeoffs between MPE resource allocation solutions. For instance, how much coverage at high collision and speed violation sites would be sacrificed to achieve more enforcement presence in school zones. A case study of an MPE program in Edmonton, Alberta, Canada, is studied and PF results are found and analyzed for one month using three years (2012-2014) of historical data from Edmonton.

This chapter provides a systematic mapping of MPE program goals to deployment decisions. This process has existed as a "black box" insofar as it has not been explicitly mapped or defined; therefore, the major contribution of this chapter lies here. Application of the model yields a pool of candidate deployment options from which program managers can choose, based on their preferences and needs at a given time. Neighborhood-level deployment plans offer city- or region-wide information regarding where enforcement needs are and how to address them, such that program managers can then schedule individual resources to individual enforcement sites within each neighborhood.

## 5.2 MODEL FORMULATION

The MRA model uses multi-objective optimization to map high-level program goals to deployment decisions. Specifically, the deployment process can be described in three parts (Figure 5-1): defining high-level program goals, the MRA model, and choosing the deployment plan for implementation.

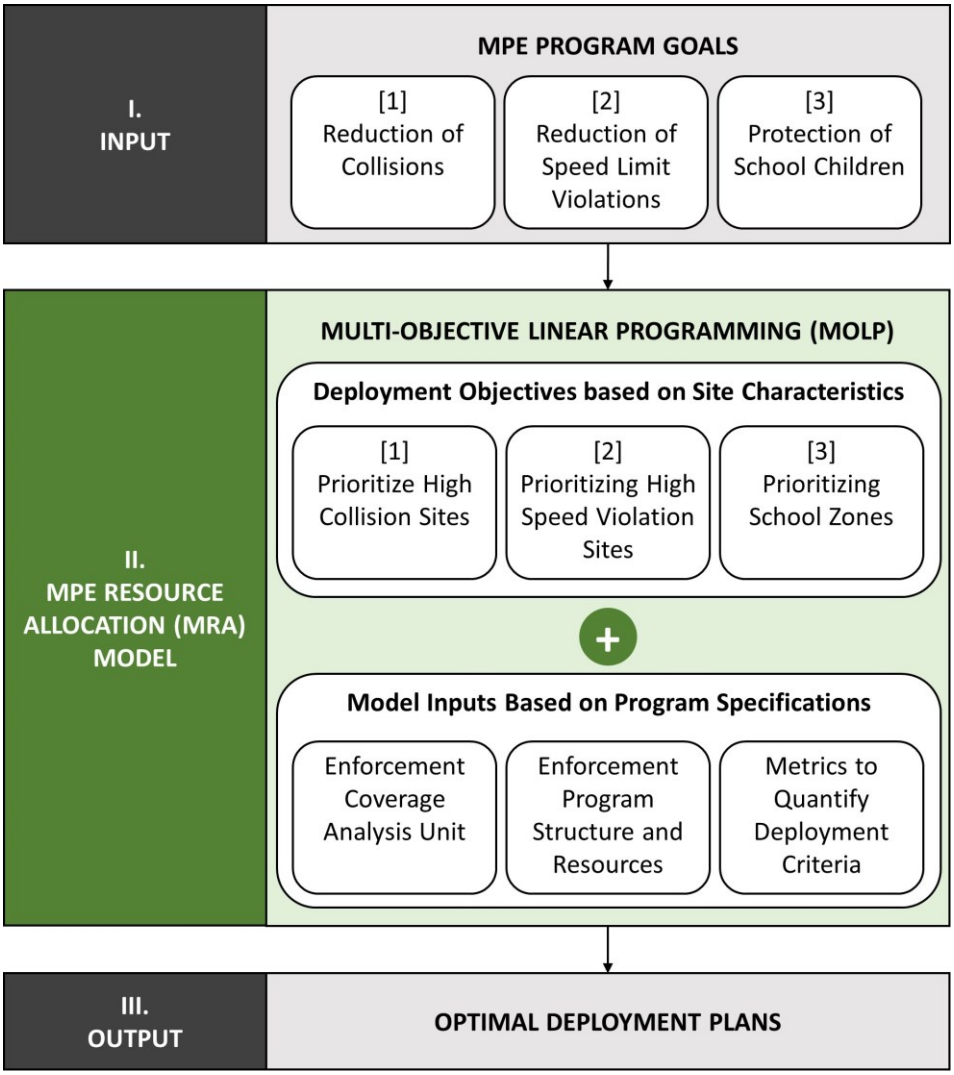


**Figure 5-1 Flow chart of the MPE resource allocation model.**

The input to the MPE resource allocation, as shown in Figure 5-1, includes the three high-level MPE program goals: reduction of collisions, reduction of speed limit violations, and presence in school zones (to increase pedestrian safety). The three deployment objectives used here are part of a larger set of six, which are commonly identified in MPE program guidelines and they have been concluded in Chapter 2. These three objectives are used in this research for two reasons. Firstly, addressing the former two (reducing collisions and speed violations) addresses the ultimate high-level goals of most MPE programs around the world. Secondly, placing priority on school zones is necessary for protecting children (Peden, 2008; Joel Warsh et al., 2009). However, any number of, and types of, goals can be considered in the MRA model.

As discussed in Section 3.2, limited research has been conducted on how to allocate and utilize MPE program resources with direct consideration for multiple program goals. We propose multi-objective linear programming (MOLP) to connect deployment decisions back to high-level program goals in Part II of Figure 5-1, which requires two major tasks. The first is to convert high-level, traffic safety-focused program goals into operational deployment objectives. In this research, the operational deployment objectives consist of the prioritization of sites with high rates of collisions, high rates of speed limit violations, and those within school zones. The second task is to identify program-specific characteristics for use in the MRA model. In this research, we have identified three: geographic units for enforcement allocation, program resources (i.e., operators, shift scheduling rules, equipment, etc.), and metrics to quantify the operational deployment objectives in the first task. The details of Part II are discussed in Sections 5.2.1 and 5.2.2. The model outputs a set of candidate deployment plan options from which decision makers can choose, based on their specific preferences and needs at a given time.

### *5.2.1 Model Inputs*

Here we discuss the three inputs of the MRA model as identified in Part II of Figure 5-1, as defined for the MPE program in Edmonton, Alberta, Canada. Data was provided by the City of Edmonton Traffic Safety Section, which oversees Edmonton's MPE program. Decision makers of other MPE programs with different operational and geographic considerations may need to adjust these inputs.

#### 5.2.1.1 Geographic Units for Enforcement Allocation

In Edmonton, MPE sites are urban mid-block sections, their locations and lengths having been assessed and approved by MPE agencies. Approval is given if there is an identified need for enforcement, and the site has a safe place to park an enforcement vehicle with a clear line of sight to license plates. Operators may only conduct photo radar enforcement activities at these predetermined sites. The MPE program has a site pool consisting of more than 1000 sites that are candidates for enforcement; with a limited set of operators, vehicles, and equipment, deciding where to send these resources can be difficult. To make the planning stage of this deployment problem tractable, we allocate enforcement resources at a neighborhood level. A neighborhood is the considered unit of study in our application because it is commonly understood, and descriptive data (that can support MPE program decision-making) is often available at this level of urban

aggregation. In the literature, neighborhoods have often been used in road safety evaluation research to support high-level management (Ho & Guarnaschelli, 1998; Poppe, 1995; Kmet, Brasher, & Macarthur, 2003; G. R. Lovegrove & Sayed, 2006; G. Lovegrove & Sayed, 2007). Neighborhood-level MPE resource allocation can provide planning-level insight into how to allocate resources to address the three priorities.

#### 5.2.1.2 Program Resources

The COE's MPE program is conducted through operator shifts that cover 20 hours of a day, seven days a week. During a shift, an operator is assigned to police speed at a set of enforcement sites. The 20-hour daily enforcement is divided into two shifts, including a daytime shift from 6AM-4PM and an evening shift from 4PM-2AM. Therefore, we quantify available program resources in terms of the total monthly number of shifts. The MRA model assigns operator shifts on a monthly basis, determining the assignment that best addresses the deployment goals in a given month. Providing a deployment plan that rotates monthly is more feasible than a weekly or yearly plan. A weekly rotation is too frequent to assess historical data, such as collision and speed survey data, because enforcement demands would not change appreciably from week to week. In contrast, a yearly rotation is too long a period; opportunities to make improvements and increase the unpredictability of enforcement may be missed (Kim et al., 2016).

#### 5.2.1.3 Metrics to Quantify Operational Deployment Objectives

We define the three neighborhood-level deployment criteria based on those proposed in Chapter 4. Equivalent property-damage-only (EPDO) collision frequency per km, the percentage of speeding vehicles, and the number of school zones are used to assess enforcement need in neighborhoods. Given that these measures are developed on a road segment basis, we reform them into neighborhood metrics in order to assess and compare enforcement need on a neighborhood level. Firstly, the total EPDO collision frequency divided by the total road length (in km) for each neighborhood is used to quantify a neighborhood's need for enforcement regarding collision rates. Secondly, a speed violation indicator ($SVI$) is used to aggregate the proportion of vehicles exceeding the speed limit per neighborhood. $SVI$ is the average percentage of speed violating vehicles across all segments in each neighborhood, weighted by the traffic volume over the length of time measured for each segment (Hakkert, Gitelman, & Vis, 2007). Thirdly, neighborhood

school zone density, computed by dividing the total number of school zones by the total neighborhood area (in sq.km), is used to assess the level of enforcement needed in a neighborhood due to the presence of schools. Neighborhoods exhibiting high metrics warrant a high level of enforcement, and the model is designed to allocate as many shifts as possible to these neighborhoods.

### *5.2.2 Multi-Objective Linear Program*

The MRA model uses multi-objective linear programming (MOLP) (Equations (5-1)-(5-3)) to allocate one month of enforcement shifts to city neighborhoods, to optimize the three deployment criteria simultaneously. The three deployment objectives are quantified using the metrics introduced in Section 5.2.1.3; the higher the total of the three metrics is for a neighborhood, the more enforcement shifts one would expect to be allocated to that neighborhood.

Decision Variables:

$x_n$ = number of operator shifts assigned to neighborhood $n$ in a given month, $n \in [1, \dots, N]$

Objective Functions:

$$max \begin{cases} (I) & \sum_{n=1}^{N} EPK_n \cdot x_n \\ (II) & \sum_{n=1}^{N} SVI_n \cdot x_n \\ (III) & \sum_{n=1}^{N} SZD_n \cdot x_n \end{cases} \quad (5\text{-}1)$$

Subject to:

$$\sum_{n=1}^{N} x_n = P \quad (5\text{-}2)$$

$$L_n \leq x_n \leq U_n, \qquad \forall\, n \in [1, \dots, N] \quad (5\text{-}3)$$

Where:

| | | |
|---|---|---|
| $n$ | = | neighborhood index, $n = 1, \dots, N$ |
| $EPK_n$ | = | EPDO collision frequency per kilometer (km) for neighborhood $n$ |
| $SVI_n$ | = | speed violation indicator for neighborhood $n$ |
| $SZD_n$ | = | number of school zones per square kilometer (sq.km) for neighborhood $n$ |
| $P$ | = | number of total shifts in one month |
| $L_n$ | = | minimum allowable shifts that may be allocated to neighborhood $n$ in one month |
| $U_n$ | = | maximum allowable shifts that may be allocated to neighborhood $n$ in one month |

Equation (5-1) consists of three objective functions, each of which sums the product (over all neighborhoods) of a neighborhood's metric in question and number of shifts assigned to that neighborhood in the one given month. Equation (5-1) maximizes the three objective functions simultaneously, with respect to the constraints on the total number of shifts available in one month, $P$ (Equation (5-2)), and the minimum and maximum shifts allowed for each neighborhood over that month, $L_n$ and $U_n$ (Equation (5-3)).

The determination of $L_n$ and $U_n$ in Equation (5-3)) can explicitly account for operational-level deployment considerations. For example, there may have been a decision to enforce neighborhood $n$ with a desired intensity in the actual program, despite that the neighborhood scores low in the three enforcement metrics. In this case, the constraint $L_n$ is set to account for this decision; without $L_n$, the model might assign few shifts (possibly none) to $n$. The maximum allowable number of shifts to $n$ ($U_n$) may be pre-set in a similar fashion.

The model searches for the optimal shift distributions to neighborhoods $[1 \dots N]$, allocating as many shifts as allowed by Equation (5-3) to neighborhoods experiencing high $EPK_n$, $SVI_n$, and $SZD_n$.

## 5.3 MULTIOBJECTIVE OPTIMIZATION APPROACHES

Say we were to maximize only one of the three objective functions in Equation (5-1). The result would be equivalent to having performed the following steps: assign to each neighborhood the minimum number of shifts required ($L_n$); order all neighborhoods from highest to lowest values of the metric quantifying the objective function in question; assign the difference of the maximum and minimum number of shifts ($U_n - L_n$) allowable to the first neighborhood on the list (i.e. the one with the highest calculated metric value), then do the same for the second, and third, and etc. until all available shifts have been assigned.

However, trade-offs between the three objective functions will be required when they are considered simultaneously. Usually there is not a single optimal solution but a set of optimal solutions; at each of these optimal solutions, one objective cannot be increased without reducing at least one of the others. These solutions are called Pareto optimal solutions (Steuer, 1986), or PF.

There are many ways to identify a PF. In this Section, we only suggest and demonstrate two multi-objective optimization methods used to generate a PF of the MRA. Section 5.3.1 presents an algorithm that combines two well-known conventional scalar optimization methods. Section 5.3.2 introduces a classic multi-objective evolutionary algorithm, the generalized differential evolution 3 algorithm.

### *5.3.1 A Weighted Sum and Epsilon Constraint Approach*

The weighted sum method (Miettinen, 1999) is one of the most well-known and simplest scalar optimization techniques for multi-objective optimization problems. Scalar optimization techniques require the determination of weights for objectives before solving the problem. A true Pareto optimal solution can be obtained by using a set of objective weights. We first employed the weighted sum method to solve the MRA model (Equations (5-1)-(5-3)). The formulation of the weighted sum method is shown in the following WSP problem.

#### 5.3.1.1 Weighted Sum Problem (WSP)

As shown in Equation (5-4), the weighted sum method formulates the three-objective model in Equations (5-1)-(5-3) as a single objective consisting of the weighted sum of the three individual

objectives. Equation (5-5) normalizes the weights $\alpha_g, \beta_g$, and $\gamma_g$ assigned to each of the three metrics such that they sum to 1. The subscript $g$ represents the algorithm iteration number (to a maximum of $G$). Equations (5-6) and (5-7) are the constraints from the original model on resources $x_n$ (introduced in Equations (5-2) and (5-3)). Equations (5-4)-(5-7) are repeatedly evaluated for each $g$; each evaluation yields a Pareto-optimal solution.

$$max\ \alpha_g \cdot \sum_{n=1}^{N} EPK_n \cdot x_n\ + \beta_g \cdot \sum_{n=1}^{N} SVI_n \cdot x_n\ + \gamma_g \cdot \sum_{n=1}^{N} SZD_n \cdot x_n \qquad (5\text{-}4)$$

Subject to:

$$\alpha_g + \beta_g + \gamma_g = 1, \qquad \forall\ g \in [1, \dots, G] \qquad (5\text{-}5)$$

$$\sum_{n=1}^{N} x_n = P \qquad (5\text{-}6)$$

$$L_n \leq x_n \leq U_n, \qquad \forall\ n \in [1, \dots, N] \qquad (5\text{-}7)$$

where:

| | | |
|---|---|---|
| $n$ | = | neighborhood index, $n = 1, \dots, N$ |
| $EPK_n$ | = | EPDO collision frequency per kilometer (km) for neighborhood $n$ |
| $SVI_n$ | = | speed violation indicator for neighborhood $n$ |
| $SZD_n$ | = | number of school zones per square kilometer (sq.km) for neighborhood $n$ |
| $P$ | = | number of total shifts in one month |
| $L_n$ | = | minimum allowable shifts that may be allocated to neighborhood $n$ in one month |
| $U_n$ | = | maximum allowable shifts that may be allocated to neighborhood $n$ in one month |
| $\alpha_g$ | = | weight given to deployment metric $EPK$ in the $g$th iteration |
| $\beta_g$ | = | weight given to deployment metric $SVI$ in the $g$th iteration |
| $\gamma_g$ | = | weight given to deployment metric $SZD$ in the $g$th iteration |
| $g$ | = | iteration index, $g = 1, \dots, G$ |

Note that the weighted sum method has a well-known drawback: it only searches for corner solutions in the feasible region of the weighted sum problem. Therefore, using various weight combinations is likely to also produce corner solutions (Branke, Deb, & Miettinen, 2008; Mavrotas, 2009). To identify intermediate (non-corner) solutions, we adopted another well-known scalar

optimization approach, the ε-constraint method (Haimes, 1971). The ε-constraint method formulation for the MRA example is described in the following ECP problem.

#### 5.3.1.2 ε-Constraint Problem (ECP)

The ε-constraint method described in Equations (5-8)-(5-11) optimizes $EPK$ (equivalent property-damage-only collision frequency per kilometer) and transforms the remaining two measures ($SVI$, speed violation indicator, and $SZD$, school zone density) into inequality constraints that are greater than or equal to the pre-set values of $\varepsilon_g^1$ and $\varepsilon_g^2$. The choice to optimize one particular measure and set the others as constraints is arbitrary; we would expect any configuration to yield the same results because this three-objective problem is convex. By changing the ε values of Equations (5-9) and (5-10), the ε-constraint method is able to generate a different Pareto-optimal solution at every iteration ($g$).

$$\max_{x \in \Omega} \sum_{n=1}^{N} EPK_n \cdot x_n \tag{5-8}$$

Subject to:

$$\sum_{n=1}^{N} SVI_n \cdot x_n \geq \varepsilon_g^1 \tag{5-9}$$

$$\sum_{n=1}^{N} SZD_n \cdot x_n \geq \varepsilon_g^2 \tag{5-10}$$

$$\Omega = \{x_n \mid \sum_{n=1}^{N} x_n = P \; and \; L_n \leq x_n \leq U_n, \forall \, n \in [1, \dots, N]\} \tag{5-11}$$

where:

| | | |
|---|---|---|
| $n$ | = | neighborhood index, $n = 1, \dots, N$ |
| $EPK_n$ | = | EPDO collision frequency per kilometer (km) for neighborhood $n$ |
| $SVI_n$ | = | speed violation indicator for neighborhood $n$ |
| $SZD_n$ | = | number of school zones per square kilometer (sq.km) for neighborhood $n$ |
| $P$ | = | number of total shifts in one month |
| $L_n$ | = | minimum allowable shifts that may be allocated to neighborhood $n$ in one month |
| $U_n$ | = | maximum allowable shifts that may be allocated to neighborhood $n$ in one month |
| $\varepsilon_g^1$ | = | lower bound value given to deployment objective $SVI$ in the $g$th iteration |

$\varepsilon_g^2$ = lower bound value given to deployment objective $SZD$ in the $g$th iteration
$g$ = iteration index, $g = 1, \ldots, G$

The major disadvantage of the ε-constraint method is that it can be difficult to specify the values of $\varepsilon_g^1$ and $\varepsilon_g^2$ without knowing the bounds of objectives $SVI$ and $SZD$ for the PF (Miettinen, 1999). However, the results from the weighted sum method in the previous step can be used to address this issue – we can define $\varepsilon_g^1$ and $\varepsilon_g^2$ values using the range of corresponding objective function values of the weighted sum solutions found in the previous step.

### 5.3.2 A Generalized Differential Evolution 3 (GDE3) Algorithm

Multi-objective evolutionary algorithms (MOEAs) are becoming increasingly popular in solving multi-objective optimization problems since 1990s. The major advantages of MOEAs include the ability to 1) handle difficult objective functions, 2) provide posteriori preference information to decision makers (i.e., no need to set the weight parameter values for each objective in advance), and 3) find an entire set of solutions after a single run.

Therefore, we use the generalized differential evolution 3 algorithm (GDE3), which is a widely used MOEA to solve the MRA (Equations (5-1)-(5-3)). The GDE3 algorithm, developed by Kukkonen and Lampinen (2005), has been shown to outperform other MOEAs (such as the non-dominated sorting genetic algorithm) in finding solutions with fewer iterations (Kukkonen & Lampinen, 2005; Antonio & Coello Coello, 2013).

The GDE3 uses floating-point encoded variable vectors as the population of evolutionary algorithms. In the process of evolution, GDE3 first creates a set of trial vectors that is a copy of the decision vectors of the population in one generation. Then GDE3 goes through each element of each trial vector and mutates the element, as long as a random number from [0, 1] assigned to the element is less than a predetermined crossover rate. The element's mutation is done by changing its value to be equal to a linear combination of three elements that are randomly chosen from three decision vectors. After evolution, GDE3 compares each pair of the decision vector and its corresponding trial vector. The vector that weakly dominates (has equal or better objective values) the other in the objective function space is selected as the population of the next generation. However, if the two vectors do not dominate each other, both are selected for the next generation.

Note that after the selection, the population size of the next generation may be larger than the size of the initial population, up to twice the initial population. The GDE3 uses the vector sorting method as described in Deb, Pratap, Agarwal, & Meyarivan (2002) to prune the population size to the initial number of population. This pruning process is done by using two measures: non-dominance level and crowdedness. First, vectors are partitioned into different non-domination levels (best level, next best level, and etc.) by comparing the number of vectors that dominate each vector and the set of vectors dominated by each vector. Vectors ranked at the best non-domination level are first added to the next generation of population. The next best-level vectors are then added to the population. Adding vectors is done one level at a time until the next level of vectors cannot be fully added to the population. At this point, to identify which vectors in the next level can be input to the population, the crowding distance of each vector of the level is computed. Based on the distance, vectors are ranked in descending order, and they are added to the population in the ranking order until the population is full.

The GDE3 approach uses the non-dominance level and crowding distance to screen the current generation of populations into the next generation. Therefore, it is an elitist algorithm. That is, each new generation of populations contains solutions that are closer to optimal frontier and more dispersed than the previous generation. Appropriate stopping criteria for the iterative process of GDE3 usually include a pre-set upper limit of the number of generations or a limit on the objective function value.

## 5.4 PARETO FRONT GENERATION RESULTS

The MRA model described in Section 5.2.2 was applied to produce candidate deployment plans for the City of Edmonton's MPE program in September 2014. We used GIS mapping to present one deployment plan produced by the MRA model, which assigned higher priority to school zones and lower to high collision and speed violation sites. Furthermore, these deployment results were visually compared against the results of the actual September 2014 MPE program deployment.

### *5.4.1 Neighborhood Metrics*

Table 5-1 presents the metrics calculated for the three deployment criteria, for the 388 Edmonton neighborhoods, from the 2012-2014 historical data. In computing EPDO collision frequency, the

direct cost of collisions of different severity levels (de Leur et al., 2010) were used as the weights for different collision severities. Specifically, according to this 2010 report, one fatal collision is equivalent to 16.6 PDO collisions and one injury collision is equivalent to 3.6 PDO collisions. Most neighborhoods have $EPK$ values between 0 and 7.7 EPDO/km, speed violation indicator ($SVI$) values between 0 and 0.6, and school zone densities (school zones/sq.km) between 0 and 1.6.

**Table 5-1 Summary of Calculated Metrics for 388 Edmonton Neighborhoods (2012-2014)**

| Metrics | Average | Standard Deviation | Minimum | Maximum |
|---|---|---|---|---|
| **EPDO/km** | 4.3 | 3.4 | 0.0 | 19.6 |
| **Speed violation indicator** | 0.3 | 0.3 | 0.0 | 0.9 |
| **School zone density (/sq.km)** | 0.7 | 0.9 | 0.0 | 4.3 |

Figure 5-2 identifies neighborhoods that have calculated metrics within the top 10% of each criterion (three in total). These neighborhoods are those that we have defined as warranting high enforcement attention. As seen in Figure 5-2, there are no neighborhoods that fall in the top 10% of neighborhoods for all three metrics simultaneously. In addition, there are only nine neighborhoods in the top 10% of neighborhoods for any two of the three metrics (marked in red). This suggests that resources to these nine neighborhoods may address two of the three goals at once. However, overall it can be concluded that the goals of prioritizing neighborhoods with high collision rates, speed violation rates, and school zone densities for enforcement are not necessarily complementary to one another, and indeed, conflict.

**Neighborhood Metrics (3-Year Average)**

| | | Number of Neighbor-hoods | EPDO/km | SVI | School Zone Density (sq.km) |
|---|---|---|---|---|---|
| Neighbor-hoods within Top 10% of Metrics | Any Two of Three Metrics | 9 | 11.1 | 0.7 | 0.3 |
| | Exclusively EPDO/km | 32 | 11.9 | 0.3 | 0.4 |
| | Exclusively SVI | 31 | 3.1 | 0.8 | 0.3 |
| | Exclusively School Zone Density | 36 | 4.5 | 0.4 | 2.7 |
| Total Neighborhoods | | 388 | 4.3 | 0.3 | 0.7 |

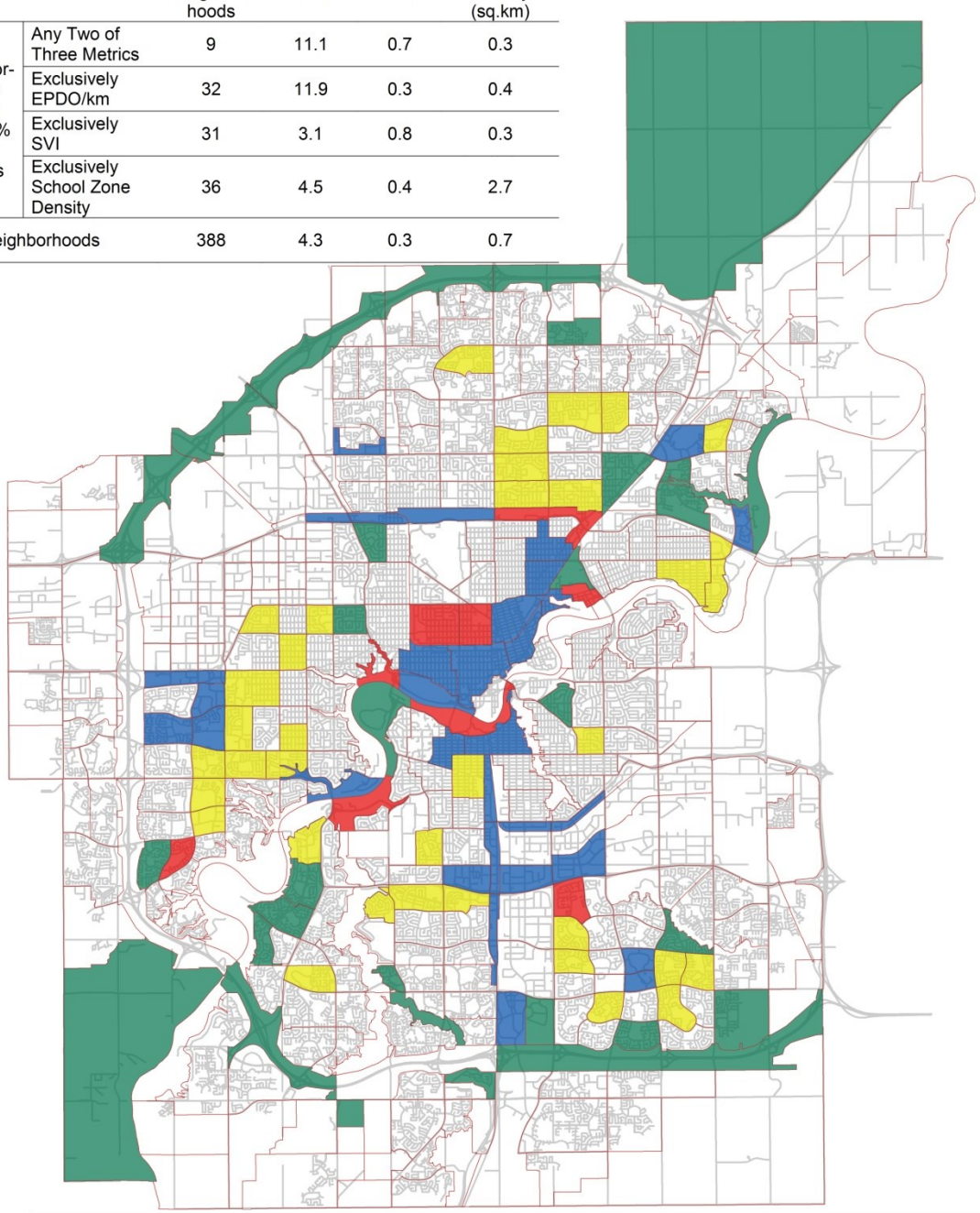


**Figure 5-2 Edmonton neighborhoods ranked by criteria, 2012-2014.**

Neighborhoods within the top 10% for only one metric include 32 neighborhoods for $EPK$ (identified in blue), 31 neighborhoods for $SVI$ (identified in green), and 36 neighborhoods for $SZD$ (identified in yellow). All three top 10% criteria groups have an average calculated metric that is more than double the average for all 388 neighborhoods, but they have values in the other two metric categories close to or even below the average of all neighborhoods. For instance, the 2012-2014 average $EPK$ of the neighborhoods exclusively in the top 10% of collision sites is 11.9 EPDO/km, which is almost three times the average $EPK$ for all 388 neighborhoods (4.3EPDO/km). However, the average $SVI$ of those neighborhoods exclusively in the top 10% of collision sites is 30% violating vehicles, mirroring the average for all neighborhoods. In addition, those neighborhoods' average school zone density is only 0.4 school zones per square kilometer (sq.km), which is about half of the average for all neighborhoods (0.7 school zones/sq.km). Similar observations can be made for the other two groups of neighborhoods that fall exclusively in the top 10% of the speed violation metric or school zone density metric. These observations imply that allocating resources to the blue, green, and yellow neighborhoods shown in Figure 5-2 will address high enforcement demand for only one of three deployment goals. Thus, these goals are in conflict. If agencies want to address conflicting program goals at the same time, they must trade off and compromise when allocating resources to meet these goals, which is difficult without support from a mathematical tool.

### 5.4.2 Results

After inputting the data introduced in Section 3.2 above to the MRA model, a model instance is created. Specifically, in the instance, the COE MPE program in September 2014 included 458 operator shifts distributed over 388 neighborhoods, based on each neighborhood's calculated $EPK$, $SVI$, and $SZD$, as well as the bounds on the number of shifts that may be allocated to each neighborhood. Sections 5.4.2.1 and 5.4.2.2 show the generated PF results for the MRA instance by using the two solution methods described in Sections 5.3.1 and 5.3.2, respectively.

#### 5.4.2.1 Pareto Front Generated by Weighted Sum and Epsilon Constraint Combined Method

To construct the weight combinations required for the weighted sum method (Equations (5-4)-(5-7)), we first set each of $\alpha_g$ , $\beta_g$ and $\gamma_g$ to values at 0.05 increments between 0 and 1, to generate a total of 9,260 weight value combinations. Then, we normalized these weight values (i.e., such

that they summed to one) by dividing by the total weight of each combination. By removing the duplicated weight combinations and a zero-valued combination, a total of 7,758 different remaining weight combinations were input to Equation (5-4). The 7,758 optimizations of Equations (5-4)-(5-7) were implemented by CPLEX in the MATLAB environment on a PC with Intel® Core i7-3770 CPU (3.4GHz) and 16GB RAM. A total of 244 unique solutions were found in 23 seconds.

Of the 244 weighted sum solutions, the objective function values for $SVI$ and $SZD$ are observed within the ranges of [208, 294] and [377, 1007], respectively. Therefore, these two ranges are used to limit the values of $\varepsilon_g^1$ and $\varepsilon_g^2$ used in Equations (5-9) and (5-10) of the ε-constraint method. We created 20,000 random numbers for $\varepsilon_g^1$ and $\varepsilon_g^2$ in a uniform sequence within the specified range. Equations (5-8)-(5-11) were implemented by the MATLAB CPLEX toolbox repeatedly at each of the 20,000 sets of $\varepsilon_g^1$ and $\varepsilon_g^2$ values. To build a dense PF, we limited the solution space of $SVI$ and $SZD$ examined per iteration to the neighborhood of $(\varepsilon_g^1, \varepsilon_g^2)$. Specifically, each implementation is constrained in a search area where the $SVI$-axis step size was set to two and $SZD$-axis step size ten. The step size (of 2×10) accounts for 2% of the corresponding objective function interval; other sizes can be determined as needed. A total of 16,544 unique solutions were obtained in 27 seconds on the same PC described above.

The solutions found by the weighted sum and ε-constraint methods are then put together and compared with each other. Although various weights were used in both methods, 97% of weighted sum solutions and 22% of ε-constraint solutions have the same objective values as the solutions in the combined set. Therefore, we eliminated these repeated solutions, and a total of 243 weighted sum solutions (black circles in Figure 5-3) as well as 12,967 ε-constraint solutions (grey points in Figure 5-3) are finally considered in the PF.

Each point shown in Figure 5-3 is the result of optimizing all metrics (represented on each of the three axes shown) simultaneously. The three red asterisks shown in Figure 5-3 represent the extreme (corner) points of the PF; each corner point represents the maximization of one of the three objectives. They are generated from the weighted sum method using weight combinations (1, 0, 0), (0, 1, 0), and (0, 0, 1) for the measures $(EPK, SVI, SZD)$.

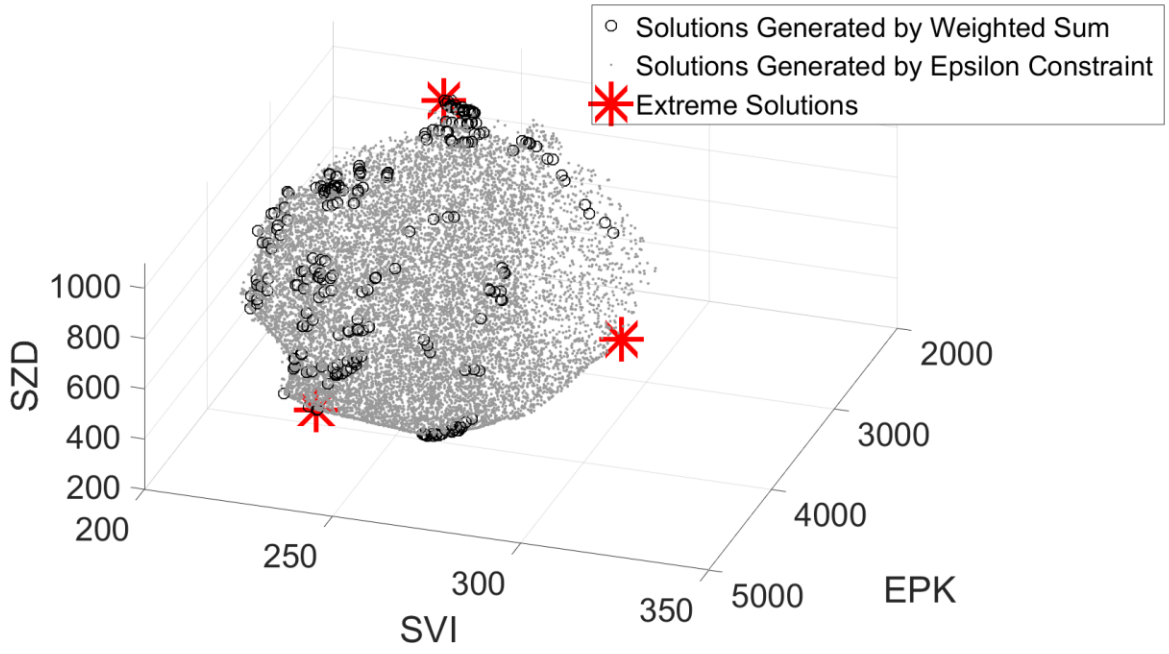


**Figure 5-3 Pareto front identified for the MRA example.**

As seen in Figure 5-3, the 243 weighted sum solutions are not evenly distributed on the Pareto front despite the evenly spaced weights. This is because, in the weighted sum method, the relationship between the objective function weights and the objective function values of the Pareto solution (based on those weights) is nonlinear. Using geometry, Das & Dennis (1997) demonstrated that the weight used in a bi-objective weighted sum method to find a Pareto solution is the reciprocal of one minus the slope (i.e., the ratio of change between the two objective functions) of the PF at a given solution point. Thus, considering a uniform distribution of weights in Equation (5-4) is unlikely to result in uniformly distributed Pareto solutions.

In addition, the identified weighted sum solutions comprise only 3% of the utilized weight combinations. This demonstrates the drawback of the weighted sum method discussed earlier: the method ignores non-corner solutions, rendering the usage of a large portion of the weight combinations redundant (Branke et al., 2008; Mavrotas, 2009). However, the solutions generated by the ε-constraint method fill the empty spaces left by the weighted sum solutions on the PF, as illustrated in Figure 5-3. Applying both solution methods results in a nearly complete PF with a relatively uniform and dense spread of solutions.

### 5.4.2.2 Pareto Front Generated by Generalized Differential Evolution 3 (GDE3) Algorithm

An open-source MOEA Java Framework (Hadka, 2015), run on a Dell Precision T1700 workstation running Windows 7 with 3.6 GHz processor and 8 GB RAM, was used to execute the GDE3 algorithm in searching for Pareto solutions. The parameter settings used in this algorithm included a population size of 200, crossover rate of 0.1, and step size of 0.5. A population size of 200 was used because we felt that this would be large enough to provide good coverage of the Pareto "surface", but not so large as to completely overwhelm MPE decision makers who would be responsible for choosing one solution among the Pareto set. The crossover rate and step size values chosen (0.1 and 0.5, respectively) are both within the recommended range for the GDE3 algorithm (Kukkonen & Lampinen, 2005). The algorithm's iterative process is stopped when the number of iterations reaches a predefined limit.

200 solutions were obtained through more than ten hours of computation, and they are plotted using the Visual Co-Plot software (Talby & Raveh, 2015) (Figure 5-4). All 200 points in Figure 5-4 represent MPE resource allocation solutions that are optimal when considering the three objective functions of Equation (5-1). MPE decision makers are expected to choose a solution from this set based on their specific needs for the month, and what trade-offs among the objectives are considered acceptable.

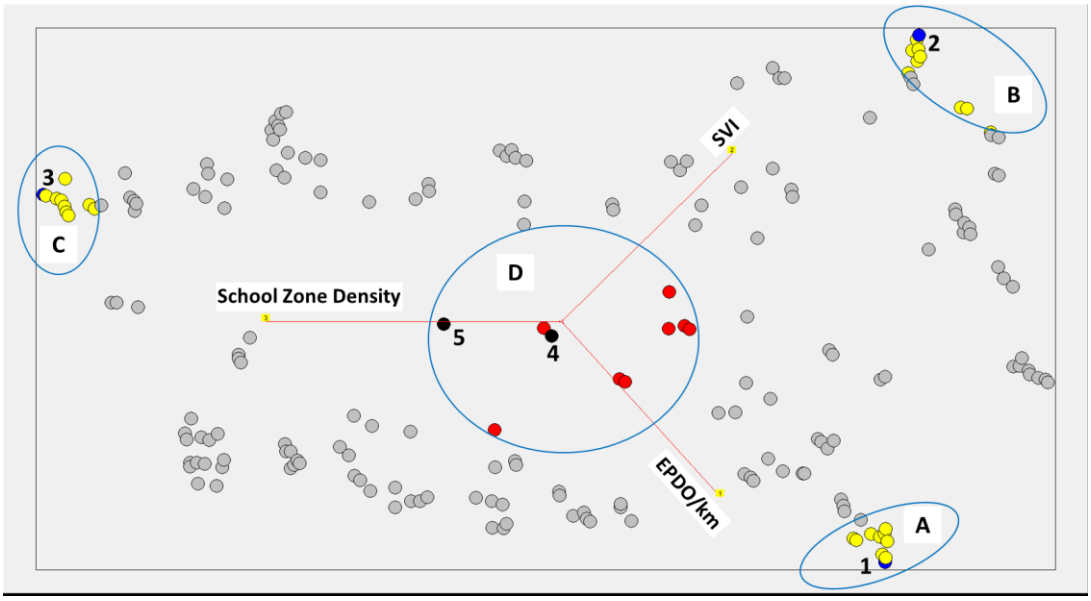


**Figure 5-4 Pareto solutions from the MRA model.**

Each axis in Figure 5-4 represents a metric associated with one of the Equation (5-1) objective functions. There are three circles labeled A, B, and C located beyond the ends of the axes; solutions contained in these circles are identified to have metric values within the top 5% of the metric represented by the axis on which they lie (10 points per group).

In addition, there is one point marked in blue in each circle (labeled 1 in circle A, 2 in circle B, 3 in circle C). These points are located at the extreme ends of each axis and represent the highest value of the corresponding axis metric. Each point represents the result obtained by maximizing one of the three objective functions of Equation (5-1). The values of these three extreme solutions maximizing $EPK$, $SVI$, and $SZD$ are (4599, 239, 470), (3059, 294, 377), and (2449, 237, 1007), respectively. They are the same as the three extreme points (three red asterisks shown in Figure 5-3) found by the weighted sum and epsilon constraint methods. Choice of one of these solutions represents the scenario where agencies have decided to allocate all enforcement resources to maximizing the one corresponding metric alone, without regard for the two others.

The solutions in, say, Group A have high values of the $EPK$ metric (first objective function in Equation (5-1)), but exhibit a range of values of the other two metrics. Selecting a solution contained within one of these groups represents a high-level decision to give greater priority to one deployment criteria over the others.

The points in circle D represent solutions that are the most balanced among the three objectives in Equation (5-1). Specifically, they represent the 10 points (5% of solutions) with the shortest Euclidean distance to the intercept, with the black point labeled “4” being the closest of them all. The solutions in this group were found to have relatively average values for each of the three metrics represented. Therefore, if MPE agencies are aiming to find deployment resource allocation plans that best balance all three deployment objectives, they would consider these solutions.

Solutions (represented by grey points) positioned between any two of the three axes exhibit relatively high values for two of the three metrics. If agencies are looking to fulfill program goals that are more nuanced (i.e., somewhere between the extremes of focusing on one goal versus balancing all of them), they might focus on one of these solutions.

#### 5.4.2.3 Summary

Using the weighted sum and ε-constraint combined methods together allows a much lower computation time compared to the GDE3 algorithm. The combined scalar optimization method is able to find almost all solutions on a PF in a time efficient manner. Conversely, the advantage of using an evolutionary algorithm (e.g., GDE3) is its ability to generate a representative subset of Pareto optimal solutions. From the representative solutions, decision makers can interactively choose answers based on their specific needs and preferences. A clustering method is presented in Section 5.5.1 to help further reduce decision fatigue.

Overall, the model delivers deployment solutions that simultaneously consider the three deployment goals at varying relative degrees of importance. The MPE agencies are provided a diverse set of solutions that yield optimal deployment allocations for any configuration of program priorities called for in a given month. In addition, the variety of options available, even when narrowed down to meet a focused program objective that is in place for longer than a single month, allows agencies to change the deployment plan from month to month within that same objective. This will help to maintain the perception of unpredictability (in time and location) of enforcement activities.

### *5.4.3 Illustrative MRA Model Solution*

Here we present one candidate deployment plan for a typical September in Edmonton. As previously mentioned, September is the beginning of the school year for kindergarten through grade 12 (as well as post-secondary), and the Edmonton MPE program will typically commit a significant portion of enforcement resources to school zones at this time. Therefore, we illustrate the deployment results of one potential deployment plan—solution 5, shown as a black point in circle D, in Figure 5-4. This solution gives the highest priority to the school zone criterion among the solutions in D (recall that D identified the 10 solutions that provide the most balance among the three objectives in Equation (5-1)).

Figure 5-5 shows the neighborhoods identified in the plan, which are colored according to the level of proposed enforcement intensity. In addition, these results are shown against the actual MPE deployment made in Edmonton in September 2014. Specifically, Figure 5-5 uses circles to

represent the MPE sites actually visited by program operators during the month. These circles are differentiated by color and size. Firstly, blue represents a road segment enforcement site located in at least one of the neighborhoods proposed by the plan; grey represents sites actually visited in neighborhoods not included in the candidate plan. Secondly, the size of the circle indicates the amount of enforcement time spent at each site over the month; the larger the circle is, the more time spent at the site. During a typical 10-hour shift in September 2014, operators spent an average of 6.7 hours on enforcement activities (with the balance spent in travel and other non-enforcement activities). However, sites that had less than 6.7 hours of enforcement over the month are represented by a lighter blue or grey colored dot that is not to scale (as they otherwise would be too small to be seen on the map).

**Candidate Deployment Plan Compared to Actual MPE Deployment in Edmonton**

| | High Intensity | Medium Intensity | Low Intensity | Total |
|---|---|---|---|---|
| Number of Neighborhoods | 5 | 17 | 22 | 44 |
| Proposed Number of Shifts | 227 (50%) | 188 (41%) | 43 (9%) | 458 |
| Number of Neighborhoods Covered by MPE | 4 | 17 | 17 | 38 |
| Actual Deployment Hours for Neighborhoods in Candidate Deployment Plan | 365 (19%) | 1147 (58%) | 456 (23%) | 1968 |

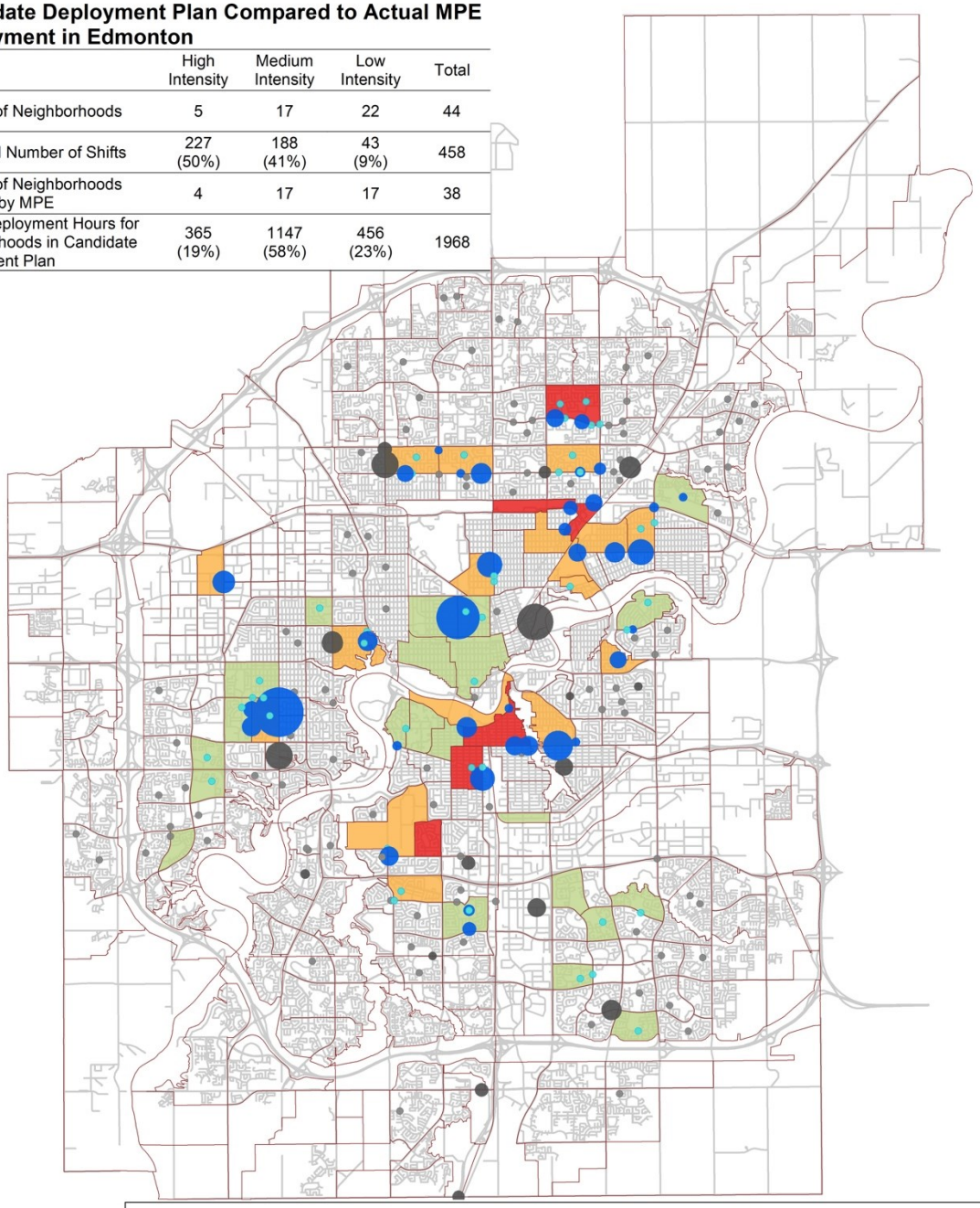


**Figure 5-5 Candidate and actual MPE deployment plans for Edmonton, September 2014.**

As shown in Figure 5-5, 44 neighborhoods were identified in the candidate deployment plan, and were further split into three categories based on the number of shifts assigned to each neighborhood: high, medium, and low enforcement intensity. Firstly, five neighborhoods (shown in red) are high enforcement intensity neighborhoods, which are assigned 227 shifts with each neighborhood allocated an average of 45 shifts in September. The average school zone density of this neighborhood group (based on the 2012-2014 data) is 2.1 school zones/sq.km, which is three times the average of all 388 neighborhoods. The high intensity neighborhoods of this group also have relatively higher values in the other two metrics, showing an average of 8.8 $EPK$ and 0.6 $SVI$ per neighborhood, which are each about twice the average figures for all 388 neighborhoods. This indicates the three program goals are all addressed with a high level of enforcement, but school zones receive the most enforcement, given that the $SZD$ metric for these neighborhoods (equal to triple the average school zone density for all neighborhoods) is optimized in the model.

Secondly, 17 neighborhoods fall within the medium enforcement intensity group and are marked in yellow in Figure 5-5; these were assigned a total of 188 shifts, with each allocated an average of 11 shifts in September. These neighborhoods have mean $SZD$, $EPK$, and $SVI$ values of 1.1 school zones/sq.km, 5.6 EPDO/km, and 0.5 $SVI$. Marked in green are 22 low enforcement intensity neighborhoods. They received the lowest enforcement intensity, with an average of two shifts allocated to each neighborhood during the month. This neighborhood group has 33% higher mean values of school zone density and 20% higher average $EPK$ metric than the medium intensity group, and similar mean $SVI$ value as the medium intensity group. The reason that these neighborhoods are assigned lower enforcement intensity than those in the medium intensity group is due to the values of the constraints in Equation (5-3). The minimum and maximum enforcement shifts allowed to a neighborhood in the MRA model were set using the actual numbers of shifts in 2013 and 2014 (this was discussed in Section 3.2). Most neighborhoods in the medium intensity group are those that had received significant enforcement attention—10 to 51 shifts per neighborhood per month. Therefore, the minimum shifts ($L_n$, Equation (5-3)) for neighborhoods in this group were quite high and they received significant enforcement attention, despite that they also exhibited the lowest average $SZD$ and $EPK$ among the three intensity groups.

In addition to the above discussion of the candidate deployment plan and the results, we provide a comparison to the actual COE MPE deployment made in September 2014. Figure 5-5 shows that

93 (40%) of 231 MPE sites enforced in September 2014 are located in neighborhoods included in the candidate plan; these are represented in blue. The remaining 138 MPE sites (represented as grey circles) in the actual deployment were in neighborhoods not covered by the candidate deployment plan. To compare how well the three goals were addressed simultaneously, we compared the values of the three objective functions in Equation (5-1) for the proposed resource allocation plan and the actual program deployment. To do the comparison, we used hours rather than shifts as the unit for the decision variable $x_n$. In the actual September 2014 deployment, some operators visited enforcement sites belonging to different neighborhoods during one shift; however, the candidate plan assigns an operator to visit sites only within one neighborhood during a shift. Therefore, it is not possible to compare the proposed candidate plan intensity with the actual deployment intensity in terms of shifts per neighborhood. Thus, we multiplied the proposed number of shifts per neighborhood in the candidate plan by 6.7 hours (recall this is the average time actually spent doing enforcement during a shift) and calculated the three metrics (also the objective function values of Equation (5-1)) when $x_n$ is in hours rather than shifts. Then, the actual hours spent enforcing sites in each neighborhood in September 2014 were used to calculate the three resulting metric values for the actual MPE deployment.

The results indicate that the $EPK$, $SVI$, and $SZD$ metrics obtained in the candidate plan are 18%, 11%, and 34% higher than those of the actual September 2014 deployment, respectively. The actual program spent a total of 1968 hours in September 2014 doing mobile photo enforcement in neighborhoods also identified for enforcement in the candidate plan; this accounts for about two-thirds of the total September 2014 enforcement hours (3068 hours). However, the actual program spent significant time in neighborhoods that were identified as warranting medium enforcement intensity in the candidate plan. Neighborhoods that were identified as part of the medium intensity group in the candidate plan were covered a total of 1147 hours in the actual program (which is 58% of the total MPE hours assigned in the candidate plan). In contrast, the actual September 2014 program spent only 19% (365 hours) and 23% (456 hours) of the total hours proposed for neighborhoods in the candidate plan on neighborhoods in the high intensity and low intensity groups, respectively. Conversely, the proposed proportion of total deployment time for high, medium, and low intensity neighborhoods over one month in the candidate plan is 50% (1521 hours), 41% (1259 hours), and 9% (288 hours), with the differences among the neighborhood

groups based on the metrics and model constraints. This comparison indicates that the actual September 2014 deployment did not invest a greater proportion of enforcement resources to neighborhoods that exhibit high levels of enforcement demand, as identified by the metrics of the three program goals considered in this study.

Overall, this application has demonstrated how the proposed model can allocate resources to balance multiple and conflicting program priorities. Visualizing the candidate plan provides agencies with insight into how the deployment goals can be quantitatively mapped to the deployment decisions, which may make the decision process simpler and evidence-based.

## 5.5 PARETO FRONT ANALYSES

This section focuses on how to explore the relationships (tradeoffs) after MRA model solutions are found. Considering that the PF constructed by the weighted sum and ε-constraint methods is more complete than that by the GDE3, we use the solutions generated by the former (as shown in Figure 5-3) as the basis for post-Pareto analyses. Section 5.5.1 explains how to cluster solutions on a PF, and Section 5.5.2 presents tradeoff analysis for the PF results.

### *5.5.1 Pareto Front Clustering*

To be able to analyze the most important and salient features of the PF generated as per Figure 5-3, we adopt the *K*-medoids algorithm (Kaufman & Rousseeuw, 1987) to group similar solutions into clusters and identify a representative solution for each cluster. *K*-medoids is a modification of the well-known *K*-means clustering algorithm (MacQueen & others, 1967), where existing data points are recognized as cluster centers (medoids) rather than creating new cluster centers. To use the existing Pareto-optimal solutions as candidates, we select *K*-medoids to conduct the clustering analysis.

Use of *K*-medoids requires a prior determination of how many data clusters should be created. A common tool for determining the optimal number of clusters is the silhouette index (Rousseeuw, 1987). The silhouette index evaluates the average distance, $a(i)$, between any data point $i$ in cluster $a$ and all other points in the same cluster. It also compares $a(i)$ with the average distance of the point $i$ to all the points of a neighboring cluster $b$, $b(i)$. The silhouette index for point $i$ is

close to one if $b(i)$ is much larger than $a(i)$ (Rousseeuw, 1987) – meaning, cluster $a$ points are closer to one another than points in cluster $b$. The optimal number of clusters is found by maximizing the average silhouette index for all data points.

We implement the R Package 'NbClust' (Charrad, Ghazzali, Boiteau, Niknafs, & Charrad, 2014) to compute the silhouette index for a pre-set range of clusters between 10 and 20 in the data set as illustrated in Figure 5-3. The maximum silhouette index is observed when the number of clusters is set to 12; thus, we took 12 as the best cluster count for our data set. Then clustering is done by a *K*-medoids algorithm in MATLAB with these 12 clusters. The *K*-medoids algorithm identifies 12 medoids and partitions all other solutions around the 12 identified cluster medoids.

Note that the scales of the three metrics (axes) shown in Figure 5-3 are not the same. This is likely to cause the Euclidean distance measure used in the computation of the silhouette index and K-medoids clustering to be dominated by metrics with large values. Therefore, to avoid biases in results due to metric domination, we normalized metric values prior to the computation of the silhouette index and *K*-medoids. The performance of a normalization method that takes the variable range (i.e. the difference between the minimum and maximum values of the variable) as the divisor has been proven to be superior over other normalization methods in cluster analysis (Milligan & Cooper, 1988); therefore, we selected this min-max normalization method to transform the objective vectors of the solutions in Figure 5-3 into the range 0 to 1.

Figure 5-6 shows the rescaled data with the clustering result. The crosses in Figure 5-6 represent each of the 12 cluster medoids. Figure 5-6 also differentiates solution clusters by colors. Table 5-2 summarizes the descriptive statistics for the 12 clusters. The size of each cluster is given. The range of objective vectors for the solutions in each cluster and the objective vectors of the 12 medoids are also indicated in Table 5-2.

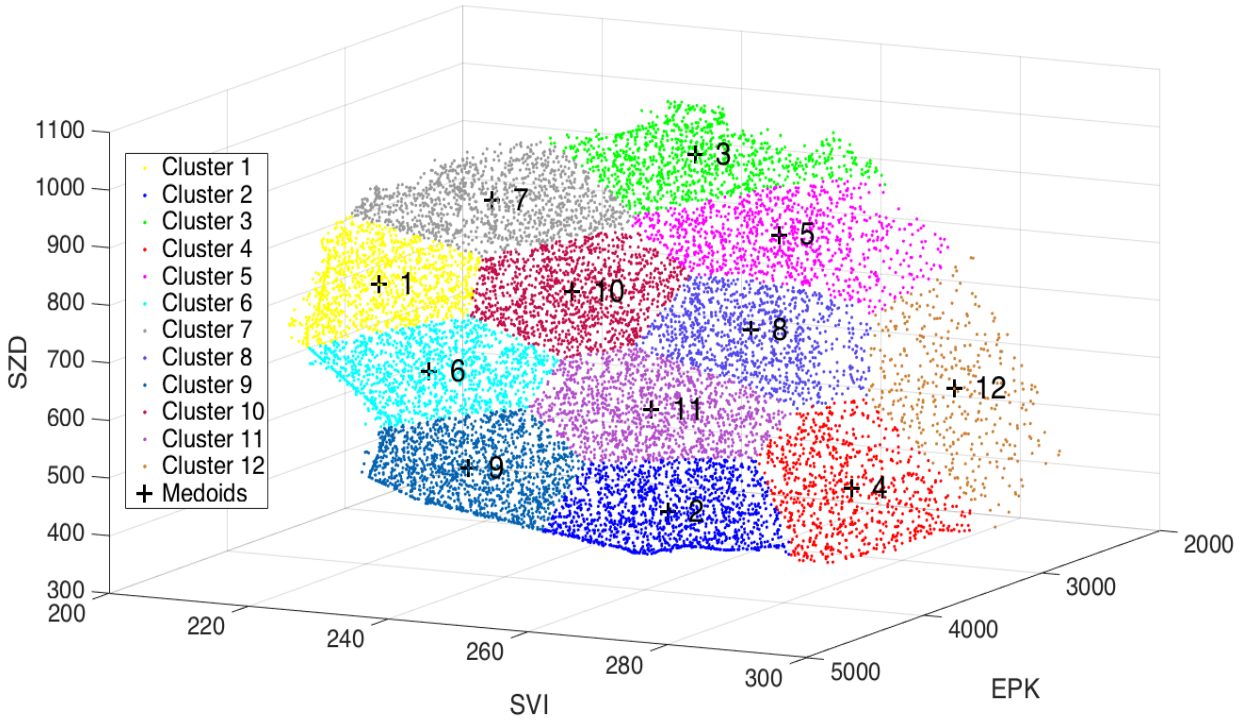


**Figure 5-6 Clustering analysis of the Pareto front of the MRA example.**

**Table 5-2 Statistical Summary of the Objective Vectors in the Twelve Partitioned Clusters**

| Clusters | No. of Solutions | EPK | | | SVI | | | SZD | | |
|---|---|---|---|---|---|---|---|---|---|---|
| | | Medoid | Min | Max | Medoid | Min | Max | Medoid | Min | Max |
| **1** | 1175 | 3865 | 3555 | 4172 | 219 | 208 | 233 | 774 | 683 | 859 |
| **2** | 1381 | 4416 | 4128 | 4572 | 270 | 255 | 284 | 477 | 402 | 557 |
| **3** | 1028 | 2850 | 2432 | 3249 | 248 | 228 | 269 | 957 | 882 | 1007 |
| **4** | 762 | 3813 | 3228 | 4184 | 286 | 278 | 294 | 491 | 378 | 623 |
| **5** | 1008 | 3131 | 2440 | 3467 | 264 | 246 | 279 | 857 | 740 | 922 |
| **6** | 1268 | 4209 | 3943 | 4438 | 233 | 215 | 248 | 663 | 581 | 742 |
| **7** | 1186 | 3371 | 2928 | 3651 | 227 | 210 | 246 | 893 | 820 | 960 |
| **8** | 1001 | 3665 | 3225 | 3902 | 270 | 257 | 283 | 736 | 624 | 803 |
| **9** | 1502 | 4503 | 4282 | 4599 | 243 | 228 | 258 | 530 | 440 | 618 |
| **10** | 1201 | 3727 | 3351 | 4016 | 245 | 231 | 258 | 779 | 693 | 857 |
| **11** | 1313 | 4128 | 3877 | 4360 | 263 | 248 | 279 | 626 | 546 | 706 |
| **12** | 385 | 2944 | 2433 | 3463 | 286 | 279 | 294 | 601 | 377 | 785 |

From Table 5-2, one can observe an average of about 1,100 solutions per cluster. In each cluster, the objective function values of the solutions with respect to $EPK$, $SVI$, and $SZD$ vary within ranges of 688, 28, and 190, respectively. It is observed that the average differences in the three objective function values of $EPK$, $SVI$, and $SZD$ between the medoid and the farthest solution in the same cluster is 344, 14, and 95, respectively. These ranges are about half that of the ranges of the objective vectors within each cluster. Thus, we can conclude that the 12 medoids are located in the relative center of each cluster, and are a reasonable representation of their respective cluster. An agency managing an MPE program could take these medoids as the initial deployment candidate options.

Table 5-2 shows that candidate options (or medoids) #1, #6, #7, and #9 have relatively low objective function values on the $SVI$ axis but high values on the $EPK$ axis. Therefore, these solutions lie on the left-hand side of the PF as illustrated in Figure 5-6. The average objective

function values of these solutions in $SVI$ and $EPK$ are 231 and 3,987, which fall in the first third of the $SVI$-axis scale (208 to 294) and in the last third of the $EPK$-axis scale (2,432 to 4,599), respectively. By choosing these solutions, one gives priority to the $EPK$ objective (enforcing high collision sites) while largely ignoring $SVI$ (enforcing high speed violation sites).

Conversely, candidate solutions occupying the PF's right-hand side on Figure 5-6, such as solutions #4, #5, and #12, show low objective function values for $EPK$ but high values for $SVI$, with average values of 3,296 (two-fifths of the $EPK$ scale) and 279 (four-fifths of the $SVI$ scale), respectively. Therefore, the solutions on the right-hand side of Figure 5-6 give enforcement attention to high speed violation sites, regardless of the locations with high collision frequencies.

Other solutions in the middle of the PF have relatively average values in both $EPK$ and $SVI$ objectives (3757 and 259), indicating a balance of the two deployment goals. Specifically, solution #3 (in the middle top of the PF in Figure 5-6) shows the highest $SZD$ objective value (957) among the 12 medoids. This solution assigns school zone enforcement the greatest priority, while maintaining relatively average enforcement intensity at high collision sites and high speed violation sites. In contrast, solution #2 (which lies in the middle bottom of the PF) presents the lowest $SZD$ value (477) among all the medoids; therefore, it gives school zone enforcement the lowest priority of the three objectives. Solutions #8, #10, and #11 are in the relative center of the PF. Their average values in $EPK$, $SVI$, and $SZD$ are 3,840, 259, and 714, which lie at the midpoints of the corresponding axis' intervals. These types of solutions represent a balance of the three conflicting enforcement deployment goals; they almost reach the optimal value for each. When MPE managing agencies have no preference among the three enforcement priorities, these solutions may be of most interest.

### 5.5.2 Pareto Front Tradeoff Analysis

After making an initial selection from the clustering result, if MPE agencies want to move from the initial selection to another solution on the PF that better suits their requirements, it would be helpful to understand what the tradeoffs are (with respect to the three objectives) in moving to another solution on the PF. In other words, if one wanted to increase attainment of one objective, how much would one need to sacrifice in the other two objectives to achieve this? In this section

we present a function fit to the Pareto data points found in Figure 5-3. Note that the data points used in this section are not normalized. The (continuous) PF fitting function can be used to quantitatively evaluate the tradeoffs between the deployment objectives as one moves between (discrete) solutions on the PF.

#### 5.5.2.1 Pareto Front Fitting Function

A (continuous) polynomial function is estimated on the discrete multi-objective optimization solutions comprising the PF of Figure 5-3. A polynomial functional form is chosen because of its simple implementation and its ability to approximate the true PF (Fang, Rais-Rohani, Liu, & Horstemeyer, 2005; Goel et al., 2007). However, other fitting techniques, such as exponential and translog functions, may also be suitable given different distributions of optimized solutions.

In a multi-objective problem, such as the MRA example (with three objectives $EPK$, $SVI$, and $SZD$), one objective should be chosen as the dependent variable of the PF fitting function while the remaining objectives are independent variables (Goel et al., 2007). To facilitate this decision, we created three quadratic polynomial functions for the three possible variable configurations using the response surface method. The quadratic polynomial is one of the most commonly used models for the response surface method, to describe the relationship between dependent and independent variables (Myers, Montgomery, & Anderson-Cook, 2016). The model is useful for generating a response surface that is reasonably close to the fitted data points (Box & Wilson, 1992), and such a model is easy to estimate and apply. Table 5-3 shows the $R^2$ values for each of these three functions, indicating the goodness of fit of each function to the Pareto data points shown in Figure 5-3. Because polynomial regression is a special case of linear regression, in that it is linear in the regression coefficients on the dependent variables, it is appropriate to use $R^2$ to determine model goodness-of-fit (Ostertagová, 2012).

**Table 5-3 R-squared Values of the Quadratic Pareto Front Fitting Function, by Variable Configurations**

| | $EPK = f(SZD, SVI)$ | $SVI = f(EPK, SZD)$ | $SZD = f(EPK, SVI)$ |
|---|---|---|---|
| $R^2$ | 0.939 | 0.899 | 0.968 |

In Table 5-3, the $R^2$ value of $SZD = f(EPK, SVI)$ is the highest (at 0.968) among all the three fitted functions. This suggests that the function taking the $SZD$ metric as dependent variable is the best-fitting function for the MRA Pareto points generated, compared to the functions generated by the other two variable configurations. Furthermore, the $R^2$ value of this best-fitting function is close to one, suggesting that a quadratic polynomial function is an appropriate fit for the identified Pareto data points. Therefore, the function $SZD = f(EPK, SVI)$ is selected to represent the PF of the MRA example, and its estimated form is shown in Equation (5-12). All estimated parameters are statistically significant at the 95% confidence level.

$$SZD = -9.63e^{-5} \cdot EPK^2 + 0.001 \cdot EPK \cdot SVI + 0.149 \cdot EPK - 0.093 \cdot SVI^2 + 38.408 \cdot SVI - 3360.688 \quad (5\text{-}12)$$

Figure 5-7 shows a plot of the PF fitting function of Equation (5-12) as a grey surface, and compares it against the set of Pareto-optimal solutions (first shown in Figure 5-3) used to fit the function. It is observed that the function fits the plotted Pareto data points closely (as the $R^2$ value would indicate).

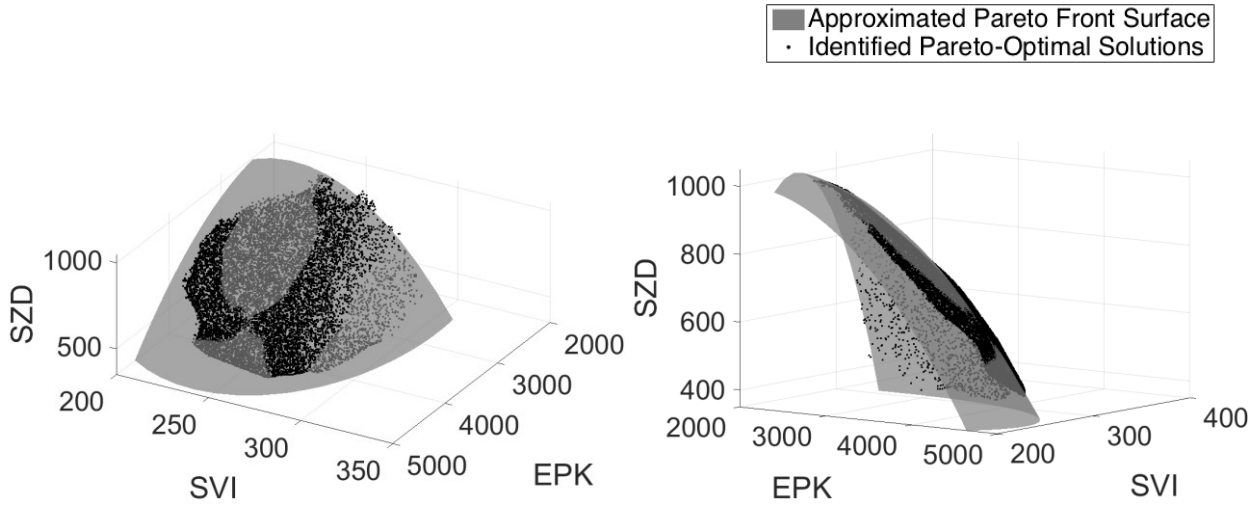


**(a) View 1** **(b) View 2**

**Figure 5-7 Pareto-optimal solutions and the fitted Pareto surface, for the MRA example.**

We observe a downward bend at the top of the fitted Pareto surface in Figure 5-7(b). This bending is attributed to the fact that the graph of a quadratic polynomial is a parabola. Since the coefficients

of the function terms with highest degree in Equation (5-12) are negative, the function graph will always decrease exponentially at its edges. Therefore, it is important to note that the PF fitting function should only be used within the range of Pareto data point values taken to fit the function.

#### 5.5.2.2 Illustrative Example of the Objective Tradeoff Analysis

Suppose Edmonton's MPE program manager (i.e. the managing agency) had chosen solution 3 from the 12 medoids identified in Figure 5-6, for the month of September 2014. According to Table 5-2, among the 12 medoids, this solution reflects an elevated priority to have enforcement presence in school zones during the start of the school year, while also maintaining some coverage of high collision and high speed violation sites. This solution has the highest $SZD$ value (at 957) of the 12 medoids, with relatively average values of $EPK$ and $SVI$ at 2,850 and 248, respectively. The three metric values of solution 3 represent an initial decision, which assigns 957, 2850, and 248 enforcement coverage units in school zones, high collision sites, and high speed violation sites, respectively.

We assess the tradeoffs between each pair of the three metrics in solution 3, where the pairwise tradeoff results are benchmarked against set values of the 3rd metric. Figure 5-8 illustrates the three cross sections of the PF fitting function along each of the three axes, viewed in solution 3. Curves in Figure 5-8(a), (b), (c) are function contour lines at the solution 3's objective values ($SVI = 248$, $EPK = 2{,}850$, and $SZD = 957$). Hence, these curves depict how a change in one objective function value of solution 3 impacts the other function values.

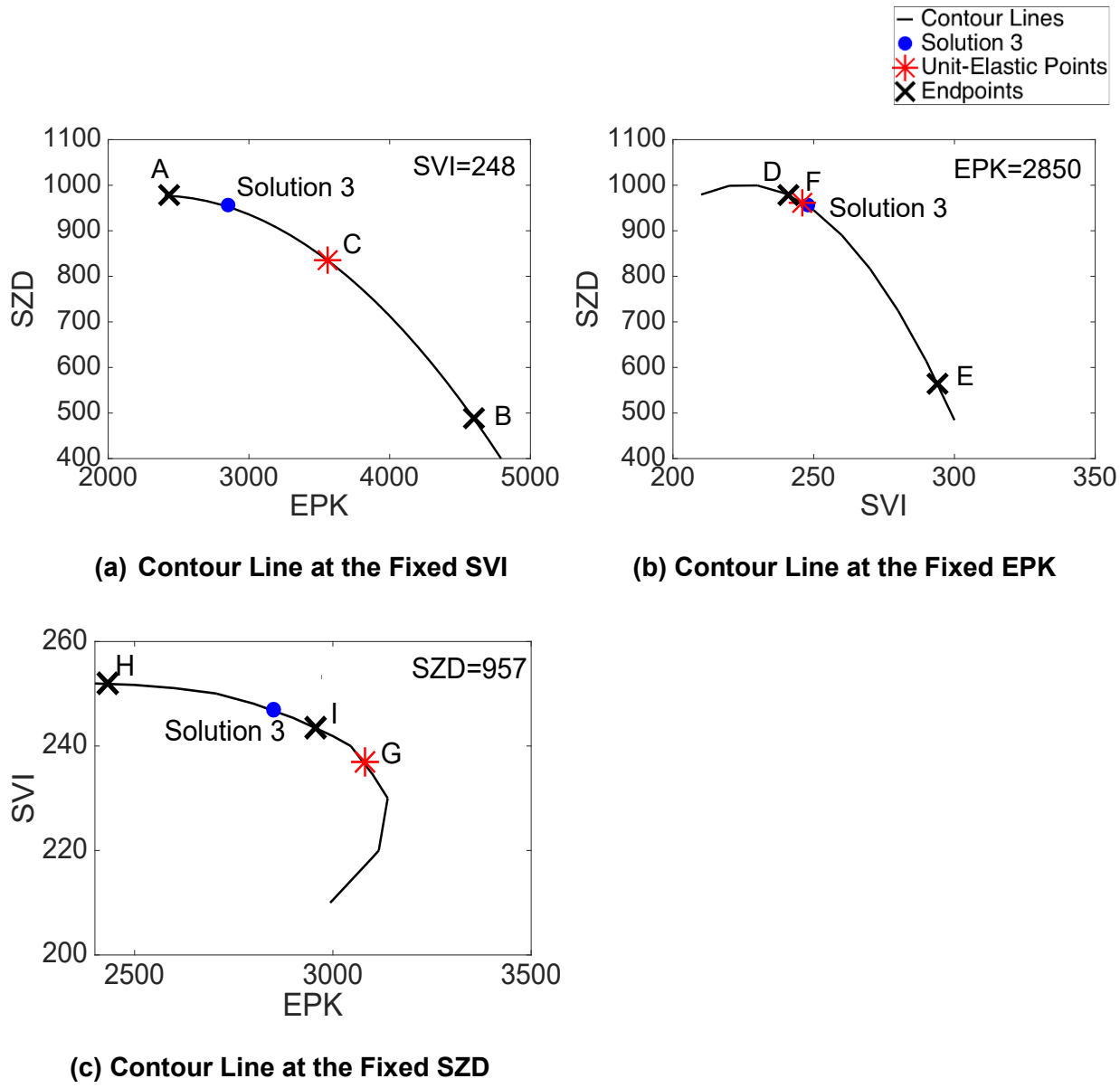


**(a) Contour Line at the Fixed SVI**

**(b) Contour Line at the Fixed EPK**

**(c) Contour Line at the Fixed SZD**

**Figure 5-8 Contours of the Pareto fitting function at MRA example Solution 3.**

Note that as discussed in Section 5.5.2.1, the polynomial function is only valid over the range of Pareto data points used to fit it. Therefore, based on the range of the found Pareto data points in the three axes (2,432-4,599 $EPK$, 208-294 $SVI$, 377-1,007 $SZD$), we found two endpoints on each curve, between which the curve is considered a valid description of objective tradeoff. The two endpoints of each curve are marked as crosses and labeled A and B, D and E, H and I, in Figure 5-8(a), (b), and (c) respectively. The three components of the objective vectors for these endpoints are shown in Table 5-4.

**Table 5-4 Objective Vectors of the Endpoints, the Unit-Elastic Points, and the Illustrative Candidate Point on the Tradeoff Curves**

| Point Labels | Endpoint, unit-elastic point, or illustrative point | EPK | SVI | SZD |
|---|---|---|---|---|
| **A** | Endpoint | 2432 | 248 | 978 |
| **B** | Endpoint | 4599 | 248 | 489 |
| **C** | Unit-Elastic Point | 3561 | 248 | 836 |
| **D** | Endpoint | 2850 | 241 | 979 |
| **E** | Endpoint | 2850 | 294 | 564 |
| **F** | Unit-Elastic Point | 2850 | 246 | 961 |
| **H** | Endpoint | 2432 | 252 | 957 |
| **I** | Endpoint | 2956 | 244 | 957 |
| **G** | Unit-Elastic Point | 3081 | 238 | 957 |
| **Solution 3** | Illustrative Point | 2850 | 248 | 954 |

The three plots in Figure 5-8 show that as one objective decreases, the other two objectives increase. The average tradeoff rate (i.e., the slope of the curves) between $SZD$ and $EPK$, $SZD$ and $SVI$, and $SVI$ and $EPK$ is -0.2, -7.8, and -0.02, respectively. This means that for everyone unit decrease in $SZD$ (i.e., one less enforcement coverage level in school zones), $EPK$ increases by 0.2 (or, 0.2 more enforcement coverage levels at high collision sites) when $SVI$ is fixed at 248 (enforcement coverage units at high speed violation sites). However, if $EPK$ remains at 2850, $SVI$ increases by 7.8 for each reduced unit in $SZD$. Additionally, a one unit decrease in $SVI$ leads to a 0.02 increase in $EPK$ when $SZD = 957$. It is difficult for MPE program decision makers to intuitively interpret the trade-off between more than two objectives. Therefore, these obtained pairwise tradeoff values provide useful information and support for multi-objective decision-making about MPE resource allocation. Specifically, decision makers can learn the result of changing a decision (choose a new PF solution), that is, when the expectations for the 3rd objective are met, how they adjust the resource allocation between the remaining two objectives.

As the ranges of the three objective values are different, the concept of curve elasticity is introduced to further understand how responsive (in a proportional manner) one objective is to a change in another objective. Elasticity is a measure that evaluates the proportional change of the abscissa divided by the proportional change of the ordinate. The metric on the abscissa is classified as being ordinate metric elastic if elasticity is greater than one, unit ordinate metric elastic if elasticity is equal to one, or ordinate metric inelastic if elasticity is less than one. The ordinate metric elasticity of the abscissa metric at a specific point $(x^*, y^*)$ on the curve is expressed by Equation (5-13), which computes the reciprocal of the curve's derivative at that point multiplied by the ratio of $y^*$ to $x^*$.

$$e = \frac{dx^*}{dy^*} \cdot \frac{y^*}{x^*} \tag{5-13}$$

As can be seen from Figure 5-8, as abscissa values increase, the slopes of each of the three curves become steeper, indicating a continuously decreasing elasticity of each curve in the abscissa direction. Thus, by manipulating Equation (5-13) and the curve function (i.e., the PF fitting function holding one variable fixed), we found the location of the unit elastic point on each curve. Specifically, the unit-elastic points in Figure 5-8(a), (b), (c) are marked as asterisks and labeled as C, F, G, respectively. Table 5-4 shows their objective function values. These unit-elastic points help divide the curve between two endpoints into two parts. The curve that lies to the left of the unit-elastic point is elastic, whereas the curve to the right side of the unit-elastic point is inelastic.

In Figure 5-8(a), it is observed that $EPK$ is elastic to the changes in $SZD$ along the part AC of the curve where $EPK$ is in the range of 2,432-3,561, and $SZD$ is in the range of 836-978 as shown in Table 5-4. Conversely, on the curve between points C and B, where $EPK$ lies between 3,561 and 4,599 and $SZD$ is between 489 and 836, $EPK$ is inelastic regardless of whether $SZD$ changes. The average elasticities of curve segments AC and CB are -3.2 and -0.7, respectively. This indicates that $EPK$ changes at 3.2 times the rate of $SZD$ change on the AC curve segment, but the rate of change of $EPK$ is reduced to 0.7 times the rate of change of $SZD$ on the CB curve segment. Since solution 3 is positioned on the AC curve segment, reducing solution 3's $SZD$ value by a small quantity, say 10%, may yield an approximately 32% increase in $EPK$. This tradeoff could be highly attractive to MPE agencies that are looking to reduce traffic collisions.

In Figure 5-8(b), the unit-elastic point F also specifies the elastic and inelastic regions for the tradeoff of the $SVI$ and $SZD$. It is worth noting that the endpoint D and unit-elastic point F are very close together. As seen in Table 5-4, they have a difference of 5 and 18 respectively on the $SVI$ and $SZD$ axes, accounting for only 6% and 3% of the corresponding axis interval. Therefore, the curve portion DF may be negligible, leading to the fact that $SVI$ is almost always inelastic in $SZD$. The reason that $SVI$ almost always responds weakly to changes in $SZD$ may be due to the fact that neighborhoods with relatively high school zone densities also experience more speed violations (in turn, due to lowered area speed limits). According to data from 2012 to 2014, Edmonton neighborhoods with the top 10% of school densities (the average $SZD$ for these neighborhoods is 2.74) exhibited an average of 43% of speeding violations, 30% higher than the average of all city neighborhoods. Reducing MPE resource allocations to neighborhoods with more school zones may also have the secondary effect of reducing MPE resources to neighborhoods with high speed violations (because these neighborhoods are the same). It can be seen that solution 3 is on the FE curve segment with an average elasticity of -0.47. This suggests that a 10% decrease in $SZD$ results in only about a 5% rise in $SVI$. Consequently, at solution 3, it may not be productive to reduce $SZD$ value to gain the expected increase in $SVI$.

Contrary to the inelasticity of $SVI$ and $SZD$, in Figure 5-8(c) it is observed from the position of the unit-elastic point G (located to the right of the curve segment HI) that $EPK$ is always $SVI$ elastic. The average elasticity between points H and I on the curve is -6.8, indicating that a 10% drop in $SVI$ will result in a 68% increase in $EPK$. This high elasticity implies the strong responsiveness of $EPK$ to decreases in $SVI$. However, between solution 3 and endpoint I, the $SVI$ value that can be traded-off for $EPK$ is very limited, only 4 in $SVI$ (as shown in Table 5-4).

Based on the tradeoff and elasticity results observed above, MPE agencies may want to locate a more suitable solution (other than solution 3) with the desired level for all objectives on the fitted Pareto surface. Suppose the manager decides to relax $SZD$ by 100 (an approximately 10% decrease) and $SVI$ by 4 (approximately 2% decrease) to improve $EPK$. By entering the (relaxed) values of $SZD$ (854) and $SVI$ (244) to the PF fitting function, we can obtain an $EPK$ value of 3,522, which is an approximately 25% increase in $EPK$ compared to that of solution 3 (we will refer this point on the fitted Pareto surface as solution $X$). This procedure can be continued until the program

manager obtains a solution that best satisfies their needs. Then, one of the Pareto-optimal solutions (Figure 5-3) closest to their preferred solution determined on the Pareto surface can be selected. A search of the nearest Pareto-optimal solution to solution $X$ is conducted and the objective values of that Pareto-optimal solution for $EPK$, $SVI$, $SZD$ are obtained (3477, 243, 839, respectively). The Pareto-optimal solution found nearest to $X$ deviates from $X$ by values of 45 ($EPK$), 1 ($SVI$), and 15 ($SZD$). Choosing this Pareto-optimal solution will generate a tradeoff that is slightly different from the tradeoff result estimated by the PF fitting function; however, the new tradeoff may not satisfy the desired tradeoff level. Therefore, it is recommended that in future research, we should further investigate how to identify the actual Pareto-optimal solution that best matches the solution found on the tradeoff surface.

#### 5.5.2.3 GDE3 Solution Assessment

In Section 5.4.2.2, the GDE3 algorithm produced a set of 200 Pareto non-dominated solutions (see Figure 5-4), when the termination criterion (i.e., the predefined bound for the number of iterations) was met. These 200 solutions are approximations of the true Pareto optimal solutions. This section evaluates the optimality of the 200 GDE3 solutions, by comparing the GDE3 solutions with the Pareto optimal surface fitted by Equation (5-12).

The most common and simplest measure used in the literature for quantifying the quality of Pareto approximate solutions is the generational distance. General distance (Van Veldhuizen & Lamont, 1998) measures the shortest distance from each approximate solution to the Pareto optimal surface, and then computes the average of these shortest distances. The smaller the generational distance is, the better the quality of approximate solutions.

We measure the shortest distance between the 200 GDE3 solutions and the fitted surface through MATLAB's fmincon function. We set the variables of the fmincon function to any point on the surface. The function objective is to find the surface points closest to the GDE3 points, subject to the surface Equation (5-12). The shortest distance measured between the two sets of points varies between 0.3 and 147. Their average value (i.e., generational distance) is 55, accounting for 1.2%, 5.7%, and 18.7% of the maximum of the three metrics $EPK$ (4599), $SZD$ (957), and $SVI$ (294), respectively.

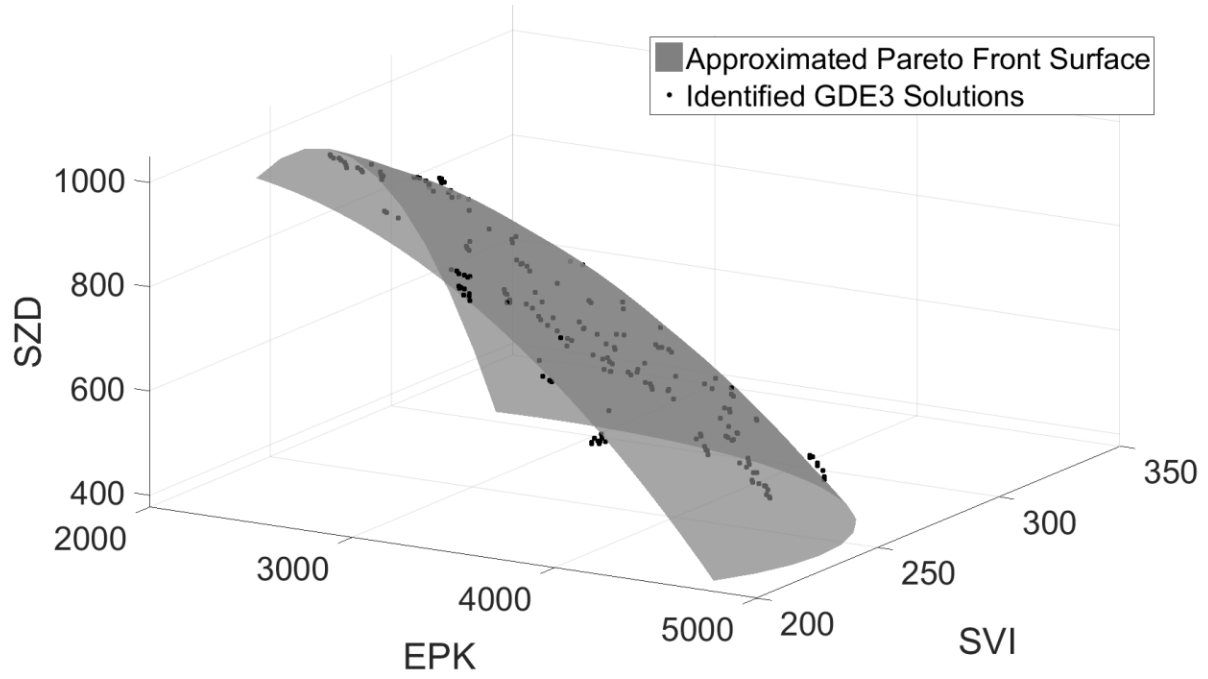


**Figure 5-9 200 GDE3 solutions and the fitted Pareto surface, for the MRA example.**

In addition, Figure 5-9 depicts the relative distance between the 200 GDE3 solutions and the surface. As seen in Figure 5-9, the GDE3 solutions approach closely to the surface, suggesting that the GDE3 solutions are close approximations to the exact solutions.

## 5.6 SUMMARY

This chapter presents a neighborhood-level resource allocation model for MPE. The model uses multi-objective linear programming to determine how enforcement resources may be allocated to city neighborhoods, when multiple deployment criteria must be considered. The model was applied to a case study of an MPE program operating in Edmonton. The model generated a set of resource allocation solutions for the program's deployment in September 2014, while simultaneously optimizing three metrics: equivalent property-damage-only collision frequency per kilometer ($EPK$), speed violation indicator ($SVI$), and school zone density ($SZD$).

Combining two scalar optimization methods (weighted sum and ε-constraint) were applicable to generate a nearly complete PF (13,210 exact solutions) over multi-dimensions in a time-efficient

manner. In contrast, an evolutionary algorithm can be used to determine a specified number of approximate solutions (we found 200 GDE3 solutions in this chapter), which can greatly reduce decision fatigue. Also, $K$-medoids clustering was used to choose 12 existing Pareto-optimal solutions as representative solutions from which the MPE agency can initially choose a solution that suits their preference.

We created a quadratic polynomial function to model the relationship between the dependent variable ($SZD$) and the independent variables ($EPK$ and $SVI$). We studied the objective relationship at a representative solution. In this study, tradeoff rate results showed that one less enforcement coverage unit in school zones will lead to 0.2 or 7.8 more enforcement coverage units at high collision sites and high speed violation sites, respectively. Additionally, every reduction in one enforcement unit coverage at high speed violation sites increases enforcement coverage at high collision sites by 0.02 units. The ability to quantitatively assess tradeoffs among objectives, allows MPE agencies to understand the amount of exchange between objective values and how responsive a change in one objective is in relation to others, when moving along the PF.

Finally, one candidate deployment plan designed for September 2014 was plotted in GIS and assessed, alongside the actual program deployment results for the same month. This candidate plan allocates one month of shifts to 44 Edmonton neighborhoods, which exhibit high enforcement demand according to the aims set out for the month. The aim, in this case, was to dedicate more enforcement resources to neighborhoods with higher school zone densities, while still giving significant consideration to sites with higher collision and speed violation metrics. Because the proposed model does not directly account for the purpose of increasing the program's perception of randomness, the resources were utilized to focus on a limited number of neighborhoods that warranted high enforcement demand according to the three program goals. The average metric values of these 44 neighborhoods are at least about 60% higher than the average metric values for all 388 neighborhoods across the city. The candidate deployment plan is shown to efficiently utilize one month's worth of shifts by varying the enforcement intensity (i.e., number of shifts allocated) for different levels of enforcement demand (as identified by the metrics) associated with the program goals: after taking special deployment considerations into account, the higher the neighborhood metrics, the higher the number of shifts assigned to the neighborhoods.

# 6 MPE RESOURCE SCHEDULING MODEL

This chapter presents a model for scheduling MPE resources. The MPE resource scheduling (MRS) model described in this chapter schedules operators over the course of a month to groups of enforcement sites, based on the neighborhood allocation determined in the previous stage (Chapter 5). The key feature of the MRS model is that it considers the time halo effects of enforcement; our model uses binary integer programming to minimize visits to an enforcement task (to visit a site group in a shift) over consecutive shifts.

The model was applied to data obtained from the MPE program in Edmonton, Canada. Because this is a large-scale integer programming problem, we solve it with the Dantzig-Wolfe decomposition and column generation approaches, which have been applied successfully to scheduling problems. This scheduling model is the final step in an MPE program that can provide enforcement agencies with a tool to systematically assign limited resources, with greater efficacy towards achieving program-level objectives such as reducing speeding, reducing collisions, and providing enforcement presence in areas with many vulnerable pedestrians (i.e. school zones).

## 6.1 INTRODUCTION

An MPE program must schedule enforcement operators and equipment to sites located throughout a city or region. Typically, there are far fewer operators and equipment than sites requiring enforcement attention. Operators work in shifts, during which they must visit a set of sites (referred to as location visit task). This chapter presents an MPE resource scheduling (MRS) model that allocates operator shifts among location visit tasks over a set period (one month).

The proposed MRS model comprises the next stage after the Chapter 5 MRA model. The MRA model employed multi-objective optimization to allocate MPE resources to city neighborhoods, using multiple enforcement coverage goals simultaneously. We developed the MRS model to schedule neighborhood-level resources to location visit tasks, in three steps: 1) determine location visit tasks in neighborhoods, 2) distribute operators to location visit tasks, and 3) create a schedule. In Step 1 we combine all predetermined enforcement sites in each neighborhood into sets. Each set is a candidate location visit task for an operator's shift. In Step 2 we distribute the shifts

allocated to each neighborhood for a given month (resulting from the MRA model of Chapter 5) to those candidate location visit tasks. Shifts are proportionally distributed to tasks based on weights assigned to each task. These weights are a direct reflection of the enforcement need at the locations within the task, quantified by the same metrics used to assign resources to neighborhoods in Chapter 5.

In Step 3, we schedule operator shifts considering enforcement time halo effects. The time halo effect can last several hours to days (Hauer, Ahlin, & Bowser, 1982; Armour, 1986; Cairney, 1988; Vaa, 1997; Gouda & El-Basyouny, 2016). As a result, it is inefficient to send operators to a location where the time halo effect remains. The scheduling model's objective is to minimize instances of resources being allocated to tasks including locations where a time halo effect remains. To solve, this binary integer programming model is first reformulated using the Dantzig-Wolfe decomposition algorithm as a set partitioning problem—a formulation used for many real-life resource scheduling problems. The reformulated problem is then solved using a column generation approach, which has been combined with the Dantzig-Wolfe decomposition to efficiently solve integer programming problems with a large number of variables.

The MRS model was implemented to one neighborhood-level deployment plan (Figure 5-5) output from the MRA model. The result is a schedule of operators assigned to perform a location visit task during each shift, for morning and afternoon shifts throughout a month of enforcement.

## 6.2 MODEL FORMULATION

Our MRS model is the second stage of an MPE deployment model. The 1st stage model (Chapter 5) allocates enforcement resources to city neighborhoods, by maximizing enforcement coverage of neighborhoods based on three chosen metrics: 1) equivalent property-damage-only (EPDO) collision frequency per km, 2) speed violation indicators, and 3) school zone density. This model identifies neighborhoods to send enforcement resources over a one-month period. The MRS model takes these allocation results and further schedules resources. The MRS model assigns resources over both space and time; it assigns resources to enforcement location visit tasks within each neighborhood over a month-long period, while accounting for enforcement time-halo effects. The model minimizes the number of sequential visits to a given task (to, more generally, minimize

"wasting" the possible effects of an enforcement time halo). The steps of our scheduling model are shown in Figure 6-1.

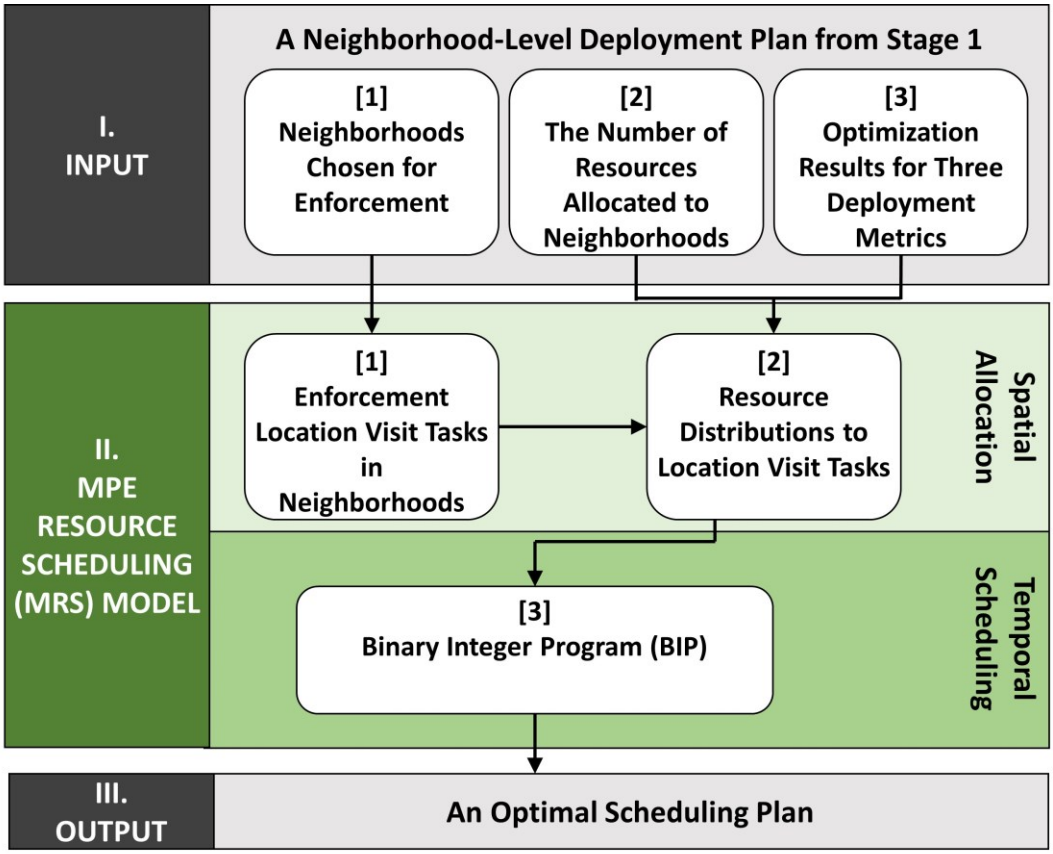


**Figure 6-1 MPE resource scheduling model.**

As seen from Figure 6-1, the neighborhood-level deployment plan of the 1st stage MRA model is input to the MRS model. This neighborhood-level plan contains three elements for input to the scheduling model: 1) the neighborhoods to receive enforcement resources, 2) the number of resources allocated to these neighborhoods, and 3) the optimization results (i.e. values of the three metrics considered).

The MRS model requires two preprocessing steps to further distribute neighborhood-level resource to enforcement location visit tasks and one binary integer programming (BIP) step to schedule resources to tasks, as illustrated in the green box of Figure 6-1. The first preprocessing step is to identify enforcement location visit tasks for each chosen neighborhood. A task is defined to be a group of predetermined enforcement sites (road segments) that can be visited by an enforcement

operator in a single shift. The second preprocessing step involves distributing the resources allocated to each neighborhood to different tasks within the neighborhood. This resource distribution is commensurate to each task's enforcement demand, measured by the three deployment metrics used in Stage 1. These two preprocessing steps above address the spatial allocation problem—allocating neighborhood-level resources to location visit tasks. The next step of the model focuses on scheduling operator work times to the tasks on the planning horizon. This is performed using a binary integer program (BIP) that minimizes time halo effect violations. The details of the preprocessing steps and BIP, are described in Sections 6.2.1 and 6.2.2. The final output is an enforcement activity timetable determining when, where, and how many enforcement operators are assigned to specific tasks over the course of a month.

### *6.2.1 Preprocessing Steps*

We developed the MRS model of Figure 6-1 based on the COEs MPE program parameters and requirements. This section describes the two preprocessing steps.

#### 6.2.1.1 Enforcement Location Visit Tasks in Neighborhoods

The COE's MPE program schedules operators into two work shifts per day: a morning shift from 06:00-16:00 and an afternoon shift from 16:00-02:00. An MPE program operator typically visits several enforcement sites during a single work shift. Hence, to assign operators to enforcement sites within each neighborhood, we first combined individual sites from a neighborhood into visiting groups.

Two assumptions are made before combining the sites. First, all operators visit the same number of sites in a shift. Second, operators cannot visit a site twice in one shift. With these two requirements, all possible combinations of (pre-approved) enforcement sites in each neighborhood were enumerated. Consequently, these site combinations (hereafter called location visit tasks) in each neighborhood serve as allocation units for receiving neighborhood resources (again, assigned in Chapter 5). This allocation unit can be changed to accommodate different MPE program operations needs and requirements. Equation (6-1) represents the possible tasks in each neighborhood in a matrix format, for input into the BIP optimization model.

$$C^n = \left\{ c_{mj} = \begin{cases} 1 & \text{if the } m^{th} \text{ site is used in} \\ & \text{the } j^{th} \text{ task} \\ 0 & \text{otherwise} \end{cases}, \ \forall m \in M_n, \forall j \in J_n \right\}, \ \forall n \in N^{(1)} \qquad (6\text{-}1)$$

Where:

| | | |
|---|---|---|
| $d$ | = | number of sites to be visited per operator per shift |
| $m$ | = | enforcement site index |
| $n$ | = | neighborhood index |
| $N^{(1)}$ | = | subset of neighborhoods identified in Stage 1 |
| $M_n$ | = | number of predetermined enforcement sites included in neighborhood $n$ |
| $j$ | = | task index |
| $J_n$ | = | number of tasks included in neighborhood $n$ |
| $c_{mj}$ | = | 1 if the $m^{th}$ site is used in the $j^{th}$ candidate task, and 0 otherwise |
| $C^n$ | = | a $M_n \times J_n$ binary matrix containing all the possible tasks for neighborhood $n$ |

As defined in Equation (6-1), each neighborhood $n$ in set $N^{(1)}$ has a matrix $C^n$. The rows of $C^n$ $(M_n)$ represent the number of predetermined enforcement sites in neighborhood $n$, while the number of columns $(J_n)$ is the number of location visit tasks identified for neighborhood $n$. $J_n$ is equal to the number of combinations $\binom{M_n}{d}$ where the total of predetermined sites $(M_n)$ of neighborhood $n$ is not less than $d$ (the number of sites to be visited per operator per shift). Otherwise, $J_n = 1$. Matrix $C^n$ is composed of binary elements $c_{mj}$ that denote whether a site in the $m^{th}$ row $(m \in M_n)$ is included in the location visit task arranged in the $j^{th}$ column $(j \in J_n)$. Each column of $C^n$ represents a possible candidate deployment plan for neighborhood $n$, providing agencies the locations of tasks to which an operator may be assigned over a shift.

#### 6.2.1.2 Resource Distribution to Enforcement Location Visit Tasks

After identifying all possible tasks, we use three metrics to assess the need to perform each task in a neighborhood. These metrics are those used for the neighborhood-level deployment plan: EPDO collision frequency per km $(EPK)$, speed violation indicator $(SVI)$, and school zone density $(SZD)$. The number of resources allocated to each neighborhood is then assigned to tasks based on their metric values.

Because each site will have a value for each of the three metrics, Equation (6-2) evaluates the relative enforcement need of a site $m$ included in neighborhood $n$, $W_m^n$, with respect to the three metrics. The weighted sum of these three metrics is shown in Equation (6-2).

$$W_m^n = w_{EPK} \cdot EPK_m + w_{SVI} \cdot SVI_m + w_{SZD} \cdot SZD_m \ , \ \ \forall m \in M_n, \forall n \in N^{(1)} \qquad (6\text{-}2)$$

Where:

$W_m^n$ = weight of enforcement site $m$ in neighborhood $n$
$EPK_m$ = EPDO collision frequency per kilometer (km) for site $m$
$SVI_m$ = speed violation indicator for site $m$
$SZD_m$ = number of school zones for site $m$
$w_{EPK}$ = weight of $EPK$
$w_{SVI}$ = weight of $SVI$
$w_{SZD}$ = weight of SZD

The relative importance (or weight) of each criterion—$w_{EPK}$, $w_{SVI}$, and $w_{SZD}$—are taken from the objective function value of the neighborhood-level deployment plan (Stage 1 results). Decision makers chose a neighborhood-level deployment plan from a set of options resulting from the MRA model, which includes the weights placed on each of the three objectives. These weights are then used in this MRS model (Stage 2), in Equation (6-2). However, the individual metric values ($EPK_m$, $SVI_m$, and $SZD_m$) are different units. Therefore, if they are to be used in Equation (6-2), each variable requires normalization.

After completing the calculation of enforcement need for each site $m$, $W_m^n$, the relative weight of a task in a neighborhood is calculated using Equation (6-3).

$$W_j^n = \sum_{m \in M_n} W_m \times c_{mj}, \quad \forall j \in J_n, \forall n \in N^{(1)} \qquad (6\text{-}3)$$

where:

$W_j^n$ = weight of task $j$ in neighborhood $n$

Equation (6-3) computes a weight $W_j^n$ for the $j^{th}$ task in $n$ by taking the sum of the product of $W_m^n$ and $c_{mj}$. If site $m$ is used in task $j$, then $c_{mj} = 1$; otherwise it is 0).

Finally, the number of shifts allocated to neighborhood $n$, $x_n$, is apportioned between all enforcement tasks identified in the neighborhood (Equation (6-4)). The allocation to tasks is computed based on the relative weight of task $j$ ($W_j^n$ as defined in Equation (6-3)) compared to the sum of the weights of all tasks in the neighborhood. The higher the weight of task $j$, the more shifts $x_j^n$ will be allocated to it.

$$x_j^n = \frac{W_j^n}{\sum_{j \in J_n} W_j^n} \cdot x_n, \qquad \forall j \in J_n, \forall n \in N^{(1)} \tag{6-4}$$

where:

$x_j^n$ = number of monthly shifts allocated to candidate task $j$ in neighborhood $n$

$x_n$ = number of monthly shifts allocated to neighborhood $n$ as determined in Stage 1

### 6.2.2 Binary Integer Program

After $x_j$ (the number of shifts allocated to candidate task $j$) is calculated using Equation (6-4), it is then input into the scheduling model as a fixed parameter. According to the neighborhood-level deployment plan results, we observed that some neighborhoods were assigned only a few shifts over the course of one month (and possibly only one). For these low intensity neighborhoods, a shift from the $x_j^n$ set may be assigned to almost any day. Without knowing the program requirements for which day the shift is assigned, we create a 'unified' schedule for all city neighborhoods.

We used a binary integer program (BIP) to determine the sequence of daily shifts that minimize consecutive shift visits to the same location visit task (in consideration of the enforcement time halo).

The BIP formulation is presented in Equations (6-5)-(6-8).

Decision Variables:

$$x_{ij} = \begin{cases} 1 & if\ visit\ occurs\ at\ location\ visit\ task\ j\ in\ shift\ i \\ 0 & otherwise \end{cases}$$

Objective Function:

$$min \sum_{i=1}^{I} \sum_{j=1}^{J} c_{ij} x_{ij} \tag{6-5}$$

Subject to:

$$dl_i \leq \sum_{j=1}^{J} x_{ij} \leq du_i, \quad \forall i = 1 \dots I \tag{6-6}$$

$$\sum_{i=1}^{I} x_{ij} = x_j, \quad \forall j = 1 \dots J \tag{6-7}$$

$$x_{ij} \in \{0,1\}, \quad i = 1 \dots I, j = 1 \dots J \tag{6-8}$$

Where:

| | | |
|---|---|---|
| $i$ | = | shift index, $i = 1, \dots, I$ |
| $j$ | = | task index, $j = 1, \dots, J$ |
| $I$ | = | total number of shifts of the given month |
| $J$ | = | total tasks identified across all neighborhoods, $J = \sum_{n \in N^{(1)}} J_n$ |
| $x_{ij}$ | = | 1 if visit occurs at location visit task $j$ in shift $i$, and 0 otherwise |
| $c_{ij}$ | = | cost of allocating an operator visit at task $j$ in shift $i$ |
| $dl_i$ | = | minimum number of visits required for shift $i$ |
| $du_i$ | = | maximum number of visits allowed for shift $i$ |
| $x_j^n$ | = | number of monthly shifts allocated to candidate task $j$ in neighborhood $n$, defined in Equation (6-4) |

We use Equations (6-5)-(6-8) to construct a table where the rows represent shifts over a month, and columns represent the tasks determined in the preprocessing step (Section 6.2.1.1). Binary variables $x_{ij}$ take value one if task $j$ is visited by an operator in shift $i$, and 0 otherwise. Each

column of the table, $X_j = (x_{1j}, x_{2j}, \dots, x_{Ij})^T$, shows in which shifts a task will be visited in the month.

Equation (6-5) is used to find the minimum cost of allocating operator visits to tasks and shifts. Cost $c_{ij}$ (used in (6-5)) is calculated using Equation (6-9) to penalize repeated visits (in consecutive shifts) to the same task, considering the enforcement time halo effect. Cost functions on goals other than time halo violations can be specified as well, if there are other program goals to be considered.

$$c_{ij} = \sum_{i}^{i+t-1} x_{[1+(i-1)\ mod\ I]j} \quad \forall i, j \tag{6-9}$$

Where:

| | | |
|---|---|---|
| $t$ | = | number of consecutive shifts over which time halo effects are observed |
| $mod$ | = | remainder of $1 + (i - 1)$ divided by $I$ |
| $I$ | = | total number of shifts in month |

Let $t$ denote the duration of the time halo after enforcement, represented by number of consecutive shifts. In this $t$-shift time halo, more than two visits are considered a violation of the time halo (and therefore, inefficient). For a feasible schedule of shifts to tasks, we count the frequency of visits in $t$ shifts as the cost of time halo violation, as illustrated in Equation (6-9). For example, if $t$ is 3, when the task's visiting sequences occurred in three patterns described as "XOX" or "XXX" or "XXO", they are considered a violation, and their cost are 2, 3, 2, respectively. The more frequently the same task (i.e., set of sites) is visited during $t$ shifts, the greater the penalty cost will be. In addition, since Equation (6-9) sums the number of visits allocated within a window of length $t$ over each shift $i$, higher costs are assigned to successive visits.

When calculating $c_{ij}$, we connect the first and last rows of the schedule to form a closed loop, calculating the cost of the last $t - 1$ shifts using a sliding window of length $t$. Equation (6-9) implements this by expressing the row index as a function of $i$. Specifically, the row index is represented as 1 plus the remainder of $i - 1$ divided by $I$, where $i$ iterates from $i$ to $i + t - 1$. For

example, suppose $t = 2$ and $I = 3$, the cost of the element in the last row ($i = 3$) and the $j$th column on the schedule, $c_{3j}$, equals to $x_{3j} + x_{1j}$ from Equation (6-9).

Equation (6-6) limits the total visits that occur in shift $i$ to the range $[dl_i, du_i]$, because there are a limited number of operators working in each shift per day. Equation (6-7) ensures that the total visits assigned to task $j$ is equal to the fixed value $x_j$ previously obtained in Equation (6-4). Equation (6-8) is the binary constraint on the variable $x_{ij}$.

Equations (6-5)-(6-8) schedule operator shifts to their corresponding tasks (sets of sites). Hence, Equation (6-9) computes penalty costs based on evaluating time-halo violations at task level, rather than by individual sites. Depending how the site set is determined, the model will not account for site-level violations. However, Edmonton neighborhoods are quite small in geographic coverage, and MPE operator presence will be felt throughout a neighborhood through a distance halo effect; in other words, enforcement halos go beyond individual sites.

## 6.3 A Dantzig-Wolfe Decomposition And Column Generation Approach

The BIP problem of Equations (6-5)-(6-8) is a variant of the generalized assignment problem. The generalized assignment problem (Gottlieb & Rao, 1990) is a classic optimization problem that minimizes the cost involved in assigning a set of agents to perform a set of tasks. As it is NP-hard, the computation time for solving BIP grows exponentially as the size of the solution space $(I, J)$ increases. This section describes a method for solving Equations (6-5)-(6-8) using the Dantzig-Wolfe decomposition and column generation algorithms.

### *6.3.1 Dantzig-Wolfe Decomposition*

To solve the BIP, we first use the Dantzig-Wolfe approach to reformulate it as a master problem. To do this, Dantzig-Wolfe treats Equation (6-7) and Equation (6-8) as $J$ sub-problems. Equation (6-7) gives the number of monthly visits assigned to individual enforcement location visit tasks, whereas Equation (6-8) specifies binary variables. $J$ is the number of all tasks. They are handled separately because enforcement tasks are mutually exclusive, as such scheduling visits to each task individually is more efficient than scheduling them together. For any task $j \in J$, assume all

possible schedules (that distribute $x_j$ visits within $I$ shifts) determined by Equations (6-7) and (6-8) are known, and there are $K_j$ schedules. Let $S_j = \{x_j^1, x_j^2, \dots, x_j^{K_j}\}$ denote a complete enumeration of the feasible shift schedules for task $j$. Each element of $S_j$ is a feasible solution (column) to Equations (6-7) and (6-8).

Then, we use Equations (6-10)-(6-12) to rewrite $x_{ij}$ from Equations (6-5)-(6-8), by introducing a new binary variable $\lambda_j^k$. $\lambda_j^k = 1$ when the $k$-th column in $S_j$ is selected, otherwise $\lambda_j^k = 0$.

$$x_{ij} = \sum_{k=1}^{K_j} \lambda_j^k \, x_{ij}^k \tag{6-10}$$

$$\sum_{k=1}^{K_j} \lambda_j^k = 1, \quad \forall j = 1 \dots J \tag{6-11}$$

$$\lambda_j^k \in \{0,1\}, \quad k = 1 \dots K_j, j = 1 \dots J \tag{6-12}$$

Equation (6-10) represents variable $x_{ij}$ as a convex combination of the elements that are positioned in the $i$-th row of the feasible columns in $S_j$. Equation (6-11) is the convexity constraint that forces the sum of $\lambda_j^k$ over $k$ to be equal to one, and Equation (6-12) states $\lambda_j^k$ is binary.

Substituting Equations (6-10)-(6-12) into Equations (6-5)-(6-8) results in Equations (6-13)-(6-16).

Master Problem (MP)

Decision Variables:

$$\lambda_j^k = \begin{cases} 1 & if\ shift\ schedule\ x_j^k\ is\ selected\ for\ task\ j \\ 0 & otherwise \end{cases}$$

Objective Function:

$$min \sum_{j=1}^{J} \sum_{k=1}^{K_j} \left( \sum_{i=1}^{I} c_{ij} \, x_{ij}^k \right) \lambda_j^k \tag{6-13}$$

Subject to:

$$dl_i \leq \sum_{j=1}^{J} \sum_{k=1}^{K_j} x_{ij}^k \lambda_j^k \leq du_i, \quad \forall i = 1 \dots I \tag{6-14}$$

$$\sum_{k=1}^{K_j} \lambda_j^k = 1, \quad \forall j = 1 \dots J \tag{6-15}$$

$$\lambda_j^k \in \{0,1\}, \quad k = 1 \dots K_j, j = 1 \dots J \tag{6-16}$$

In the master problem (MP), the original BIP objective function (Equation (6-5)) and row constraints (Equation (6-6)) are rewritten as Equations (6-13) and (6-14), respectively. The two constraints of the original BIP problem (Equations (6-7) and (6-8)) are now included in $\lambda_j^k$. Note that $x_{ij}^k$ is no longer a decision variable in Equation (6-13), but is selected from the feasible set ($S_j$) determined in the sub-problem corresponding to $j$.

The Dantzig-Wolfe decomposition method reformulates the original problem (Equations (6-5)-(6-8)) to the master problem using new variable $\lambda_j^k$. This reformulation is an equivalence operation between the original problem and the master problem. The master problem is a set partitioning problem (or equality-constraint set covering problem), which is the most widely used formulation in integer programming (Balas & Padberg, 1976). Equation (6-15) is the partitioning constraint enforcing that only one column in $S_j$ is selected for task $j$. When using a classical branch-and-bound integer program algorithm to solve the master problem, branching on $\lambda_j^k$ is equivalent to branching on the convex combination of feasible columns for $j$. Therefore, tighter bounds can be obtained from solving the master problem rather than the original problem (branching on a single element of column $j$), speeding up the solution process.

Solving the master problem requires the enumeration of $S_j$ (the set of all feasible schedules for task $j$). However, it is unrealistic to enumerate each column in $S_j$ in many real applications,

because the number of shift schedules satisfying Equations (6-7) and (6-8) can be enormous. Thus, a column generation approach is applied instead, as described in Section 6.3.2.

### *6.3.2 Column Generation*

To help better understand how column generation is applied to Dantzig-Wolfe, Figure 6-2 shows the process of using the two algorithms.

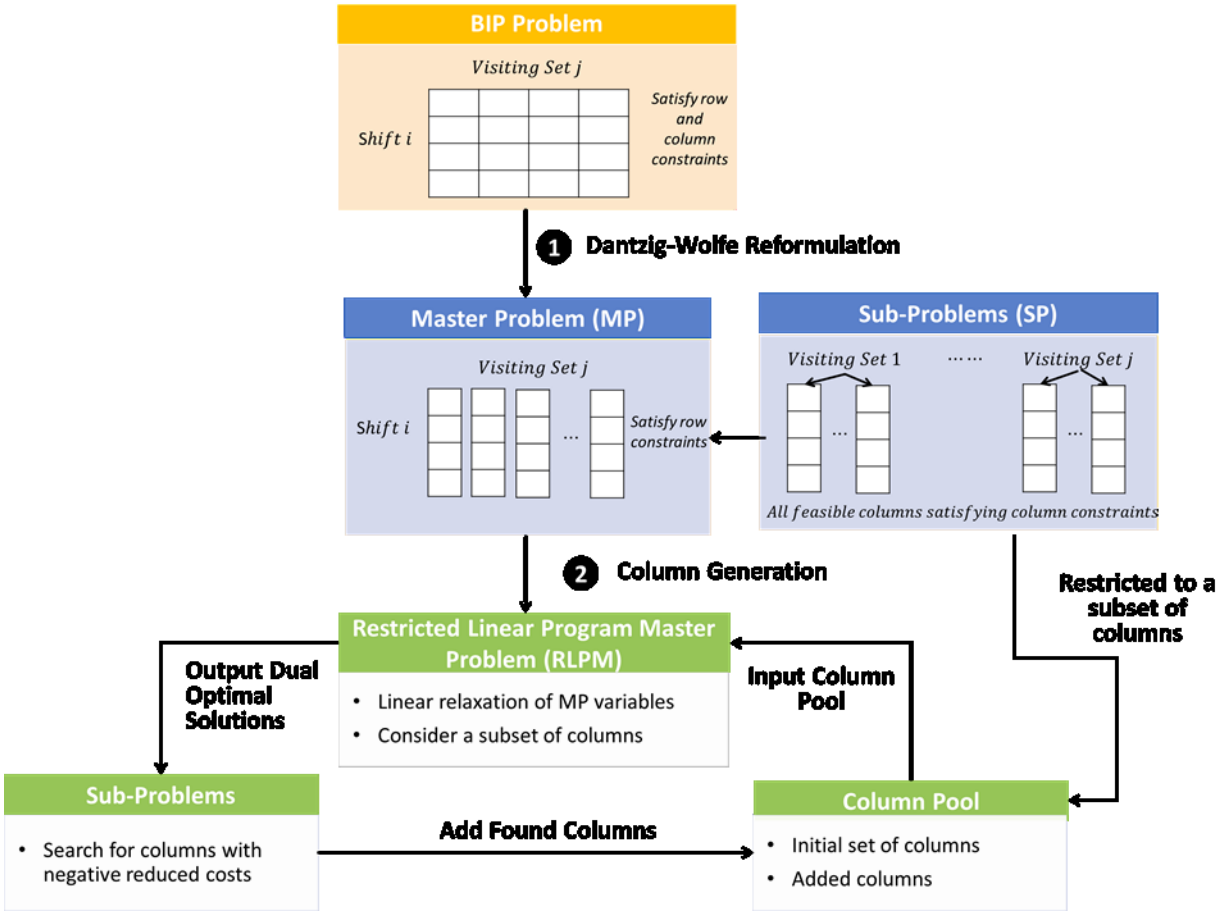


**Figure 6-2 Process of implementing Dantzig-Wolfe and column generation algorithms.**

As mentioned previously, the Dantzig-Wolfe algorithm is used to reformulate the BIP as an MP (Figure 6-2, blue box on the left). This is done by defining feasible schedules (columns in the right blue box, Figure 6-2) that have been enumerated for individual tasks as variables. However, due to the heavy computational effort for enumeration, we use the column generation method (green boxes, Figure 6-2) to solve an LP-relaxed master problem in a column pool whose size is restricted.

The pool is first generated by an initial set of columns satisfying the constraints from the BIP. Then, the pool is expanded by adding a single column identified for each task (the column identification is referred to a sub-problem). Column generation moves back and forth between the sub-problems and the relaxed master problem until an optimal solution to the relaxed master problem is found. The details of this solution process are described below.

First, instead of solving the master problem (MP) of Equations (6-13)-(6-16) directly, column generation handles a restricted linear programming master problem (RLPM), where the MP's decision variable $\lambda_j^k$ is relaxed to be continuous and the total number of variables for each $j$, $K_j$, is restricted to a given number $\widehat{K}_j$. Let $\lambda'^k_j \in [0,1]$ denote the relaxed variable, where $k = 1 \dots \widehat{K}_j < K_j$, and $j = 1 \dots J$. Equations (6-17)-(6-21) present the formulation of RLPM using a restricted number of continuous variables.

#### 6.3.2.1 Restricted Linear Programming Master Problem (RLPM)

Decision variables:

Objective Function:

$$min \sum_{j=1}^{J} \sum_{k=1}^{\widehat{K}_j} \left( \sum_{i=1}^{I} c_{ij}\, x_{ij}^k \right) \lambda'^k_j \tag{6-17}$$

Subject to

$$\sum_{j=1}^{J} \sum_{k=1}^{\widehat{K}_j} x_{ij}^k\, \lambda'^k_j \geq dl_i, \quad \forall i = 1 \dots I \tag{6-18}$$

$$-\sum_{j=1}^{J} \sum_{k=1}^{\widehat{K}_j} x_{ij}^k\, \lambda'^k_j \geq -du_i, \quad \forall i = 1 \dots I \tag{6-19}$$

$$\sum_{k=1}^{\widehat{K}_j} \lambda'^k_j \geq 1, \quad \forall j = 1 \dots J \tag{6-20}$$

$$\lambda'^k_j \geq 0, \quad k = 1 \dots \widehat{K}_j < K_j, j = 1 \dots J \tag{6-21}$$

To allow the simplex algorithm to efficiently find feasible solutions, we rewrite the constraint matrix of RLPM to single-sided inequality constraints. Equations (6-18) and (6-19) are two single-sided inequality constraints restated from the two-sided inequality constraint of Equation (6-14). Equation (6-20) relaxes the partitioning constraint in Equation (6-15) to covering constraint: from selecting exactly one column to at least one column for $j$. This relaxation is often done because solving the LP relaxation of set covering constraints requires less computational efforts than solving the LP relaxation of set partitioning constraints (Albers, 2009). Also, use of Equation (6-20) will not produce a different optimal solution than Equation (6-15), as the objective function in Equation (6-17) is to minimize, which adds as few schedules as possible to each task.

#### 6.3.2.2 Initialization of a Feasible Schedule

To solve RLPM, we begin with an initial schedule (a starting subset of columns) in the column generation process (see Figure 6-2). There are different ways to construct the initial schedule. Since randomized enforcement activities are shown to produce better safety outcomes than fixed schedules ( L. M. W. Leggett, 1997), we initialize our optimization using a randomized schedule.

Figure 6-3 shows the process of creating the initial schedule.

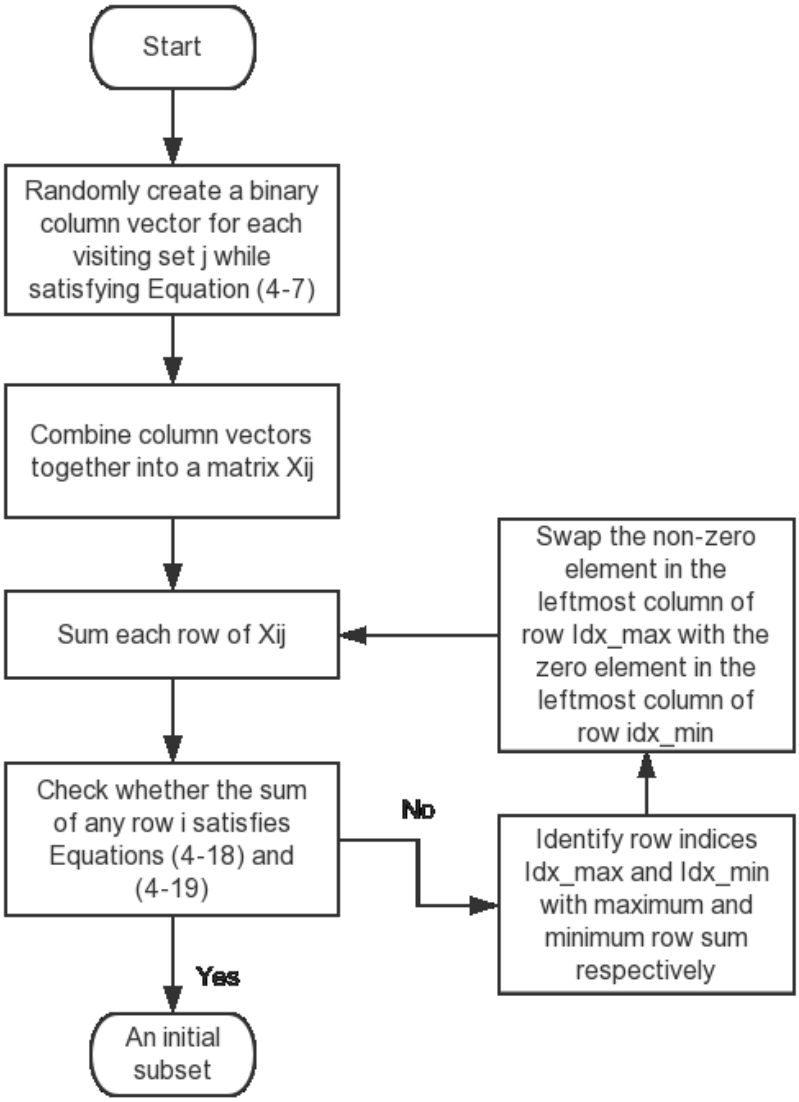


**Figure 6-3 Generating an initial subset of columns in RLPM.**

For each task $j = 1 \ldots n$, a binary column vector is randomly created whose sum is equal to $x_j$ (derived from Equation (6-4)). This column vector contains feasible solutions to Equations (6-7) and (6-8). Combining the columns of each task produces a matrix $X_{ij}$, which can be a schedule (when the initial RLMP solution $\lambda^0$ selects all columns of the matrix $X_{ij}$) if it is feasible to RLPM (i.e., row constraints in Equations (6-18) and (6-19) are satisfied). To check the feasibility of $X_{ij}$, we sum each row of $X_{ij}$. Rows that do not satisfy Equation (6-18) or (6-19) are identified, indexed. To ensure all the identified rows are feasible, we start with two rows: minimum and maximum

row sums, because they have the largest difference from $dl_i$ and $du_i$, which are the bounds specified in Equations (6-18) and (6-19). We swap leftmost zero in the minimum row with the leftmost non-zero in the maximum row. In this iterative process, a matrix $X_{ij}$ (schedule) feasible to RLMP is created.

After a feasible initial schedule is found, the simplex method (a classic algorithm for solving linear programming problems) is used to solve RLPM with the starting schedule. To get the final optimal solution and schedule, we search the columns that can replace the current pool, so that the objective value of RLPM decreases until no such column exists. This search process, shown in the green boxes in Figure 6-2, is elaborated in detail by the following sub-problems (Equations (6-22)-(6-24)).

#### 6.3.2.3 Sub-Problems (SPs)

Decision Variables:

$$x_{ij} = \begin{cases} 1 & if\ visit\ occurs\ at\ task\ j\ in\ shift\ i \\ 0 & otherwise \end{cases}$$

Objective Function:

$$min \sum_{i=1}^{i=I} (c_{ij} - \mu_i + v_i)\, x_{ij} - \omega_j, \qquad \forall j = 1 \dots J \tag{6-22}$$

Subject to

$$\sum_{i=1}^{I} x_{ij} = x_j, \quad \forall j = 1 \dots J \tag{6-23}$$

$$x_{ij} \in \{0,1\}, \quad i = 1 \dots I, j = 1 \dots J \tag{6-24}$$

Equation (6-22) minimizes the reduced cost of a feasible column $(x_{1j}, \dots, x_{Ij})^T$ for task $j$. The reduced cost of an additional column is the marginal unit deduction in the objective function value of RLPM. When replacing current columns with new ones found with negative reduced costs, the objective value of RLMP is further reduced. The reduced cost is computed using the optimal dual

solutions obtained each time RLPM is solved with the current matrix. The optimal dual solution is the optimal solution to the RLPM dual problem, which represents each constraint of RLPM as a variable. Equation (6-22) expresses the dual solutions corresponding to constraints of RLMP Equations (6-18), (6-19), and (6-20) using $\mu_i$, $v_i$, and $\omega_j$, respectively. Equations (6-23) and (6-24) ensure that $(x_{1j}, \dots, x_{mj})^T$ satisfies the conditions for a feasible shift schedule. Note that because $c_{ij}$ is a function of $x_{ij}$ as per Equation (6-9), the objective function in Equation (6-22) contains quadratic terms. With linear constraints in Equation (6-23), the sub-problems (Equations (6-22)-(6-24)) can be solved by quadratic programming.

In each iteration, column generation compares the optimal value $Z^{(SP_j)}$ obtained between the sub-problems and identifies the column with the lowest $Z^{(SP_j)}$ value. If $Z^{(SP_j)} < 0$, this column is added to the current column pool of RLMP for re-optimization until all $Z^{(SP_j)} \geq 0$.

The optimal solution of RLMP is usually fractional but does provide a tight bound to the master problem (equivalent to BIP). We re-optimize RLPM containing the final column pool using integer variables to quickly find an approximate solution for BIP.

## 6.4 Application And Results

The BIP model (Sections 6.2-6.2) is applied to generate a schedule for a September 2014 candidate neighborhood-level deployment plan. We first input a neighborhood-level allocation from the MRA model; solution #5 was chosen from the results in Figure 5-4. The enforcement location visit tasks in the 44 neighborhoods identified in the September 2014 Edmonton MPE deployment are created. The shifts allocated to these 44 neighborhoods are then distributed to tasks within each neighborhood. Finally, since each day has two shifts, the shifts paired with specific tasks are scheduled to either morning or afternoon shifts in the 30 days of September 2014.

### *6.4.1 General Results*

The scheduling model is implemented using MATLAB and CPLEX, on an OS X with a 1.6 GHz Intel® Core i5 processor. MATLAB R2015b is first used to solve Equations (6-1)-(6-4), in order to complete the two resource assignment steps described in Sections 6.2.1. The data used for model parameter estimation was introduced in Section 3.2. In addition, we set parameter $d$ in Equation

(6-1) – the average of number of sites per shift in September 2014 – to 3. Consequently, using Equation (6-1) we identified 203 possible tasks from the 44 neighborhoods chosen for enforcement in Stage 1. Weights $w_{EPK}$, $w_{SVI}$, and $w_{SZD}$ in Equation (6-2) are taken from Solution #5 on Figure 5-4, which returned objective function values of $EPK = 3441$, $SVI = 248$, and $SZD = 797$. The metrics were normalized to be within [0,1] using these weights. These normalized values are entered into Equation (6-2) to calculate the weights for each enforcement site, and then these weights are used in Equation (6-3) to calculate weights for tasks. Then, we use Equation (6-4) to split a monthly total of 458 shifts between tasks. Only 145 of the 203 identified tasks have been assigned shifts; thus, these $J = 145$ tasks and their received shift allocations $x_{j \in J}$ are input into the BIP model.

Task #77 (three sites in the Strathcona neighborhood, shown in blue in Figure 6-5), was allocated 69 shifts ($x_{77} = 69$) in the above step. This frequency exceeds the maximum $I = 60$ shifts during a month (2 shifts per day for 30 days). Given the BIP model assumes that the same task cannot be assigned to a shift more than once, we force the number of shifts assigned to this task to 60. Thus, we have decreased the total number of shifts in September 2014 from 458 to 449. The constraint of the BIP on the maximum number of shifts (i.e., 60 over one-month period) should be added to the 1st stage neighborhood-level resource allocation (MRA model). Hence, the 2nd stage resource scheduling (MRS model) will be abided by the constraint directly as part of the pervious stage optimization.

Then, to solve the scheduling problem (BIP, Equations (6-5)-(6-9)), we programmed an instance of a restricted linear programming master problem (RLPM, Equations (6-17)-(6-21)) and its associated sub-problems (SPs, Equations (6-22)-(6-24)) in MATLAB and CPLEX. The instance determines the sequence of the 449 shifts assigned to 145 tasks within 30 days, while a 5-day time halo is considered ($t = 10$ consecutive morning and afternoon shifts in Equation (6-9)). The reason for considering the 5-day time halo has been stated in Section 3.2. The instance was solved in 2.4 hours and an optimal solution for RLPM was found. The solution contains fractional values so the RLPM is re-optimized by solving integer variables in the column pool lastly generated. An optimal integer solution to the re-optimization problem was found in 0.1 seconds, which is taken as the approximate solution to BIP. Although reducing computational time should be a future

priority, we feel it is reasonable given that our model solves the MPE scheduling problem for an entire month. Shorter time halos would allow for faster solution generation.

A sample of the schedule from the approximate solution is given in Figure 6-4. The schedule has been transposed into the sample of resulting schedule in Figure 6-4, with tasks on the rows and daily shifts (M = morning, A = afternoon) on the columns. "X" indicates a shift during which visits were made to a neighborhood task (with included sites identified). For example, task # 53 was visited twice in a month, in the morning shift of Day 4 and the morning shift of Day 27. This task is composed of three enforcement sites #10073, #10091, and #10866, which are located in the neighborhood of Queen Mary Park.

| Task No. | Neighborhoods | Days and Shifts / Enforcement Site No. | | | D1 | | D2 | | D3 | | D4 | | D5 | | … | D26 | | D27 | | D28 | | D29 | | D30 | |
|---|---|---|---|---|---|---|---|---|---|---|---|---|---|---|---|---|---|---|---|---|---|---|---|---|---|---|
| | | | | | M | A | M | A | M | A | M | A | M | A | … | M | A | M | A | M | A | M | A | M | A |
| … | … | … | … | … | … | … | … | … | … | … | … | … | … | … | … | … | … | … | … | … | … | … | … | … | … | … |
| 53 | Queen Mary Park | 10073 | 10091 | 10866 | | | | | | | X | | | | … | | | X | | | | | | | |
| … | … | … | … | … | … | … | … | … | … | … | … | … | … | … | … | … | … | … | … | … | … | … | … | … | … | … |
| 134 | Terrace Heights | 5185 | 10214 | 10534 | | | | | X | | | | | | … | | | | | | | | | | |
| 135 | | 5185 | 10218 | 10534 | | | | X | | | | | | | … | | | | | | | | | | |
| … | … | … | … | … | … | … | … | … | … | … | … | … | … | … | … | … | … | … | … | … | … | … | … | … | … | … |

**Figure 6-4 Sample of the resulting schedule.**

The final output schedule assigns visits at different frequencies. The most frequently visited task is visited each day of the month, whereas the least frequent is only visited once. We do not specify that sites must be visited for the same durations or in the same order during a shift, such that variations of both can contribute to the perception of enforcement randomness.

### *6.4.2 Time Halo Violation Analysis*

The optimal objective value of Equation (6-17) is 1263, indicating that the schedule shown in Figure 6-4 produced a total of 1263 cost units due to violations of the 5-day time halo. This value is 14% lower than the objective value obtained using the initial solution (i.e., a randomly generated schedule). This objective value gap shows that by using the time halo of enforcement, the schedule obtained after optimization is more efficient than a randomly-generated schedule.

Visits assigned to 80 out of 130 sites (included in the 145 tasks) have violated the 5-day time halo. Figure 6-5 shows the locations of these 80 sites and their neighborhoods. Most violations occur in the neighborhoods that received medium and high enforcement intensities (marked as yellow and red polygons) as determined by the first stage allocation (MRA model). Only three low intensity neighborhoods (green polygons) had sites with time halo violations. Because neighborhoods warranting high enforcement attention are allocated a large number of visits in Stage 1, these neighborhoods are also more likely to have time halo violations.

Among all the violating visits, the most common case is when a site is visited twice within 10 shifts (5 days). This case occurred a total of 610 times (501 non-successive visits and 109 successive visits), and they mainly occurred at 48 sites represented by grey lines in Figure 6-5. Each site was visited seven times on average over a month. In scheduling seven visits in 60 shifts, with a 10-shift time halo, it is highly likely that violations will occur.

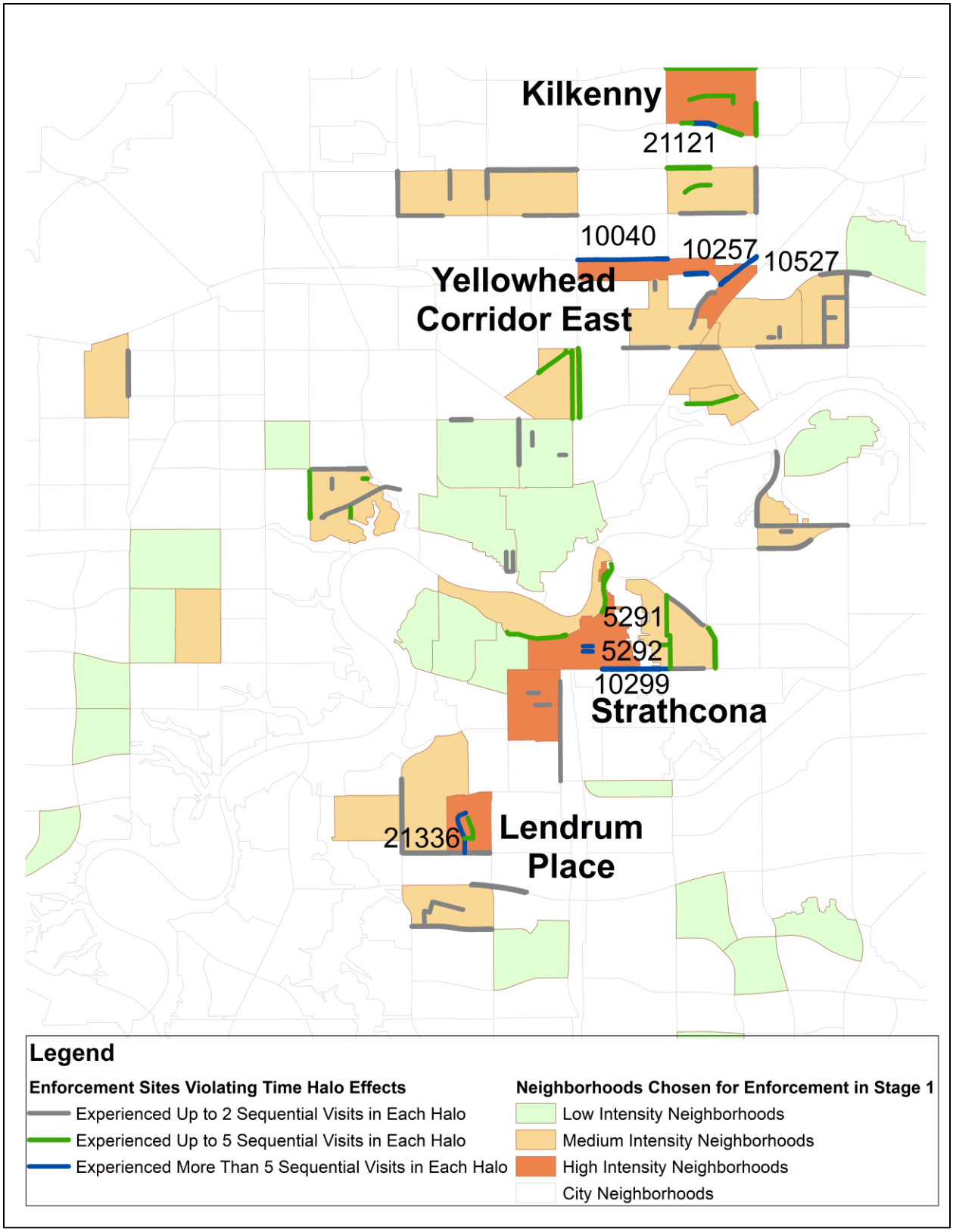


**Figure 6-5 Task locations with shift schedule violating the time halo effect, Edmonton.**

A high number of time halo violations (three or four consecutive visits) occurred at 24 sites (green lines in in Figure 6-5), at an average of two such visits per site. Each of these 24 sites was assigned an average of 16 visits, which is twice the average of the 48 locations shown above. These locations were allocated high intensity enforcement attention because they are in neighborhoods with average $SVI$ (percentage of vehicles violating speed limits) and $SZD$ (number of schools per sq.km) 62% and 1.7, respectively – 30% higher than neighborhoods of the 48 sites above.

There are eight sites (blue lines in Figure 6-5) where frequent five to ten consecutive visits are observed. Sites #5291, #5292, #10299 and Sites #10040, #10257, #10527 are the only enforcement sites in Strathcona and Yellowhead Corridor East, respectively. Strathcona is a central Edmonton neighborhood, with an average of 12.2 EPDO/km ($EPK$) and 1.9 $SZD$. The Yellowhead Corridor East neighborhood, containing a section of the Yellowhead Expressway on which frequent speeding occurs, experienced an average of 16.6 $EPK$ and 75% $SVI$. The two neighborhoods were assigned 60 and 40 visits, which are further allocated to their only enforcement sites that were formed into a single location visit task. Consequently, visits assigned to these two neighborhoods repeated 10 and six times on average during each 10 shifts. Another two sites (Sites #21121 and #21336) in Kilkenny and Lendrum Place were assigned high intensity enforcement, with 56 and 40 shifts in one month, respectively. Kilkenny's average $SZD$ and $SVI$ values were 2.9 and 56%, while Lendrum Place's were 3.5 and 64%. Sites #21121 and #21336 are visited 31 and 27 times over the month, respectively. The highest repetitions are found to be six consecutive visits during 10 shifts.

Repeat visits at sites are assigned because they are deemed necessary by the metrics and models used. As mentioned in the formulation of BIP, Section 6.2.2, our model schedules visits for tasks and calculates time halo violations at a task rather than individual site level. Hence, it does not consider cases when two tasks that contain several of the same enforcement sites are scheduled for visits in successive shifts. For instance, the Terrace Heights neighborhood in Figure 6-4 contains sets #134 and #135, both of which contain enforcement sites #5185 and #10534. They are visited sequentially in the Day 2 afternoon shift and Day 3 morning shift. This sequential visit violates the 5-day enforcement time halo from a site-level perspective. This type of violation occurred at 35 sites (9 neighborhoods), and they constitute about half of the 109 two-shift consecutive visits

discussed above. Future work is needed to improve the way in which the tasks in a neighborhood are selected, thereby reducing duplication between sites in the same task.

## 6.5 SENSITIVITY ANALYSIS

In our scheduling model, the enforcement time halo duration $(t)$ is critical to model outcomes and computational time. Therefore, we explored the results of five values of $t$. The last row of Table 6-1 (where $t = 10$ shifts) corresponds to the results we have presented and explored in the previous section.

**Table 6-1 Results for Varying Enforcement Time Halo Duration $t$**

| Time Halo Duration $t$ (shifts) | Days represented by $t$ | Objective Value of RLMP $Z$ | | | Total Computation Time (min) |
|---|---|---|---|---|---|
| | | Initial Solution $\lambda^0$ | Optimal Solution $\lambda$ | Gap | |
| 2 | 1 | 556 | 529 | 5% | 5.3 |
| 4 | 2 | 782 | 696 | 11% | 9.7 |
| 6 | 3 | 990 | 878 | 11% | 23.1 |
| 8 | 4 | 1203 | 1069 | 11% | 67.8 |
| 10 | 5 | 1477 | 1263 | 14% | 141.6 |

Columns 3 and 4 of Table 6-1 show objective value $Z$ for the initial solution $\lambda^0$ and the approximate optimal solution $\lambda$, while Column 5 shows the gap between $\lambda^0$ and $\lambda$. The final column shows the total computation time (in minutes) to reach solutions.

As seen from Table 6-1, when $t$ increases from 2 to 10, the difference between $Z(\lambda^0)$ and $Z(\lambda)$ increases from 5% to 14%. This suggests that the solution $\lambda$ is better than a randomly generated schedule (i.e., the initial generated solution $\lambda^0$) for all values of the time halo seen.

The computational time is highly sensitive to $t$, growing exponentially with $t$ as expected. Specifically, when $t = 2$ shifts, an approximate integer solution can be found in about 5 minutes. If $t \leq 6$ shifts, solution times are below 25 minutes. However, when $t = 8$, solution time exceeds one hour. Increasing $t$ from 8 to 10 resulted in doubled computational time. The exponential relationship between $t$ and the solution time is because the model enumerates the possible visits

to be made in the next $t-1$ shifts after each visit assignment to a shift. The larger $t$ is, the greater the number of possible visit schedules will be in $t$ shifts.

## 6.6 SUMMARY

This chapter describes the MRS model that determines where and when enforcement resources should be assigned, using the results of the neighborhood-level resource allocation model (MRA model, Chapter 5). Both models use optimization techniques for the purpose of generating MPE deployment plans that account for program goals and resource constraints. The MRS model introduced in this chapter, in conjunction with the MRA model of Chapter 5, provides a tool for MPE agencies to systematically and efficiently allocate and schedule limited resources, and ultimately meet their goals of improving road safety.

The MRS model was implemented using a case study of the Edmonton MPE program. Model inputs include the neighborhood-level enforcement resource allocation determined in the previous MRA model for September 2014. This model produces a varied schedule of 449 operator shifts throughout the morning and afternoon shifts in the month. Compared to a randomly generated schedule, the model is 14% more efficient based on the three metrics used, while minimizing resource scheduling conflicts considering a 5-day time halo effect.

Enforcement visits to 60% (80 sites) of the 130 studied sites violated the 5-day time halo. The intensity of violations (i.e., number of consecutive visits) increases as the number of visits assigned to an enforcement location increase. 24 locations that are assigned an average of 16 monthly visits end up with 3-4 consecutive visits. Another eight locations have been assigned a much higher number of monthly visits (40-60 visits). Consequently, in these locations, 5 to 10 visits occur every 10 shifts, heavily violating time halos. However, some enforcement sites do require frequent visits given safety considerations and specific program needs as determined by model metrics.

The calculation time of the model increases exponentially with time halo $t$, measured in shifts. For the Edmonton case study presented, when $t$ is less than six shifts, the model can be solved in about 20 minutes. Above this value, the solution time is increased to hours. It is recommended that more empirical studies of time and distance halos in Edmonton be conducted.

# 7 CONCLUSIONS

This chapter concludes the thesis by summarizing the research work, key findings and contributions, as well as research limitations and future work.

## 7.1 RESEARCH OVERVIEW

The decision-making process for deploying an MPE program has been a black box; the process of how deployment objectives are mapped to deployment decisions has lacked evidence-based decision support, leading to extensively-documented suspicion and misunderstanding of MPE programs by the public. Despite this, little attention has been paid in the literature to how to allocate MPE resources according to program goals. Therefore, we have constructed a quantitative and systematic resource allocation model for MPE programs, in order to assist enforcement agencies in identifying efficient resource allocation plans while considering a set of program goals and resource constraints.

Because deploying MPE programs involves both spatial and temporal resource allocations, our model uses a decomposition-based optimization procedure to solve the resource allocation and scheduling problems in two stages. This decomposition makes the two problems tractable (solvable in polynomial time) for realistic instances. Prior to these two optimization stages, we also presented a set of quantitative measures to assess the degree of attaining problem-level objectives required by operational MPE program guidelines.

Our resource allocation model uses multi-objective optimization to maximize coverage of city neighborhoods that have shown high enforcement demands in relation to a set of considered deployment objectives, by one month's worth of operator work shifts. Since the Pareto solution set generated by a multi-objective optimization algorithm may be relatively large, the decision to select a solution in the set becomes difficult. To facilitate this decision, $K$-mediods is applied to reduce the solution size and a polynomial function is formed to quantify the tradeoffs between solutions in the set.

The scheduling model builds on the results of the neighborhood-level allocation model. It matches operators' work shifts to enforcement location visit tasks (sets of a given number of enforcement sites) in each neighborhood, and then determines monthly work shift schedules for operators to visit the locations included. Integer programming is employed to determine daily shift sequences of operator visits—specifically, we minimize the number of visits scheduled in a shift sequence that violate the enforcement's time halo. To solve large MPE scheduling instances, we reformulated the model using the Dantzig-Wolfe decomposition and solved it by column generation.

We apply the model to an MPE program in Edmonton, Alberta, Canada. The deployment results determined by the two-stage model are visualized using Geographic Information Systems (GIS). The results are also compared to the actual MPE program operations.

## 7.2 RESEARCH FINDINGS

The use of MPE technology is typically governed by automated speed enforcement guidelines that specify deployment priorities related to road safety outcomes. Six priorities are often highlighted in the guidelines, and they are high collision sites, high speed violation sites, school zones, construction zones, high pedestrian volume sites, and sites with community speeding complaints. Increasing enforcement at these priority sites is one concrete means of implementing the multi-national Vision Zero road safety strategy, which aims to completely eliminate serious traffic injuries and deaths through transportation system design and government interventions.

A spatial analysis of Edmonton's five-year (2010-14) historical data using GIS show that the city's MPE program addressed all the six priorities with varying degrees of attention. Because reducing speeding vehicles is a direct goal of implementing the MPE program, high speed violation sites were assigned the longest enforcement time (a total of 800 hours per site) during the five-year study period, compared to other priorities. In addition, school zones gained the largest program coverage (84%) over five years, considering that school children are the most vulnerable road users.

The resource allocation model developed in this thesis found optimal allocation solutions for a demonstrated 3-objective MPE deployment problem in Edmonton. The problem balanced enforcement presence in September 2014 at high collision sites, high speed violation sites, and

school zones. Each optimal solution corresponds to a set of values for enforcement coverage units at three types of sites. Choosing a solution represents a decision that gives a quantitative trade-off between the three goals. A candidate solution was further visualized on a GIS map, which assigned 248, 797, and 3441 enforcement coverage units to high speed violation sites, school zones, and high collision sites, respectively. This candidate solution allocates one month's shifts to 44 neighborhoods, achieving higher enforcement coverage than the actual deployment in September 2014, with 11%, 34%, and 18% more coverage units at high speed violation sites, school zones, and high collision sites, respectively. This suggests that using our optimization model produces greater efficacy in achieving program objectives than the expert defined approach.

The tradeoff rate between any pair of objectives calculated at an example solution indicates that reducing one unit of enforcement coverage in school zones can increase the coverage of 7.8 units at high speed violation sites or increase the coverage of 0.2 units at high collision sites. Alternatively, sacrificing one unit of coverage at high speed violation sites will compensate 0.02 units of coverage at high collision sites. These pairwise tradeoff values (contingent on the 3rd objective's set value) can provide useful information and insights to MPE program decision makers when making a tradeoff decision between more than one program objective.

The scheduling optimization model created a timetable for a candidate neighborhood-level resource allocation solution. One month's shifts were allocated to 145 neighborhood tasks and 30 days of the month. The created timetable is 14% more resource-efficient than a randomly established enforcement schedule. 60% of the sites were assigned visits violating the 5-day time halo. Violations at these sites are necessary to maintain enforcement coverage of high collision sites and high speed violation sites at certain units, which are determined in the neighborhood-level resource allocation stage.

## 7.3 RESEARCH CONTRIBUTION

This thesis contributes to both academic research and practice in speed enforcement. The details of these two aspects are discussed in the following sections.

### 7.3.1 Academic Contributions

This thesis presents a systematic and quantitative deployment model for MPE programs. The model employs decomposed-optimization techniques to solve MPE resource allocation and scheduling problems sequentially. This is the first time in the literature that such a model is proposed to allocate enforcement operators and equipment in speed enforcement programs.

Metrics are designed and used in our model to quantify the interpretation of official guidelines on where enforcement operators should be deployed to reach high-level, safety-oriented MPE goals. Through this work, the deployment results from the model can be strictly consistent with the guidelines and MPE program goals.

The first stage MRA model builds on a maximum covering location model to maximize enforcement coverage of demands associated with program goals. In addition, multi-objective linear program is employed to simultaneously consider multiple goals without predefined weights assigned to each goal. The model produces a set of solutions with posteriori weights, allowing MPE agencies to choose based on their considerations and preferences toward the tradeoff between goals. Additionally, it produces a city-wide neighborhood-level deployment plan, which can then be used for detailed resource scheduling (assigning shifts to enforcement locations).

Clustering and response surface methods are demonstrated to analyze the resource allocation solutions (Pareto-optimal solutions) obtained from the multi-objective MRA model. A large set of resource allocation solutions is reduced to a limited number of clusters whose center solutions are used as representative decision options. A polynomial model is established to produce the tradeoff values at any solution between conflicting objectives. The above two post-optimization steps greatly reduce agencies' decision fatigue and improve their judgement by providing quantitative objective tradeoffs.

The second stage MRS model considers the time halo effect of enforcement in the establishment of MPE resource schedules. This is the first time in the literature that time halo is utilized to improve MPE resource use. The results of our study indicate that considering time halo can generate an efficient and dynamic shift schedule. We employed the Dantzig-Wolfe decomposition and column generation algorithms to successively solve a large-scale scheduling instance

implemented by the MRS model. Before our model, such a large MPE scheduling case has not been successfully solved in the literature.

### 7.3.2 Practical Contributions

Since the MRS model considers the high-level program goals set in the allocation model and uses the same metrics as the MRA model for quantifying goals, these two models form a systematic decision-making framework assisting MPE agencies in addressing high-level program goals by efficient usage of limited resources.

The two-stage model facilitates decisions of the MPE agency in two ways. First, it allows agencies to explicitly make resource deployment decisions that directly reflect their high-level program priorities. Thus, the model supports a more transparent and defensible MPE resource allocation decision-making, in sharp contrast to existing MPE programs that rely on black box (i.e. qualitative, expert run) decisions. Second, the model allows agencies to consider multiple enforcement objectives simultaneously, and it delivers deployment solutions with quantitative tradeoff information among objectives. Traceable and informed decisions about how MPE deployment strategies respond to goals can be achieved.

Then, GIS is used to visualize the spatial resource allocation of an MPE program's deployment strategy and its relation to the achievement of program goals. The mapping of traffic safety data and enforcement activities was demonstrated to be an impactful method of organizing the spatial information of an MPE program. It can help agencies better interpret the requirements articulated in the ASE program guidelines and review their allocation of deployment resources so as to increase program efficiency and effectiveness in terms of safety outcomes.

The MPE deployment is based on multiple urban safety considerations, and sites are not stationary. Thus, MPE deployment decisions can be the most difficult resource allocation problem not only among automated speed enforcement programs but other automated enforcement activities as well, including red light enforcement, impaired driving checkpoints, etc. The approach proposed in this thesis is transferrable to other automated enforcement programs across jurisdictions, simply by tailoring the high-level program goals and corresponding metrics to local program specifications.

## 7.4 RESEARCH LIMITATIONS AND FUTURE WORK

Details on our modeling limitations and potential methods of improvement are described as follows.

### *7.4.1 Limitations of the Research*

The MRA model only considers the three most critical MPE program goals: reducing collisions, reducing speed violations, and increasing safety for school children. Although other metrics can easily replace these, we have not considered others in this study.

The key limitation of the MRS model is the application of enforcement time halo effects on groups of predetermined sites (referred to shift tasks) rather than individual enforcement sites. The model calculates the penalty cost incurred due to time halo violations based on shift tasks in neighborhoods. Therefore, the model ignores the cost of some violations that happened at same sites included in different site groups.

### *7.4.2 Future Research*

To address the above mentioned model limitations, we will first perform a data collection effort to identify MRA model metrics associated with program goals that are not considered in this thesis but may also be important, such as prioritizing enforcement in construction zones, high pedestrian volume sites, and sites with community speeding complaints. Then, we will adjust the MRS model's method of generating enforcement tasks within each neighborhood, to reduce tasks containing unnecessary duplications of sites warranting low enforcement needs.

We also envision some additional future work to complement the use of the two-stage model. First, we used clustering techniques to prune the Pareto optimal solutions generated from the MRA model to a set of representative solutions. This pruned solution set serves as initial options for decision makers to choose from. Future research will explore methods to help decision makers choose the final solution by applying clustering techniques to the tradeoff analysis. Second, we only solved approximate optimal scheduling solutions. The next step may apply branching strategies to determine the integer optimal solution of the MRS model—specifically, by integrating the approximate solutions and developing a search tree. In addition, strategies may be investigated

to further reduce the solution time of the model. Third, when scheduling resources, we used a fixed duration (five days) of enforcement time halo. However, the time halo duration is affected by the execution time and frequency of enforcement. To more accurately utilize time halo in schedule, a function should be developed to model the relationship between time halo duration and enforcement intensity, so that this function can be incorporated into the MRS model. Fourth, there is a trade-off between making the most advantage of time halo and implementing enforcement goals, because some sites requiring high enforcement attention will receive shift schedules that violate enforcement's time halo. In the future, we will study how to reallocate those violated visits that are considered "wasted" during the time halo to non-violation sites. This work will further improve the resource utilization in the schedule delivered by the MRS model, while maintaining the pre-set model objective values in both optimization stages at a certain level. Finally, because enforcement operators must spend part of their shift hours in traveling between enforcement sites, current work may also be expanded to develop a resource routing model based on the scheduling model results.

Future model improvement efforts will also include the consideration of more specific project operational requirements. For example, resource allocation to some neighborhoods that contain the Edmonton's major expressways may be managed separately due to specific program needs and considerations. In addition, school hours should be considered when scheduling enforcement resources to school zones. Also, resources will be scheduled to tasks within individual neighborhoods given specific operational needs, in contrast to the current MRS model which joins all identified location visit tasks of each neighborhood and schedules them at the same time. The results provided by the two-stage model should be compared with the existing deployment schemes and the random allocation methods.

# BIBLIOGRAPHY


AASHTO, A. A. of S. H. and T. O. (2010). *Highway Safety Manual* (Vol. 529).

Abdulhafedh, A. (2017). Road traffic crash data: an overview on sources, problems, and collection methods. *Journal of Transportation Technologies*, *7*(02), 206.

Adler, N., Hakkert, A. S., Raviv, T., & Sher, M. (2014). The traffic police location and schedule assignment problem. *Journal of Multi-Criteria Decision Analysis*, *21*(5–6), 315–333.

Albers, M. (2009). *Freight railway crew scheduling: models, methods, and applications*. Logos Verlag Berlin GmbH.

Alberta Justice and Solicitor General. (2014). *Automated Traffic Enforcement Technology Guidelines*. Edmonton: Province of Alberta Government.

Alberta Ministry of Transportation. (2007). *Guidelines For School And Playground Zones And Areas Version 2*. Retrieved from http://www.transportation.alberta.ca/content/doctype233/production/schlpgnd.pdf

Antonio, L. M., & Coello Coello, C. (2013). Use of cooperative coevolution for solving large scale multiobjective optimization problems. In *Evolutionary Computation (CEC), 2013 IEEE Congress on* (pp. 2758–2765). IEEE.

Armour, M. (1986). The effect of police presence on urban driving speeds. *ITE Journal*, *56*(2), 40–45.

Bai, Q., Labi, S., & Sinha, K. C. (2011). Trade-off analysis for multiobjective optimization in transportation asset management by generating Pareto frontiers using extreme points nondominated sorting genetic algorithm II. *Journal of Transportation Engineering*, *138*(6), 798–808.

Balas, E., & Padberg, M. W. (1976). Set partitioning: A survey. *SIAM Review*, *18*(4), 710–760.

Berkuti, C., & Osburn, W. (1998). PHOTO ENFORCEMENT IN THE WILD WEST: NATIONAL CITY'S EXPERIENCE WITH PHOTO RADAR ENFORCEMENT PROGRAM. In *1998 Compendium of Technical Papers*. Retrieved from http://trid.trb.org/view.aspx?id=581327

Berman, O., Drezner, Z., & Krass, D. (2010). Generalized coverage: New developments in covering location models. *Computers & Operations Research*, *37*(10), 1675–1687.

Bjørnskau, T., & Elvik, R. (1992). Can road traffic law enforcement permanently reduce the number of accidents? *Accident Analysis & Prevention*, *24*(5), 507–520.

Box, G. E., & Wilson, K. B. (1992). On the experimental attainment of optimum conditions. In *Breakthroughs in statistics* (pp. 270–310). Springer.

Brackett, R. Q., & Beecher, G. P. (1980). Longitudinal evaluation of speed control strategies. College Station. *Human Factors Division, Texas Transportation Institute/Texas A&M University (Final Report–Vol 1)*.

Brackett, Robert Quinn, & Edwards, M. L. (1977). *Comparative evaluation of speed control strategies*. Texas A & M University. Retrieved from http://elibrary.ru/item.asp?id=7223339

Branke, J., Deb, K., Dierolf, H., Osswald, M., & others. (2004). Finding knees in multi-objective optimization. In *PPSN* (Vol. 3242, pp. 722–731). Retrieved from http://repository.ias.ac.in/83511/1/15-a.pdf

Branke, J., Deb, K., & Miettinen, K. (2008). *Multiobjective optimization: Interactive and evolutionary approaches* (Vol. 5252). Springer Science & Business Media. Retrieved from https://books.google.ca/books?hl=en&lr=&id=N-1hWMNUa2EC&oi=fnd&pg=PA1&dq=multi+objective+optimization+interactive+and+evolutionary+approaches&ots=eDBBYx0K9R&sig=3fr86o7wvF8JbPCQMl2biJvR90A

Cairney, P. T. (1988). The effect of aerial enforcement on traffic speeds. In *AUSTRALIAN ROAD RESEARCH BOARD PROCEEDINGS*. Retrieved from https://trid.trb.org/view.aspx?id=339835

Champness, P. G., Sheehan, M. C., & Folkman, L.-M. (2005). Time and distance halo effects of an overtly deployed mobile speed camera. Retrieved from http://eprints.qut.edu.au/archive/00003952

Charrad, M., Ghazzali, N., Boiteau, V., Niknafs, A., & Charrad, M. M. (2014). Package 'NbClust.' *J. Stat. Soft*, *61*, 1–36.

Chen, G., Wilson, J., Meckle, W., & Cooper, P. (2000). Evaluation of photo radar program in British Columbia. *Accident Analysis & Prevention*, *32*(4), 517–526.

Christie, S. M., Lyons, R. A., Dunstan, F. D., & Jones, S. J. (2003). Are mobile speed cameras effective? A controlled before and after study. *Injury Prevention*, *9*(4), 302–306.

Church, R., Sorensen, P., & Corrigan, W. (2001). Manpower deployment in emergency services. *Fire Technology*, *37*(3), 219–234.

Church, R., & Velle, C. R. (1974). The maximal covering location problem. *Papers in Regional Science*, *32*(1), 101–118.

Cities of Beaverton and Portland. (1997). *Photo Radar Demonstration Project Evaluation*. Cities of Beaverton and Portland.

Coleman, J. A., Paniati, J. F., Cotton, R. D., Parker Jr, M. R., Covey, R., Pena Jr, H. E., … Morford, G. (1996). *FHWA Study tour for speed management and enforcement technology*. Washington, DC: Federal Highway Administration, US Department of Transportation.

Curtin, K. M., Qiu, F., Hayslett-McCall, K., & Bray, T. M. (2005). Integrating GIS and maximal covering models to determine optimal police patrol areas. *Geographic Information Systems and Crime Analysis Hershey: IDEA Group Publishing*, 214–235.

Dantzig, G. B., & Wolfe, P. (1960). Decomposition principle for linear programs. *Operations Research*, *8*(1), 101–111.

Das, I., & Dennis, J. E. (1997). A closer look at drawbacks of minimizing weighted sums of objectives for Pareto set generation in multicriteria optimization problems. *Structural and Multidisciplinary Optimization*, *14*(1), 63–69.

Daskin, M. S. (1982). Application of an expected covering model to emergency medical service system design. *Decision Sciences*, *13*(3), 416–439.

Davis, G. A. (2001). *NASCOP: An Evaluation of the Photo-Radar Speed Enforcement Program*. San Jose, Calif.: City of San Jose.

de Leur, P., Thue, L., & Ladd, B. (2010). *Collision Cost Study*. Capital region intersection safety partnership.

Deb, K., Pratap, A., Agarwal, S., & Meyarivan, T. (2002). A fast and elitist multiobjective genetic algorithm: NSGA-II. *Evolutionary Computation, IEEE Transactions On*, *6*(2), 182–197.

Delaney, A., Diamantopoulou, K., & Cameron, M. (2003). *MUARC's Speed enforcement research: Principles learnt and implications for practice* (No. 200). Victoria: Monash University Accident.

Desaulniers, G., Desrosiers, J., Dumas, Y., Solomon, M. M., & Soumis, F. (1997). Daily aircraft routing and scheduling. *Management Science*, *43*(6), 841–855.

Desaulniers, G., Desrosiers, J., & Solomon, M. M. (2002). Accelerating strategies in column generation methods for vehicle routing and crew scheduling problems. In *Essays and surveys in metaheuristics* (pp. 309–324). Springer.

Desrochers, M., & Soumis, F. (1989). A column generation approach to the urban transit crew scheduling problem. *Transportation Science*, *23*(1), 1–13.

Desrosiers, J., Soumis, F., & Desrochers, M. (1984). Routing with time windows by column generation. *Networks*, *14*(4), 545–565.

Edwards, M. L., & Brackett, R. Q. (1978). The management of speed. *Traffic Safety*, *78*, 19–30.

Elvik, R. (1997). Effects on accidents of automatic speed enforcement in Norway. *Transportation Research Record: Journal of the Transportation Research Board*, (1595), 14–19.

Elvik, R. (2011). Developing an accident modification function for speed enforcement. *Safety Science*, *49*(6), 920–925.

Ernst, A. T., Jiang, H., Krishnamoorthy, M., & Sier, D. (2004). Staff scheduling and rostering: A review of applications, methods and models. *European Journal of Operational Research*, *153*(1), 3–27.

Fang, H., Rais-Rohani, M., Liu, Z., & Horstemeyer, M. F. (2005). A comparative study of metamodeling methods for multiobjective crashworthiness optimization. *Computers & Structures*, *83*(25), 2121–2136.

FHWA. (2015). Facts and Statistics: Work Zone Injuries and Fatalities. Retrieved from http://www.ops.fhwa.dot.gov/wz/resources/facts_stats/injuries_fatalities.htm

Ford Jr, L. R., & Fulkerson, D. R. (1958). A suggested computation for maximal multi-commodity network flows. *Management Science*, *5*(1), 97–101.

Gamache, M., Soumis, F., Marquis, G., & Desrosiers, J. (1999). A column generation approach for large-scale aircrew rostering problems. *Operations Research*, *47*(2), 247–263.

Goel, T., Vaidyanathan, R., Haftka, R. T., Shyy, W., Queipo, N. V., & Tucker, K. (2007). Response surface approximation of Pareto optimal front in multi-objective optimization. *Computer Methods in Applied Mechanics and Engineering*, *196*(4), 879–893.

Goldenbeld, C., & van Schagen, I. (2005). The effects of speed enforcement with mobile radar on speed and accidents: An evaluation study on rural roads in the Dutch province Friesland. *Accident Analysis & Prevention*, *37*(6), 1135–1144.

Gottlieb, E. S., & Rao, M. R. (1990). The generalized assignment problem: Valid inequalities and facets. *Mathematical Programming*, *46*(1–3), 31–52.

Gouda, M., & El-Basyouny, K. (2016). Investigating time halo effects of mobile photo enforcement on urban roads. *Submitted for Presentation at the 96th Annual Meeting of Transportation Research Board and Publication in Transportation Research Record: Journal of Transportation Research Board*.

Graham, P., Bean, R., & Matthews, L. (1992). Random high-visibility enforcement at rural blackspots. In *National Road Safety Seminar* (pp. 2–4).

Hadka, D. (2015). MOEA Framework - A Free and Open Source Java Framework for Multiobjective Optimization (Version 2.9). Retrieved from http://www.moeaframework.org/

Haimes, Y. Y. (1971). On a bicriterion formulation of the problems of integrated system identification and system optimization. *IEEE Transactions on Systems, Man, and Cybernetics*, *1*(3), 296–297.

Hakkert, A. S., Gitelman, V., & Vis, M. A. (2007). *Road safety performance indicators: Theory* (Deliverable D3.6 of the EU FP6 project SafetyNet).

Hauer, E., Ahlin, F. J., & Bowser, J. S. (1982). Speed enforcement and speed choice. *Accident Analysis & Prevention*, *14*(4), 267–278.

Hess, S. (2004). Analysis of the effects of speed limit enforcement cameras: Differentiation by road type and catchment area. *Transportation Research Record: Journal of the Transportation Research Board*, (1865), 28–34.

Ho, G., & Guarnaschelli, M. (1998). *Developing a Road Safety Module for the Regional Transportation Model, Technical Memorandum One: Framework*. Vancouver, Canada: Insurance Corporation of British Columbia.

Humberside Police. (2008). *Rules Governing Site Selection, Signage & Visibility in Humberside*. Kingston: Humberside Police.

Huntley, H. C. (1970). Emergency health services for the nation. *Public Health Reports*, *85*(6), 517.

Jørgensen, N. O., Koornstra, M., Broughton, J., Glansdorp, C., & Evans, A. (1999). Exposure Data for Travel Risk Assessment: Current Practice and Future Needs in the EU. Retrieved from https://www.mysciencework.com/publication/show/96750915939821883d65bd03ec1cec80

Kaufman, L., & Rousseeuw, P. (1987). *Clustering by means of medoids*. North-Holland. Retrieved from https://lirias.kuleuven.be/handle/123456789/426382

Kim, A. M., Wang, X., El-Basyouny, K., & Fu, Q. (2016). Operating a mobile photo radar enforcement program: A framework for site selection, resource allocation, scheduling, and evaluation. *Case Studies on Transport Policy*, *4*(3), 218–229.

Kmet, L., Brasher, P., & Macarthur, C. (2003). A small area study of motor vehicle crash fatalities in Alberta, Canada. *Accident Analysis & Prevention*, *35*(2), 177–182.

Kukkonen, S., & Lampinen, J. (2005). GDE3: The third evolution step of generalized differential evolution. In *Evolutionary Computation, 2005. The 2005 IEEE Congress on* (Vol. 1, pp. 443–450). IEEE.

Lamm, R., & Kloeckner, J. H. (1984). *Increase of traffic safety by surveillance of speed limits with automatic radar devices on a dangerous section of a German Autobahn: A long-term investigation*. Retrieved from https://trid.trb.org/view.aspx?id=216819

Larson, R. C. (1974). A hypercube queuing model for facility location and redistricting in urban emergency services. *Computers & Operations Research*, *1*(1), 67–95.

Leggett, L. M. (1988). The effect on accident occurrence of long term, low intensity police enforcement. In *Australian Road Research Board (ARRB) Conference, 14th, 1988, Canberra* (Vol. 14). Retrieved from https://trid.trb.org/view.aspx?id=1197507

Leggett, L. M. W. (1997). Using police enforcement to prevent road crashes: The randomised scheduled management system. *Policing for Prevention: Reducing Crime, Public Intoxication and Injury. Crime Prevention Studies*, *7*, 175–97.

Li, R., El-Basyouny, K., & Kim, A. (2015). Before-and-after empirical Bayes evaluation of automated mobile speed enforcement on urban arterial roads. *Transportation Research Record: Journal of the Transportation Research Board*, (2516), 44–52.

Li, R., El-Basyouny, K., Kim, A., & Gargoum, S. (2016). Relationship between Road Safety and Mobile Photo Enforcement Performance Indicators: A Case Study of the City of Edmonton. *Journal of Transportation Safety & Security*, (just-accepted), 00–00.

Li, Y., Kim, A., & El-Basyouny, K. (2017). Scheduling resources in a mobile photo enforcement program. In *Transportation Information and Safety (ICTIS), 2017 4th International Conference on* (pp. 645–652). IEEE.

Lovegrove, G. R., & Sayed, T. (2006). Macro-level collision prediction models for evaluating neighbourhood traffic safety. *Canadian Journal of Civil Engineering*, *33*(5), 609–621.

Lovegrove, G., & Sayed, T. (2007). Macrolevel collision prediction models to enhance traditional reactive road safety improvement programs. *Transportation Research Record: Journal of the Transportation Research Board*, (2019), 65–73.

Ma, L. (2003). Integrating GIS and combinatorial optimization to determine police patrol areas. *Unpublished Masters Thesis, University of Texas at Dallas, Dallas, TX*.

MacQueen, J., & others. (1967). Some methods for classification and analysis of multivariate observations. In *Proceedings of the fifth Berkeley symposium on mathematical statistics and probability* (Vol. 1, pp. 281–297). Oakland, CA, USA. Retrieved from https://books.google.ca/books?hl=en&lr=&id=IC4Ku_7dBFUC&oi=fnd&pg=PA281&dq=some+methods+for+classification+and+analysis+of+multivariate+observations&ots=nOSgD0IftM&sig=a5ROjuhGomjpKTeWahT03YSAA08

Mattson, C. A., Mullur, A. A., & Messac, A. (2004). Smart Pareto filter: Obtaining a minimal representation of multiobjective design space. *Engineering Optimization*, *36*(6), 721–740.

Mavrotas, G. (2009). Effective implementation of the ε-constraint method in multi-objective mathematical programming problems. *Applied Mathematics and Computation*, *213*(2), 455–465.

Miettinen, K. (1999). *Nonlinear Multiobjective Optimization, volume 12 of International Series in Operations Research and Management Science*. Kluwer Academic Publishers, Dordrecht.

Milligan, G. W., & Cooper, M. C. (1988). A study of standardization of variables in cluster analysis. *Journal of Classification*, *5*(2), 181–204.

Mohan, D. (2006). *Road traffic injury prevention training manual*. World Health Organization. Retrieved from https://books.google.ca/books?hl=en&lr=&id=9_dU2MFGA6UC&oi=fnd&pg=PT11&dq=Road+Traffic+Injury+Prevention+Training+Manual&ots=1hF0B8UkA9&sig=vj4S34_KWY1yDc-29ydPxNaYFd4

Morse, J. N. (1980). Reducing the size of the nondominated set: Pruning by clustering. *Computers & Operations Research*, *7*(1–2), 55–66.

Myers, R. H., Montgomery, D. C., & Anderson-Cook, C. M. (2016). *Response surface methodology: process and product optimization using designed experiments*. John Wiley & Sons. Retrieved from https://books.google.ca/books?hl=en&lr=&id=T-BbCwAAQBAJ&oi=fnd&pg=PR13&dq=R.H.+Myers,+D.C.+Montgomery,+Response+Surface+Methodology&ots=O1fePof63N&sig=nH6uxG4jwv0uQQm6Zzwy6Hf22_I

Newstead, S., & Cameron, M. H. (2003). *Evaluation of the crash effects of the Queensland speed camera program*. Monash University Accident Research Centre Victoria, Australia. Retrieved from http://acrs.org.au/files/arsrpe/RS030116.pdf

NHTSA. (2008). *Speed enforcement program guidelines*. Washington, DC: National Highway Traffic Safety Administration (NHTSA), US Department of Transportation.

NHTSA, N. H. T. S. A. (2013). Traffic Safety Facts, 2013 Data: Pedestrians.

NHTSA, N. H. T. S. A. (2015). *Traffic safety facts 2013 data*.

Nilsson, G. (1992). *Försök med automatisk hastighetsövervakning 1990-1992*. Statens Väg-och Trafikinstitut. VTI, rapport 378.

OECD, O. for E. C. and D. (1990). *Behaviour adaptations to changes in the road transport system*. Paris: OCDE.

OECD/ECMT (Ed.). (2006). *Speed management*. Paris: Organisation for Economic Co-operation and Development (OECD), European Conference of Ministers of Transport (ECMT), OECD/ECMT Transport Research Centre.

Ostertagová, E. (2012). Modelling using polynomial regression. *Procedia Engineering*, *48*, 500–506.

Peden, M. (2008). *World report on child injury prevention*. World Health Organization.

Peden, M., Scurfield, R., Sleet, D., Mohan, D., Hyder, A. A., Jarawan, E., & Mathers, C. D. (2004). *World report on road traffic injury prevention*. World Health Organization Geneva.

Poppe, F. (1995). *Risk Figures in the Traffic and Transport Evaluation Module (EVV): A Contribution to the Definition Study Traffic Safety in EVV* (SWOV Report No. R-95-21). Leidschendam, Netherlands: SWOV Institute for Road Safety Research.

Pulugurtha, S. S., Krishnakumar, V. K., & Nambisan, S. S. (2007). New methods to identify and rank high pedestrian crash zones: An illustration. *Accident Analysis & Prevention*, *39*(4), 800–811.

Queensland Police. (2016). *Traffic Manual* (No. TM Issue 28). Brisbane: State of Queensland Government. Retrieved from https://www.police.qld.gov.au/corporatedocs/OperationalPolicies/tm.htm

Retting, R., & Farmer, C. (2003). Evaluation of speed camera enforcement in the District of Columbia. *Transportation Research Record: Journal of the Transportation Research Board*, (1830), 34–37.

ReVelle, C. S., & Eiselt, H. A. (2005). Location analysis: A synthesis and survey. *European Journal of Operational Research*, *165*(1), 1–19.

Rodier, C. J., Shaheen, S. A., & Cavanagh, E. (2007). Automated speed enforcement in the US: a review of the literature on benefits and barriers to implementation. In *Transportation Research Board 87 th Annual Meeting. CD-ROM. Washington, DC*.

Rosenman, M. A., & Gero, J. S. (1985). Reducing the Pareto optimal set in multicriteria optimization (with applications to Pareto optimal dynamic programming). *Engineering Optimization*, *8*(3), 189–206.

Rousseeuw, P. J. (1987). Silhouettes: a graphical aid to the interpretation and validation of cluster analysis. *Journal of Computational and Applied Mathematics*, *20*, 53–65.

Scott, M. S., & Maddox, D. K. (2001). *Speeding in residential areas*. US Department of Justice, Office of Community Oriented Policing Services. Retrieved from http://www.cops.usdoj.gov/html/cd_rom/speeding/pubs/Speeding.pdf

Steuer, R. E. (1986). *Multiple criteria optimization: theory, computation, and applications*. Wiley.

Taboada, H. A., Baheranwala, F., Coit, D. W., & Wattanapongsakorn, N. (2007). Practical solutions for multi-objective optimization: An application to system reliability design problems. *Reliability Engineering & System Safety*, *92*(3), 314–322.

Taboada, H. A., & Coit, D. W. (2007). Data clustering of solutions for multiple objective system reliability optimization problems. *Quality Technology & Quantitative Management*, *4*(2), 191–210.

Talby, D., & Raveh, A. (2015). Visual Co-Plot (Version 5.5). Retrieved from http://www.davidtalby.com/vcoplot/

The Office of Traffic Safety. (2013). *2013 Vulnerable Road User Collisions*. the City of Edmonton.

Toregas, C., Swain, R., ReVelle, C., & Bergman, L. (1971). The location of emergency service facilities. *Operations Research*, *19*(6), 1363–1373.

Transport Canada. (2010). *Transportation in Canada 2010: An Overview*. Minister of Public Works and Government Services, Canada. Retrieved from https://www.tc.gc.ca/media/documents/policy/overview2010.pdf

Transport Canada. (2011). *Transportation in Canada 2011: Comprehensive Review*. Retrieved from https://www.tc.gc.ca/media/documents/policy/Transportation_in_Canada_2011.pdf

Transport Canada. (2015). *Canadian Motor Vehicle Traffic Collision Statistics 2013*. Retrieved from https://www.tc.gc.ca/media/documents/roadsafety/cmvtcs2013_eng.pdf

Vaa, T. (1997). Increased police enforcement: effects on speed. *Accident Analysis & Prevention*, *29*(3), 373–385.

Van Veldhuizen, D. A., & Lamont, G. B. (1998). Evolutionary computation and convergence to a pareto front. In *Late breaking papers at the genetic programming 1998 conference* (pp. 221–228). Retrieved from https://pdfs.semanticscholar.org/f329/eb18a4549daa83fae28043d19b83fe8356fa.pdf

Vasudevan, V., Pulugurtha, S., & Nambisan, S. (2007). Methods to prioritize pedestrian high-crash locations and statistical analysis of their relationships. *Transportation Research Record: Journal of the Transportation Research Board*, (2002), 39–54.

Victoria Police Traffic Camera Office. (2006). *Mobile Cameras Policy Manual*. Melbourne: Victoria State Government. Retrieved from http://www.carr.org.au/d-mobile-cameras-policy-manual.pdf

Waiz, F. H., Hoefliger, M., & Fehlmann, W. (1983). *Speed limit reduction from 60 to 50 km/h and pedestrian injuries*. SAE Technical Paper. Retrieved from http://papers.sae.org/831625/

Walz, F. H., Niederer, P., & Kaeser, R. (1986). The car-pedestrian collision, injury reduction, accident reconstruction, mathematical and experimental simulation, headinjuries in two wheeler collisions. *Interdisciplinary Working Group for Accident Mechanics, University of Zurich and Swiss Federal Institute of Technology*.

Warsh, J., Rothman, L., Slater, M., Steverango, C., & Howard, A. (2009). Are school zones effective? An examination of motor vehicle versus child pedestrian crashes near schools. *Injury Prevention*, *15*(4), 226–229. https://doi.org/10.1136/ip.2008.020446

Weisel, D. L. (2004). Residential Speeding in Raleigh, North Carolina. Retrieved from http://www.popcenter.org/Library/researcherprojects/Speeding.pdf

Yin, Y. (2006). Optimal fleet allocation of freeway service patrols. *Networks and Spatial Economics*, *6*(3–4), 221–234.

Zitzler, E., & Thiele, L. (1999). Multiobjective evolutionary algorithms: a comparative case study and the strength Pareto approach. *IEEE Transactions on Evolutionary Computation*, *3*(4), 257–271.